T-4270

THE EFFECT OF IMPULSIVE FORCES ON OFFSHORE PIPELINES: A CASE OF SHIP ANCHOR IMPACT

by

A.I. AL-WARTHAN

ProQuest LLC.
789 East Eisenhower Parkway
P.O. Box 1346
Ann Arbor, MI 48106 – 1346

T-4270

A thesis submitted to the Faculty and the Board of Trustees of the Colorado School of Mines in partial fulfillment of the requirements for the degree of Master of Science (Applied Mechanics)

Golden, Colorado

Date July 10, 1992

Signed: _____

A. I. AL- Warthan

Signed: _____

Prof. J. S. Chung

Golden, Colorado

Date July 13, 1992

_____

Dr. Joan Gosink
Professor and Head,
Engineering Department

ABSTRACT

A discrete element method (DEM) has been used to analyze the effect of anchor impact on offshore pipeline. The DEM is a powerful tool for numerical modeling of nonlinear dynamic pipe problem. The DEM pipe formulation is based upon a system of rigid elements connected with axial and bending stiffnesses.

The deflection, and axial and bending stresses on three types of free span pipeline subjected to three different loading function were analyzed and presented in this study. It is concluded that the anchor impact on the offshore pipeline could lead to pipeline failure, and protective means should be considered in the design of an offshore pipeline.

TABLE OF CONTENTS

page

page

LIST OF FIGURES

Figures Page

Figures Page

Figures Page

Figures Page

Figures Page

Figures Page

Figures Page

LIST OF TABLES

ACKNOWLEDGEMENTS

Thanks and appreciation to Professor Jin S. Chung, professor of Engineering at Colorado School of Mines for his great assistance and continuous encouragement in advising me to complete this project. He has been more than as advisor to me and this association with him over the last two years was invaluable.

I would like to thank Dr. H.-P. Huttelmaier for not only being a member of my committee but who has been very inspiring in many ways.

Appreciation is also extended to committee members Dr. G.G.W. Mustoe, and Prof. Wang for their great help and useful comments.

CHAPTER 1

INTRODUCTION

1.1 Background:

Risks of anchor damage to offshore pipelines is a major subject in offshore pipeline technology as it can influence a decision about the burial depth and protection cover. A dragged or dropped anchor can displace and damage a pipeline and cause permanent impact damage. Such accidents could happen to a pipeline crossing an anchorage area or during emergency ship stopping and mainly due to a vessel operating close to a platform or loading/unloading terminal.

In the last few years several incidents have been reported concerning pipeline anchor interaction in the North Sea (Strating, 1981). The effect, however, of this type of interaction was not evaluated.

In this study the interaction of a 21,880 ton displacement tanker's anchor with a pipeline is investigated using:

(i) three different free span lengths

(ii) three different types of loading: impulse impact, ramp impact and anchor dragging of the free span pipeline.

1.2 Aim of the Present Work:

The aim of this investigation is to analyze the dynamic responses of an offshore free span pipeline, to different possible loading conditions. An existing discrete element method (DEM) code (Mustoe, Huttelmaier and Chung, 1992) is extended to model a horizontal pipeline and carry out the analysis. A DEM model analysis is prepared to simulate a 16-in diameter pipeline with properties as shown in Table 1.1.

Two possible interaction modes between the anchor and the pipeline will be analyzed:

1. Dropped anchor, where the anchor is dropped into the interaction corridor, whose width is the pipe diameter plus the anchor width as illustrated in Fig. 1.
2. An anchor hooked to the pipeline which drags the pipeline while the tanker is being drifted by waves and currents at a constant velocity.

The dynamic pipeline response is studied assuming that the pipe behaves elastically. The effects of plastification and local buckling, therefore, are not considered in this analysis. The effect of anchor-pipeline interaction will be studied for the three pipe span lengths and the three types of loading conditions.

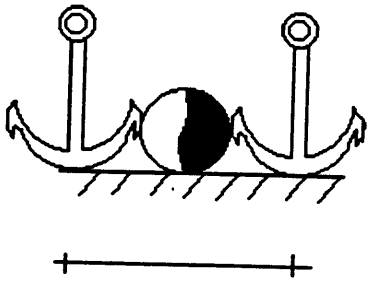

Figure 1 Interaction Corridor

Table 1.1 Pipe Geometry and Properties

Outer Pipeline Diameter	16-in
Span Length	45 ft - 90 ft - 160 ft
Wall Thickness	0.5-in
Pipe Mass Density	15.21 slug/ft^3
Young's Modules	4.32 x 10^9 lb/ft^2
Drag Coefficient	1.0
Water Density	1.99 slugs/ft^3

1.3 Layout of Thesis:

Chapter 2 presents a literature survey relevant to the present investigation. Several publications related to offshore pipeline incidents and the associated potential problems are cited.

Chapter 3 presents a theoretical formulation of impact phenomena and a brief overview of the discrete element method.

Chapter 4 presents pipeline model description within the DEM numerical analysis approach.

Chapter 5 presents numerical modeling results, and discusses the relevance of the result to the engineering design of a pipeline.

Chapter 6 presents the recommended pipeline protection method.

Chapter 7 describes the conclusions for this works. Further research recommendation are also discussed.

CHAPTER 2

BACKGROUND AND LITERATURE REVIEW

2.1 Literature Review:

Laboratory experiments, mathematical models and field tests have been widely used to investigate some of the accidents offshore pipelines encountered during their operation. Special attention was given to trawl-fishing-gear interactions with free-span pipeline. This subject was investigated both theoretically and experimentally.

Williams (1990) identified the impact from trawl gear or vessel anchor to be the largest cause of damage to operating pipelines. These accidents represented one half of the reported cases of damages.

Bruschi, Tomine and Vitali (1990) conducted a risk study to analyze anchor damage to offshore pipelines. It was concluded that anchor damage to pipelines is a major risk during pipeline construction and operations.

Verley (1991) presented a model test to investigate the trawl forces on a free-span pipeline. Three types of trawl doors were considered at different initial velocities and wrapping forces. The effects of tow velocity and span

height were included. Force-time trace for the three doors was presented.

Moshagen and Kjeldsen (1980) conducted laboratory and field studies on the conflict between pipelines laid on the seabed and trawl gear. The pipeline was subjected to an impact and a pull-over load for varying initial velocities. It was concluded that the resulting stress from the pull-over is higher than that from direct impact. A new trawl gear design was recommended to reduce the probability of hooking.

Jensen (1981) developed a numerical model using Hertz's theory (Hunter, 1957) to determine the impact strength of concrete on a submarine pipeline. A finite element model was used to estimate the deflection of the pipeline caused by a single impact load.

Chung and Fellippa (1981) developed numerical solutions to the coupled axial-bending deformation of a deep-ocean pipe using the finite element method. However, numerical instability and inaccuracies can occur when pipe velocities, relative to the surrounding fluid particles, exceed certain critical values.

Mustoe, Huttelmaier and Chung (1992) developed a new approach using the discrete element method (DEM) for the nonlinear, dynamic coupled bending-axial, analysis of ocean

pipes and risers, for which a FORTRAN program code was developed. The computer code developed (Mustoe Huttelmaier and Chung, 1992) is extended in this study to include the horizontal orientation of a pipeline with corresponding hydrodynamic forces.

2.2 Previous Incidents:

A survey of pipeline incidents in the North Sea showed that several incidents of anchor hooking to offshore pipelines have occurred. Some of these incidents (Strating 1981) have lead to shutdown of the pipeline operation for approximately six months to perform the required maintenance.

2.3 Expected Impact Frequency:

The frequency (or probability) of anchor interactions with offshore pipeline has been analyzed by Brown (1978), for various vessel sizes that are anticipated to be dragging an anchor in the vicinity of a pipeline during a 30 year period. Figure 2 shows the estimated frequency of incidents of anchor interactions with a pipeline. It is estimated that a pipeline with four markers during 30 years could

experience four interactions with a tanker's anchor of the same size used in the present study.

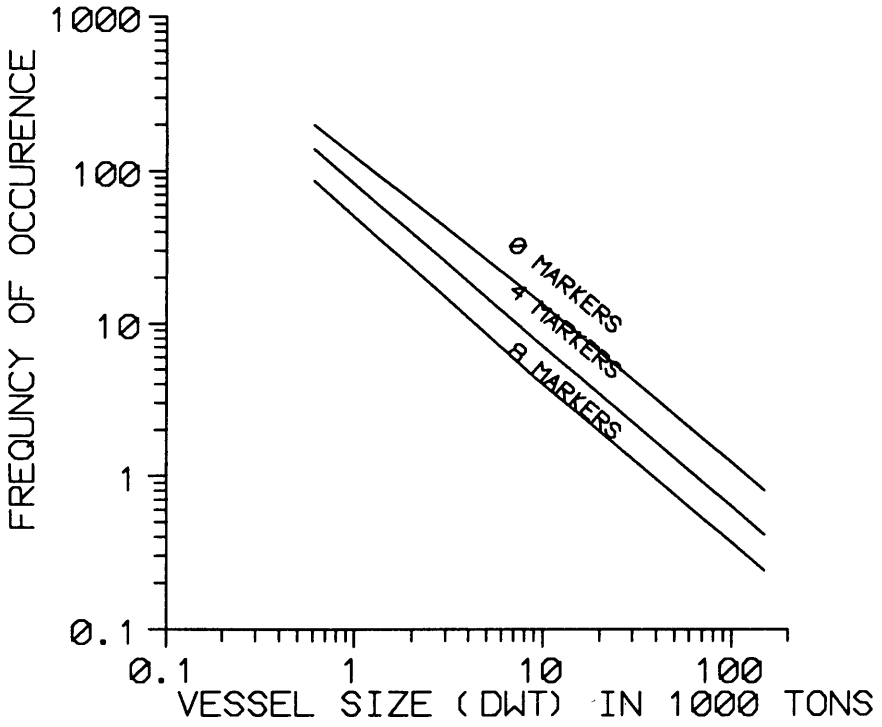

Figure 2 Estimated Number of Anchor-Pipeline Interactions

2.4 Potential Problems:

Offshore pipelines play a very important role in the economical and safe transport of oil and gas onshore from the offshore production areas and at loading and unloading terminals. Among many practical problems, a pipeline during its operation may encounter accidents such as the pipeline impacts with underwater vehicles and falling or moving objects.

Resulting impact loads can cause serious damages on the pipeline and the resulting dynamic problems. There are impact loads of various kinds;

1) Trawl doors from fishing vessels may hit the pipeline on the seafloor (Verley and Moshagen, 1991).

2) Anchors, that are pulled along the seafloor, may hit and drag the pipeline.

3) A pipeline riser installed on the jacket of an offshore bottom-fixed platform could be subjected to the impact load by floating objects such as supply vessels and workboats and falling equipment.

4) Waves generated from offshore explosions can cause damage or vibrations to the pipeline.

5) On production platforms there exists the possibility that objects (casing, drill collar, mud pipe, etc.), falling from

the platform deck can strike the pipeline, causing damage to the pipeline.

Impact loads on pipelines can affect the pipeline design and operation in many different ways. From impact, the pipe may experience an additional local denting and increased stresses which could prevent pig passage, and shorten the fatigue life of the pipe.

Dynamic characteristics of offshore pipelines in response to the loads as described above are important for several reasons. They might cause a lateral displacement of the pipe, creating cracks in the protective coating. The cracks can propagate along the pipe span and could lead to corrosion of the pipe, shortening the material life. Furthermore, pipeline vibration can shorten the fatigue life.

Failure of an offshore pipeline may lead to the leakage of the transported fluids, which could pose a serious pollution problem to the environment in addition to high repair costs.

CHAPTER 3

THEORETICAL FORMULATION

3.1 Anchor Impact:

The direct impact force on the pipe is represented by an impulse loading denoted by I, and is equal to the integral of the impact load F, over the entire impact duration from time t_1 to t_2:

$$I = \int_{t_1}^{t_2} F \, dt = mv_2 - mv_1 \qquad (3\text{-}1)$$

With the knowledge of the mass m and the initial and final velocities, v_1 and v_2, respectively of the anchor, the impulse load I can be evaluated.

The impulse load of a mass m and velocity v can be written as:

$$I = m v = C F t_d \qquad (3\text{-}2)$$

where F is the maximum impact load, $t_d = t_2 - t_1$, duration of impact, and C is the impulse shape factor (for example

for a triangular impulse load, as shown in Fig. 3, C = $\frac{1}{2}$), m = mass of the anchor, and v_o = initial velocity of the anchor.

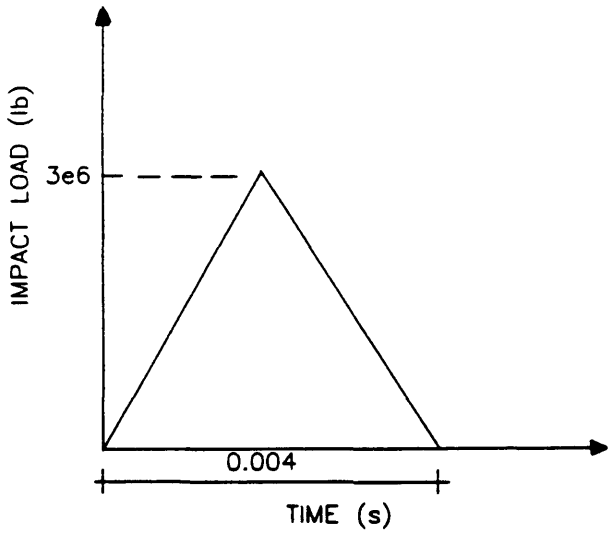

Figure 3 Triangular Impulse Loading Function Applied to a Pipeline

A 21,880 ton displacement tanker, with a loading capacity of 141,000 barrels and anchor weight of 9,504 lb will be considered in this study.

Sizing of the vessel's anchor in this study was determined by the American Bureau of Shipping (ABS) formula:

$$\text{Equipment Number} = 1.012\ \Delta^{2/3} + 0.186\ Bh + 0.00929A \quad (3\text{-}3)$$

where Δ = vessel displacement(tons), B = molded breadth(ft), h = vessel height(ft), and A = vessel profile area(ft^2).

If the equipment number is known, the anchor size can be found in the ABS manual (ABS Rules for Building and Classing Steel Vessels Table, 28.1).

The maximum impact load could be evaluated using the following equation (Jensen, 1981):

$$F = \frac{m\ v}{C\ t_d} = \frac{m\ v}{2\ t_d} \quad (3\text{-}4)$$

3.1.1 Duration of Impact:

The duration of an impact can be evaluated using Hertz's theory (Jenson, 1981) for an elastic impact by:

$$t_d = k_1\ v_o^{-1/5} \quad (3\text{-}5)$$

$$\text{where } k_1 = 2.94\ \left(\frac{15}{16}\frac{m\ m_1}{m+m_1}\ g\right)^{2/5} R^{-1/5} \quad (3\text{-}6)$$

with

$$g = \left[\frac{1-\upsilon^2}{E} + \frac{1-\upsilon_1^2}{E_1}\right] \qquad (3\text{-}7)$$

and where the following quantities are defined as:

m and m_1 are the pipe and anchor masses respectively

R is the radius of curvature

υ, υ_1 are Poisson's ratios for pipe and anchor, respectively

E, E_1 are the Young's Moduli for pipe and anchor, respectively

The initial velocity, v_o of the falling anchor prior to hitting the pipeline can be evaluated using the following equation:

$$W - F_B - \frac{1}{2}C_D \rho v_o^2 A = 0 \qquad (3\text{-}8)$$

therefore

$$v_o = \sqrt{\frac{2(W - F_B)}{C_D \rho A}} \qquad (3\text{-}9)$$

where W is the anchor weight, F_B is the anchor buoyancy, C_D is the drag coefficient, ρ is the sea water density, and A is the projected area.

3.1.2 Ramp Loading:

In this case an anchor is assumed to be dropped on a pipeline, and to remain in contact on top of the pipe span. A ramp loading function is used to simulate this loading. Such a function is illustrated in Fig. 4.

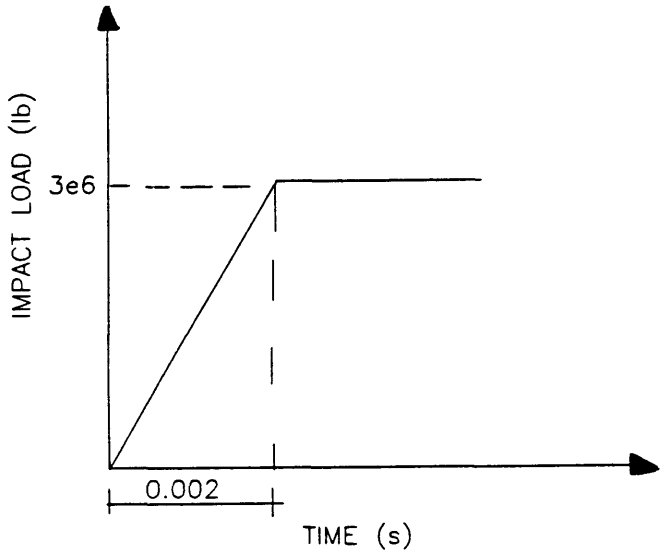

Figure 4 Ramp loading function applied to the pipeline

3.2 Anchor Hook Loading to a Pipeline:

When an anchor is hooked to a pipeline, and drags the pipeline between supports, tension develops in the pipeline, as the vessel drifts by the current and wave drift force, see Fig. 5.

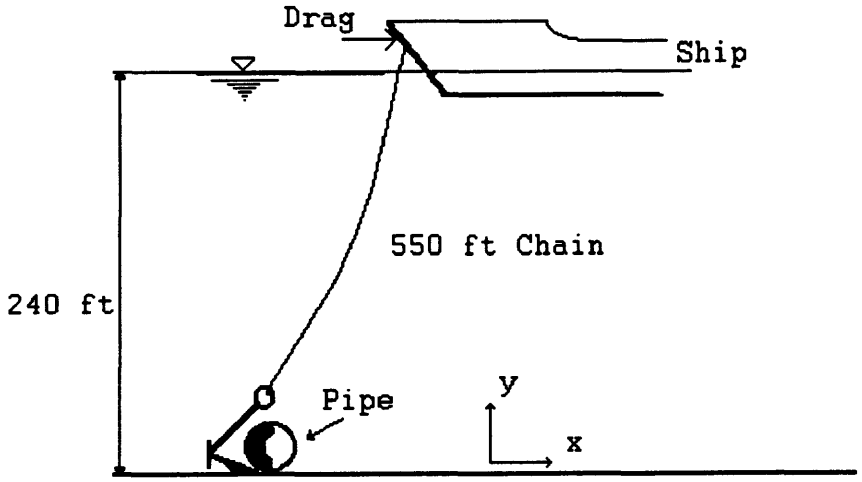

Figure 5 Anchor Hooked to Offshore Pipeline

A simplified case of tension load is considered where the applied transverse load is assumed to be in the upward vertical direction. The applied tension could be evaluated using the following procedure (Chung, the lecture note, 1992):

Calculate the downstream excursion x_t from the anchor chain with:

$$\sinh\left(\frac{x_t}{2a}\right) = \frac{11}{2a}\sqrt{L^2-h^2} \qquad (3\text{-}10)$$

where,

a is a catenary parameter which is defined as $a = \frac{T_x}{w}$,

T_x is, the tension in the x-direction (= drag force on the vessel in the x-direction),

w is the total chain weight + anchor weight

L is the chain length, and

h is the water depth.

Knowing x_t, the applied tension may be evaluated with:

$$T = aw\left[1+\left(\sinh\left(\frac{x-x_1}{a}\right)^2\right)^{0.5}\right] \qquad (3\text{-}11)$$

where,

$x_l = x_r - x_t$, and

$$x_r = a \tanh^{-1}(h/L) + (x_t/2) \qquad (3\text{-}12)$$

The above procedures were used to calculate the anchor hook loading function applied on a pipeline as shown in Fig. 6.

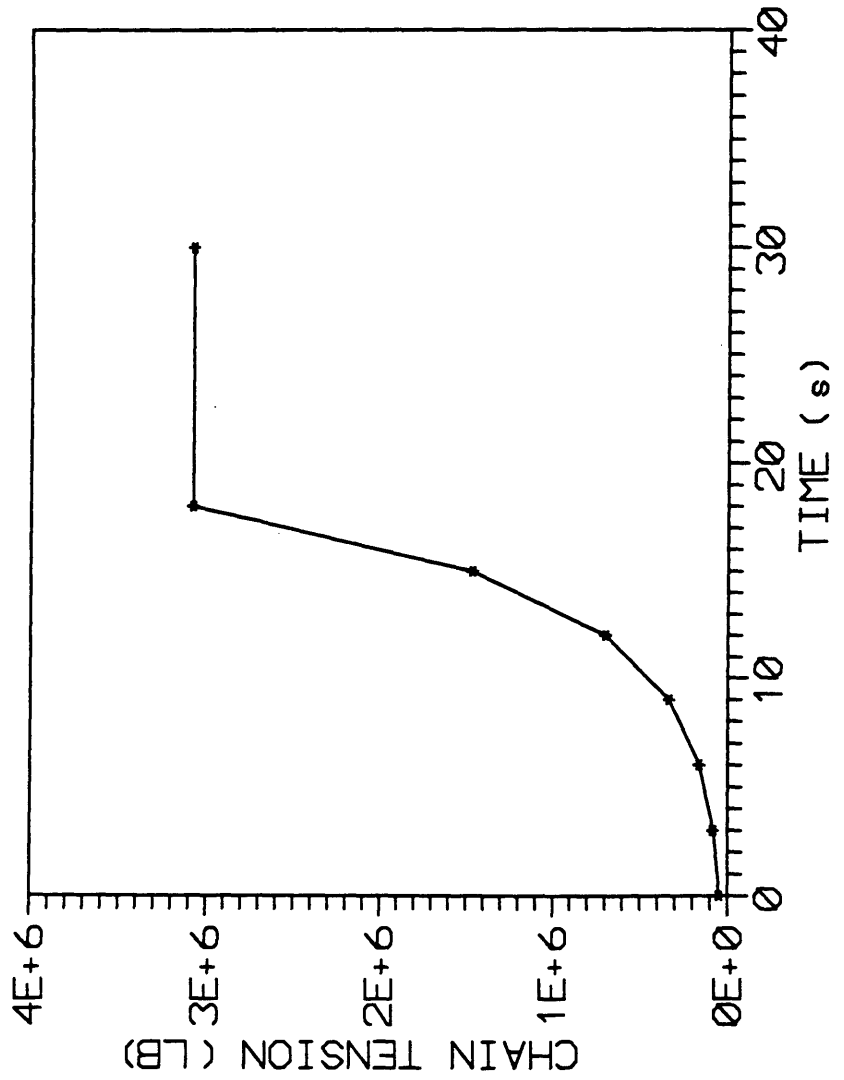

Figure 6 Applied Tension Loading Function.

CHAPTER 4

COMPUTATIONAL APPROACH

4.1 The Discrete Element Method (DEM) for a Horizontal Pipeline:

The discrete element method (DEM) is a numerical method which is capable of analyzing a system of bodies exhibiting discontinuous behavior while undergoing large motion. This method does not require the assumption of continuity as implied in other numerical techniques such as the finite element method and finite difference techniques. DEM also allows for dynamic large displacement analyses for dynamic large displacement analyses for certain type of structure such as flexible deep-ocean pipes or pipelines. The latter is discussed in this study.

In this section an overview of the mathematical basis of the DEM (OCEAN) code used is briefly presented (for more information see Mustoe, Huttelmaier and Chung, 1992). The program structure and a brief description for each subroutine is presented in Appendix A.

The DEM method developed for the dynamic analysis of a offshore pipelines was based upon modeling a pipeline with rigid body elements connected with concentrated axial, shear

and bending stiffnesses. For this study the DEM (OCEAN) computer code was modified to include the horizontal orientation of the pipeline. This required computation of the initial equilibrium state due to the pipelines self weight.

4.1.1 Equation of motion:

The equations of motion for a rigid element, e, undergoing two dimensional planar motion including damping effects are:

$$\begin{aligned} m_e \ddot{u}_e^x &= \Sigma F_e^x \\ m_e \ddot{u}_e^y &= \Sigma F_e^y \\ I_e \ddot{\theta}_e &= \Sigma M_e \end{aligned} \qquad (4\text{-}1)$$

where the resultant forces and moments ΣF_e^x , ΣF_e^y and ΣM_e include both internal loads due to the interelement stiffnesses and external loads due to applied forces and damping effects, m_e = element mass, θ_e = element angular coordinate, x and y define the element centroidal location (in Cartesian coordinates), u = displacement, $\dot{u}$ = velocity, $\ddot{u}$ = acceleration, I_e = element moment of inertia.

The numerical solution of the above element equations was obtained with a numerical time integration scheme in

conjunction with an updated Lagrangian approach to deal with the large deformations and rigid body motion. The time integration was performed with an explicit central difference time stepping scheme which is performed in two parts, a velocity update followed by a position update for each of the rigid body elements in the DEM idealization.

i) Velocity update:

The velocity is calculated at time $t^n + \Delta t/2$ using the known velocity at time $t^n - \Delta t/2$ and known loading at time t^n, where Δt = time step.

The generalized velocity $\dot{q}_e^i$ for a typical element is defined for i=1,2 and 3 as the element centroidal velocities $\dot{u}_e^x$ $\dot{u}_e^y$ and the angular velocity $\dot{\theta}_e$, respectively. The appropriate generalized velocity update for the i^{th} component using the central difference method is formulated as follows:

$$^{n+1/2}q_e^i = b\ (a(^{n-1/2}q_e^i) + \Delta t^n\ (F^n{}_e^i\ /\ M_e^i)) \qquad (4\text{-}2)$$

where $a = 1 - \dfrac{\alpha_i \Delta t}{2}$

$$b = \frac{1}{1+\alpha_i \Delta t/2}$$

and α_i is the mass proportional damping coefficient for the i^{th} generalized velocity.

ii) Position update:

The position update for the generalized element position q_e^i is evaluated using the following equation:

$$^{n+1}q_e^i = {}^{n}q_e^i + \Delta t(^{n+1/2}q_e^i) \qquad (4\text{-}3)$$

4.1.2 Computational Procedure for Two Dimensional Model:

Compute the velocity of the two adjacent nodes p_i and q_{i-1} for element i (Fig.7):

$$V^x_p = V^x - 0.5\omega_1 \, l \, \sin(\theta_1)$$

$$V^y_p = V^y - 0.5\omega_1 \, l \, \cos(\theta_1)$$

$$V^x_q = V^x - 0.5\omega_2 \, l \, \sin(\theta_2) \qquad (4\text{-}4)$$

$$V^y_q = V^y - 0.5\omega_2 \, l \, \cos(\theta_2)$$

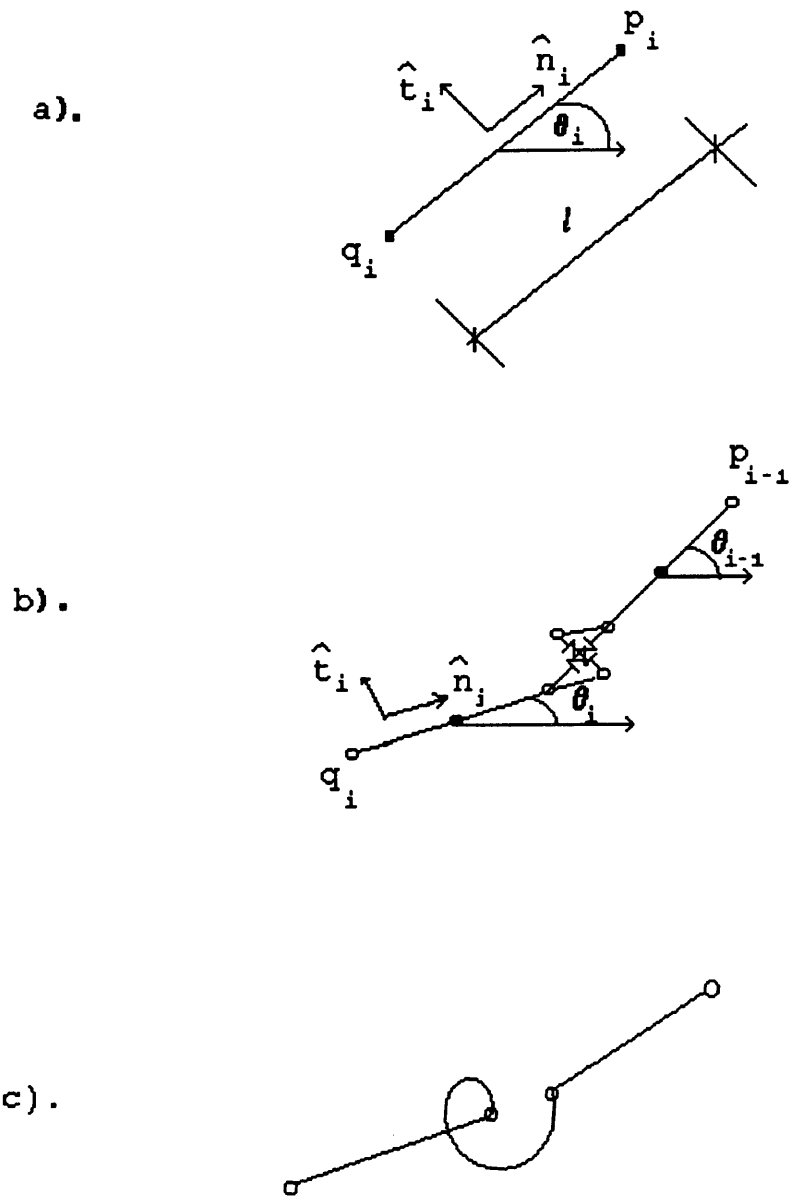

Figure 7 Angular Position of Two Adjacent Element a) Local Axes(n_i,t_i) for Element i b) Axial and Shear Stiffness Between Element i-1 and i c) Bending

Find the relative velocity $V_{q/p}$ and find the relative velocities in the axial and shear direction, v_a and v_s:

$$\begin{bmatrix} V_a \\ V_s \end{bmatrix} = \begin{bmatrix} \cos\theta & \sin\theta \\ \sin\theta & \cos\theta \end{bmatrix} \begin{bmatrix} V^x_{q/p} \\ V^y_{q/p} \end{bmatrix} \quad (4\text{-}5)$$

where $\theta = (\theta_1+\theta_2) / 2$, the average angle between two adjacent element.

Then compute the incremental forces resulting in an axial incremental force:

$$\Delta F_{axial} = k_a \Delta t \; V_a \quad (4\text{-}6)$$

a shear incremental force:

$$\Delta F_{shear} = k_s \Delta t \; V_s \quad (4\text{-}7)$$

and the incremental moment:

$$\Delta M_e = k_r \Delta t \; \dot{\theta} \quad (4\text{-}8)$$

Parameters k_a, k_s and k_r are stiffnesses in the axial, shear and rotational direction. Note, that $\Delta t \; V_a$, for

example is the incremental axial displacement during a time step.

The incremental forces are then resolved into global axes and introduced into the update equations (Eqs. (4-2) , (4-3)).

4.1.3 Incremental Strain and Stresses Calculation:

The component of logarithmic incremental kinematic strain at the joint between elements e and e+1 are computed in the following manner:

i) the incremental strain because of axial deformation, $\Delta\varepsilon_a$ is given by:

$$\Delta\varepsilon_a = \Delta u_e / (l_e /2 + l_{e+1} /2 + u_e) \qquad (4\text{-}9)$$

where Δu_e is the incremental axial displacement at the joint between element e and e+1.

ii) the incremental strain because of bending deformation, $\Delta\varepsilon_b$ is given by:

$$\Delta\varepsilon_b = t_e \Delta\theta_e / [2(\theta_{e+1} - \theta_e) R_e] \qquad (4\text{-}10)$$

where t_e, and R_e are the element thickness and radius of curvature at the joint between element e and e+1.

The corresponding total stresses at the element joint between element e and e+1 are computed in an incremental manner, in which the incremental stress calculations due to axial and bending deformation are performed, using Hooke's

law. These incremental axial and bending stresses $\Delta\sigma_a$ and $\Delta\sigma_b$, are given by:

$$\Delta\sigma_a = E\ \Delta\varepsilon_a \quad \text{and} \quad \Delta\sigma_b = E\ \Delta\varepsilon_b \tag{4-11}$$

where E is the Young's modulus.

Note that the current stress state due to the coupled axial and bending effect is then computed by a simple superposition of the total updated axial and bending stresses, σ_a and σ_b.

4.1.4 Hydrodynamic Forces:

The OCEAN computer program models the effect of normal fluid forces as vector $\overline{F}$, due to inertia and drag in the x- and y-direction using a simplified form of the equation by Chung (1980) assuming a zero wave velocity and constant current velocity:

$$\overline{F}_n = -\rho_w(\pi d^2/4)C_m\ \dot{\overline{v}}_{rn}+\rho(\pi d^2/4)\ \dot{\overline{v}}_{wn}-1/2\ \rho_w\ d\ C_d\ v_{rn}\ \overline{v}_{rn} \tag{4-13}$$

where, ρ_w is the water density, $\overline{v}_{rn}$ is the normal component of the relative velocity vector defined by $\overline{v}_{rn} = \overline{v}_r - \overline{v}_{rt}$.

The normal component of the relative acceleration is defined by $\dot{\bar{v}}_{rn} = \dot{\bar{v}}_r - \dot{\bar{v}}_{rt}$. The relative velocity vector $\bar{v}_r$ is defined by $\bar{v}_r = \bar{v}_p - \bar{v}_c - \bar{v}_w$, where $\bar{v}_p$ is the pipe velocity, $\bar{v}_c$ is the steady current velocity, and $\bar{v}_w$ is the time dependent wave velocity. The vector $\bar{v}_{rt}$ is the tangential component of the relative velocity, C_m and C_d are inertia and drag coefficients, respectively. For the present investigation, $\bar{v}_{rt} = 0$, $\bar{v}_c = 0$, and $\bar{v}_w = 0$.

4.2 Model Description:

The safe operating life of an offshore pipeline depends, primarily, on the stress level maintained on the pipeline during its operation. An unsupported span due to the loss of contact with the seabottom can experience excessive stresses due to its weight in addition to other factors such as impact loads.

Freespan can occur when a pipeline is layed on an uneven bottom, or it can develop due to varying erosion and scouring under the pipeline, initiated by waves and current which affect mostly buried pipelines.

In this study the above two cases will be modeled by a beam with fixed ends as illustrated in Fig. 8.

The span length due to erosion can be evaluated using the Fedsϕe (1983) equation:

$$\text{Span length} = 3.35 \quad S^{1/4} \, L_s^{3/4} \qquad (4\text{-}14)$$

Where

$$L_s = \sqrt[3]{\frac{EI}{p}}$$

p is the weight of the pipe /unit length, and S is the scour depth under the pipeline.

Three different span lengths will be analyzed in this study, these are 45 ft, 90 ft and 160 ft.

By using the span symmetry, the execution time is reduced by approximately 50%, and the span is analyzed by fixing one end and the beam at mid span is allowed to move in the y direction only, and is fixed rotationaly. Half of the impact load will be applied for this model at the mid span.

4.3 Model Discretaization:

In order to evaluate the effect of the impulse load, the effect of high vibration modes, and accurately model the wave propagation effects through the pipeline, the DEM

models were discretized with a constant element length l_e given by:

$$l_e < 1/4 \quad t_d \sqrt{E/\rho} \tag{4-11}$$

This condition ensures that the spatial impulsive disturbance is modeled with at least four discrete elements.

The pipe was discretized with equal element lengths of 5 ft each as illustrated in Fig. 9.

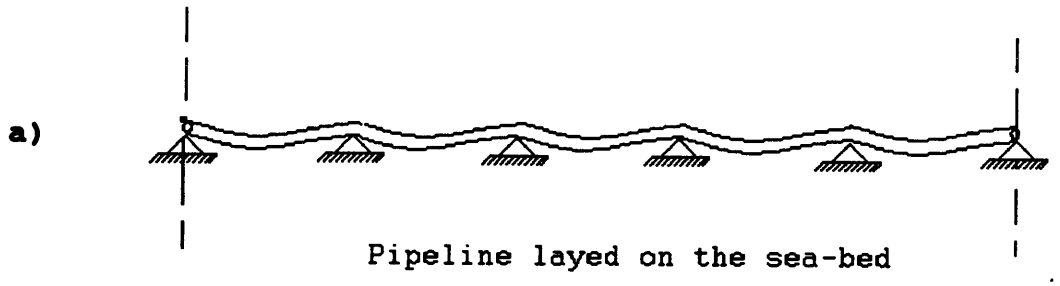

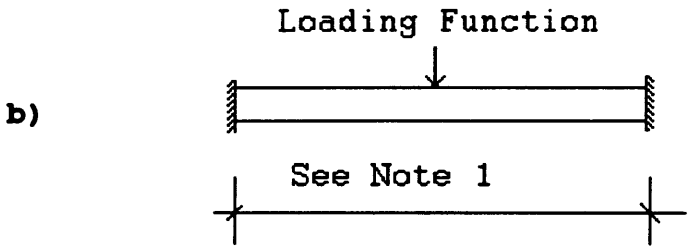

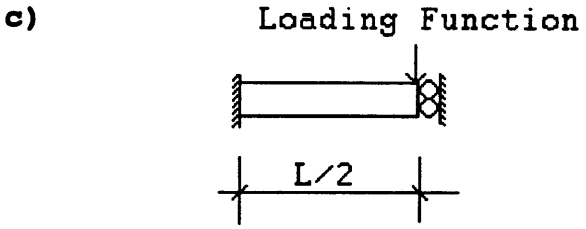

Note 1:
Three cases are considered
L = 45 ft
L = 90 ft
L = 160 ft

Figure 8 Model Description: a) Actual Case; b) Modeled Case; and c) Symmetrical DEM Idealization

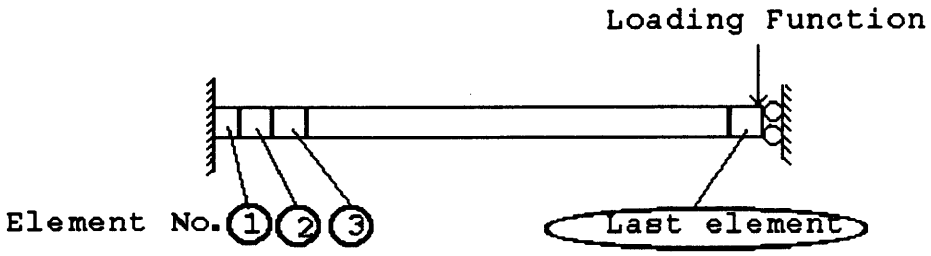

Element length= 5 ft each

Span Length	No. of Elements
45 ft	5 elements
90 ft	9 elements
160 ft	15 elements

Figure 9 Span Discretization

CHAPTER 5

RESULTS and DISCUSSIONS

5.1 Code Verification Without Contact:

A number of problems were solved to validate the DEM code. Some of these example problems were presented in Mustoe, Huttelmaier and Chung (1992). Further validation analyses are reported here with two additional examples which are compared with the analytical solutions. The differences between the results of the DEM components and analytical solution were within the range of 1%. The program was executed for two examples with the effect of mass damping, until it reached the equilibrium state. The result were compared with the analytical solution.

5.1.1 Transverse loading applied at the end of cantilever beam:

Beam Properties:

length = 1.0 ft

Young's Modulus = 4.32×10^9 lb/ft^2

Transverse load = 100 lb

Result of the analysis are shown in Table 5.1.

Table 5.1

Code Verification Without Contact

Transverse Load

ELEMENT NO.	DEM DISPLACEMENT	ANALYTICAL DISPLACEMENT	ERROR %
1	0.00	0.00	0.00
2	-2.92E-06	-2.80E-06	-2.70
3	-1.11E-05	-1.10E-05	-1.56
4	-2.39E-05	-2.40E-05	-1.20
5	-4.05E-05	-4.00E-05	-0.69
6	-6.05E-05	-6.00E-05	-0.65
7	-8.31E-05	-8.30E-05	-0.57
8	-1.08E-04	-1.10E-04	-0.83
9	-1.34E-04	-1.30E-04	-0.82
10	-1.60E-04	-1.60E-04	0.00

5.1.2 Axial Loading Applied at the End of Cantilever Beam:

Beam Properties:

length = 1.0 ft

Young's Modulus = 4.32×10^9 lb/ft^2

Axial load = 1.0×10^{10} lb

Result of the analysis are shown in Table 5.2.

Table 5.2

Code Verification Without Contact

Axial Load

ELEMENT NO.	DEM DISPLACEMENT	ANALYTICAL DISPLACEMENT	ERROR %
1	0.00	0.00	0.00
2	13.70	13.70	-0.02
3	27.40	27.39	-0.02
4	41.00	41.09	0.22
5	54.70	54.78	0.16
6	68.40	68.48	0.12
7	82.10	82.18	0.10
8	95.50	95.88	.039
9	109.50	105.58	0.07
10	123.00	123.27	0.22

5.2 Types of anchor/pipeline interaction:

Three types of anchor pipeline interactions are considered in this study:

Type 1:

A triangular impulse loading where the anchor hits the side of the mid span of a pipeline with a duration of impact t_d as illustrated in Fig. 3.

Type 2:

A direct impact where the anchor hits the mid span and stays on the pipeline. This type is implemented by using a ramp loading function as illustrated in Fig. 4.

Type 3:

An anchor is hooked to a pipeline span applying a tension loading (T) at the mid span with a loading function as shown in Fig. 6, and the ship is moving at constant velocity of 1 knot (1.689 ft/s).

The resultant forces and displacement from the above interaction for the horizontal free-span pipeline is presented in this chapter using an extended version of the

DEM code OCEAN (Mustoe, Huttelmaier and Chung, 1992) to include the horizontal orientation of a pipeline.

5.3 Self Weight Effect:

The three different types of anchor pipeline problems were analyzed in two steps:
i) compute the equilibrium configuration of the pipeline due to self weight, and ii) subject the pipeline to a specified impulsive loading history.

Each model is initially executed with the self weight only, until it reaches an equilibrium state. During this stage, damping is introduced by applying the artificial hydrodynamic forces with an unrealistic drag coefficient C_D, (C_D= 45-150). This damping is used in order to get the pipeline into its initial equilibrium state. The deflection time histories are shown in Figs. 10-12. The loading function was applied after the pipeline reached its equilibrium state.

The resulting deflected shape and axial and bending stresses are shown in Figs. 13-21, and the maximum values are listed in Table 5.3.

Table 5.3

Equilibrium Values for Central Deflection, Maximum Axial and Bending Stresses

SPAN LENGTH	DEFLECTION	AXIAL STRESSES	BENDING STRESSES
45 FT	-0.0038 ft	104 lb/ft^2	111000 lb/ft^2
90 FT	-0.0576 ft	5420 lb/ft^2	416000 lb/ft^2
160 FT	-0.757 ft	228000 lb/ft^2	1320000 lb/ft^2

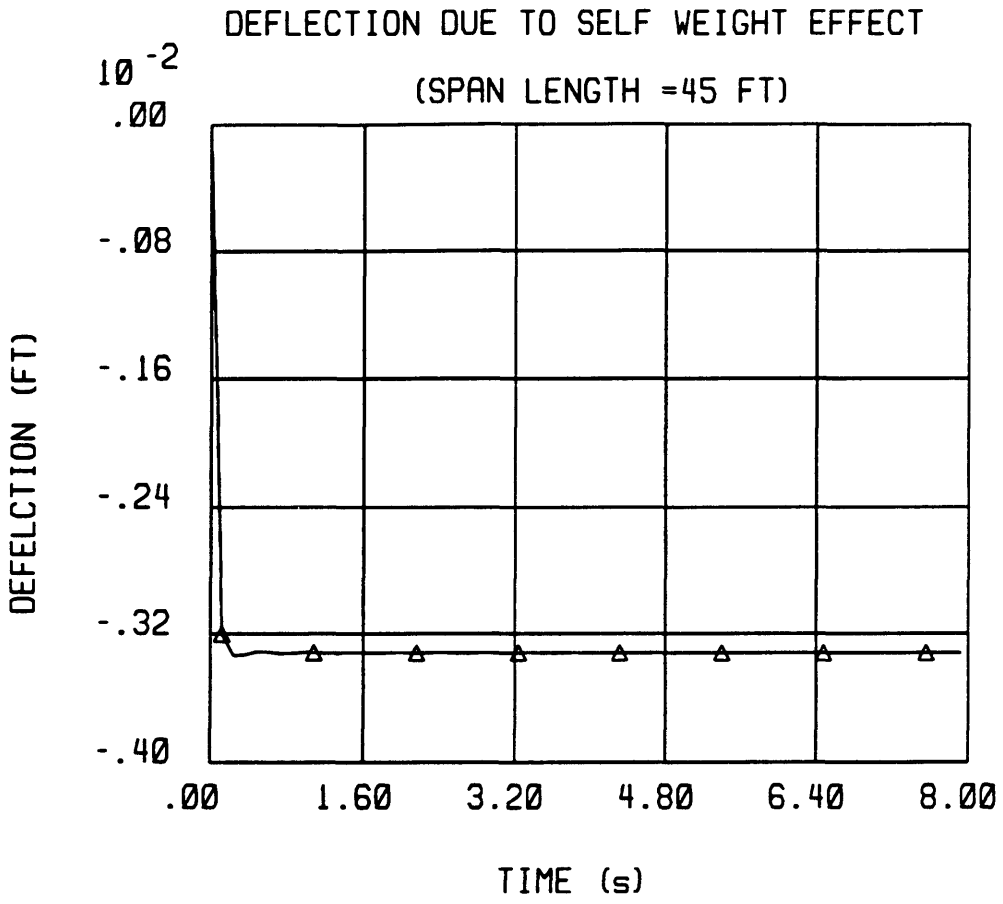

Figure 10 Time History of Pipeline Central Deflection Due to Self Weight (Span Length =45 ft)

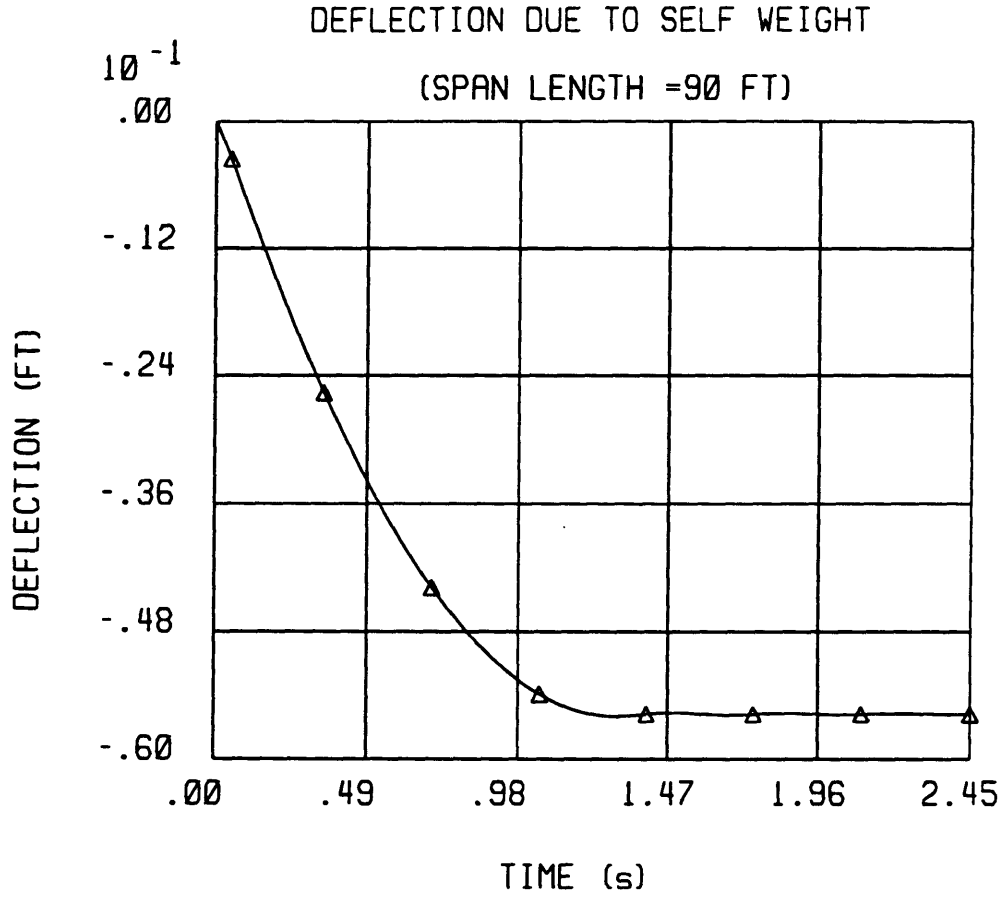

Figure 11 Time History of Pipeline Central Deflection Due to Self Weight (Span Length =90 ft)

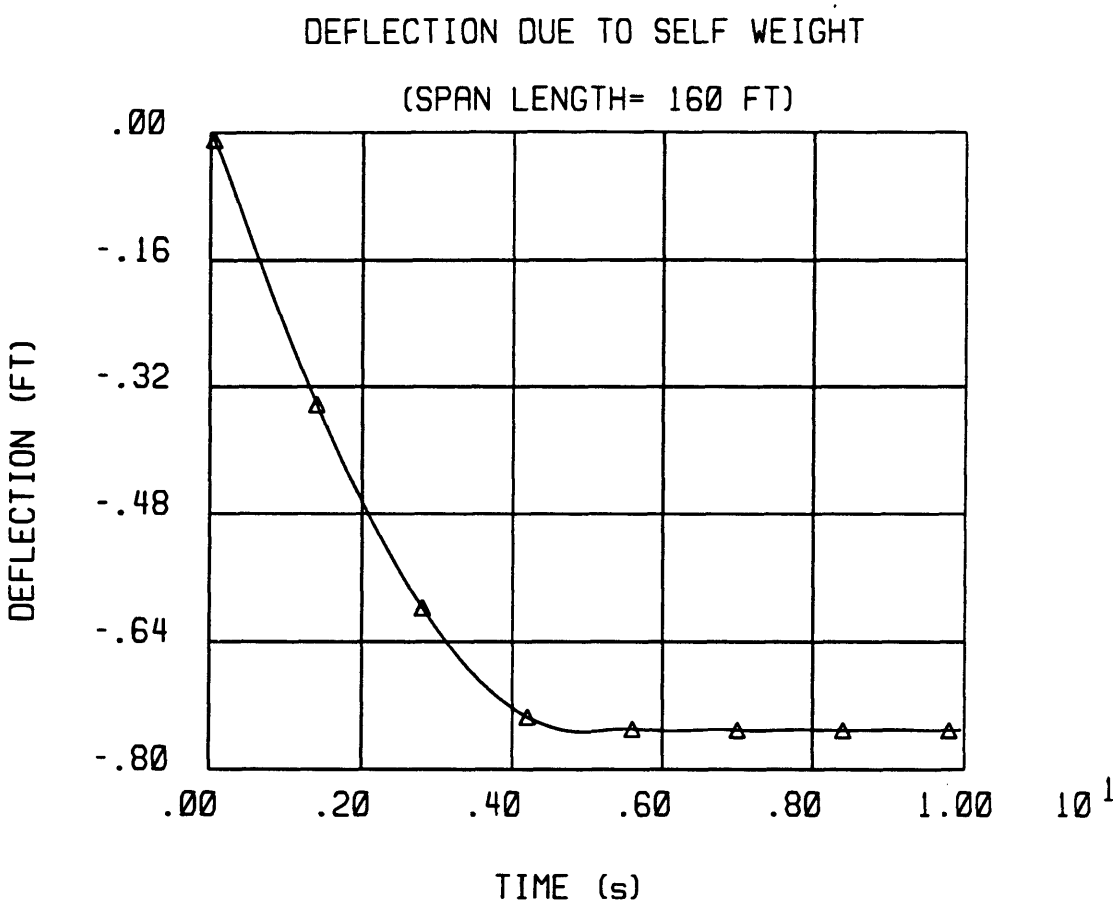

Figure 12 Time History of Pipeline Central Deflection Due to Self Weight (Span Length =160 ft)

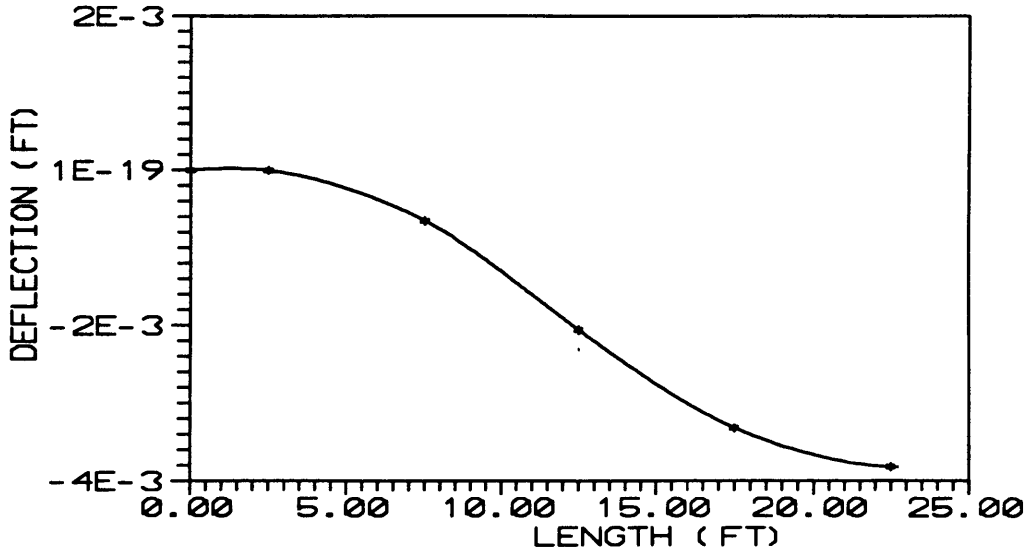

Figure 13 Pipeline Deflection Due to Self Weight
(Span Length =45 ft)

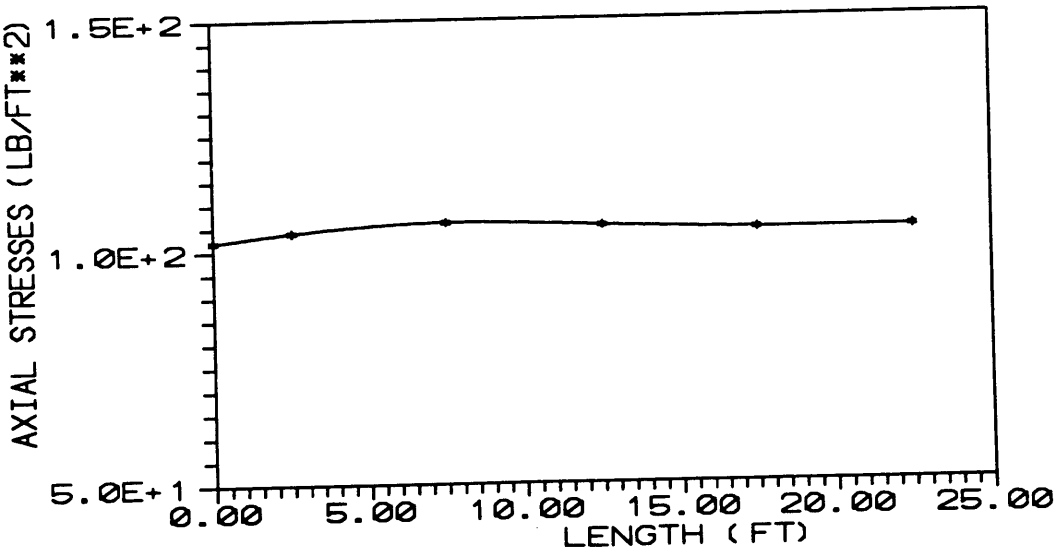

Figure 14 Axial Stresses Due to Self Weight
(Span Length =45 ft)

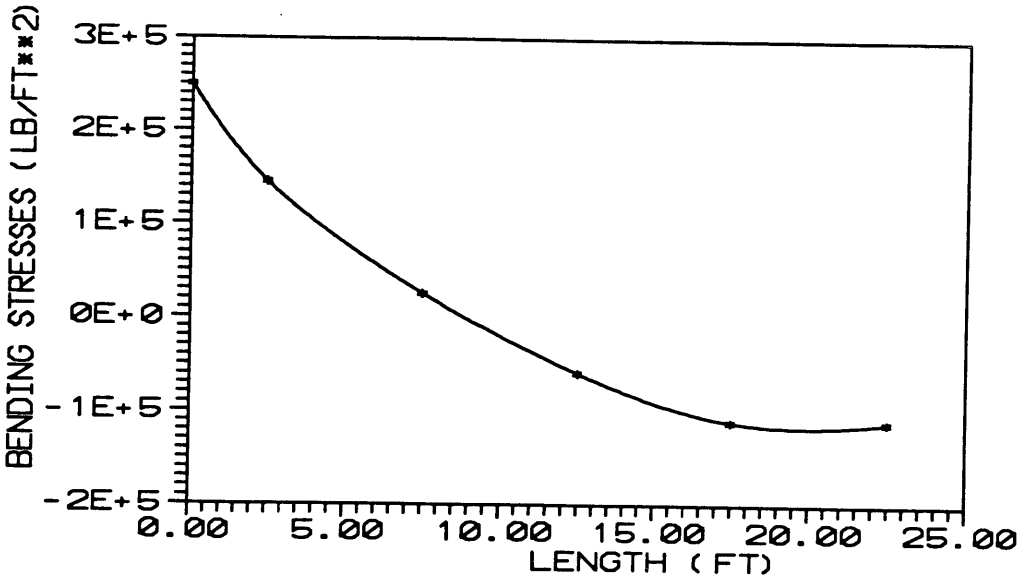

Figure 15 Bending Stresses Due to Self weight
(Span Length =45 ft)

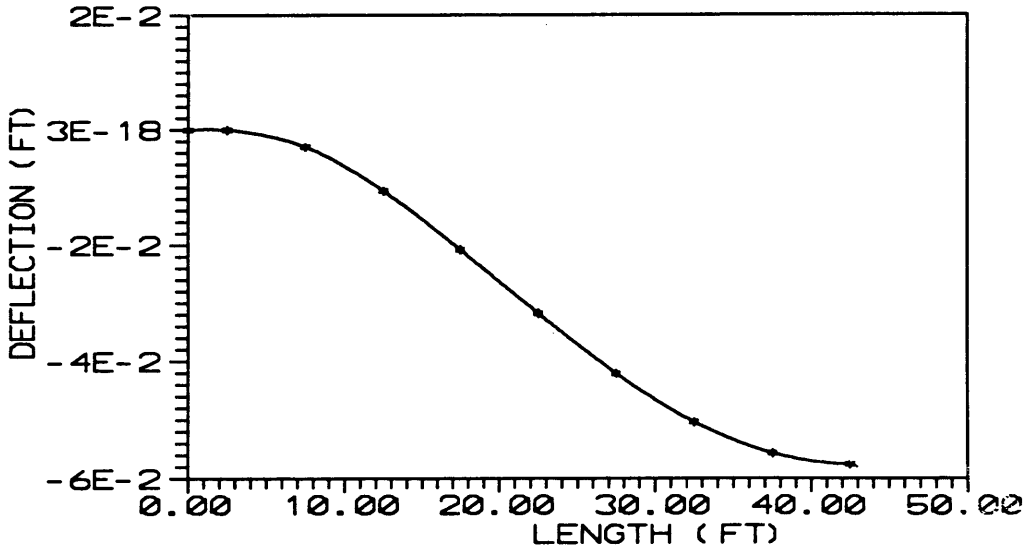

Figure 16 Pipeline Deflection Due to Self Weight
(Span Length =90 ft)

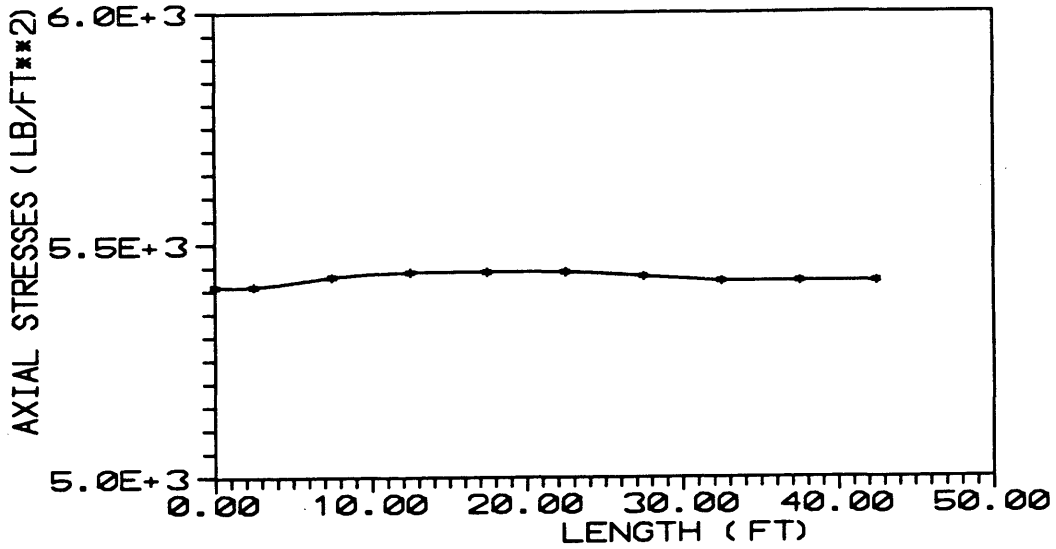

Figure 17 Axial Stresses Due to Self Weight
(Span Length =90 ft)

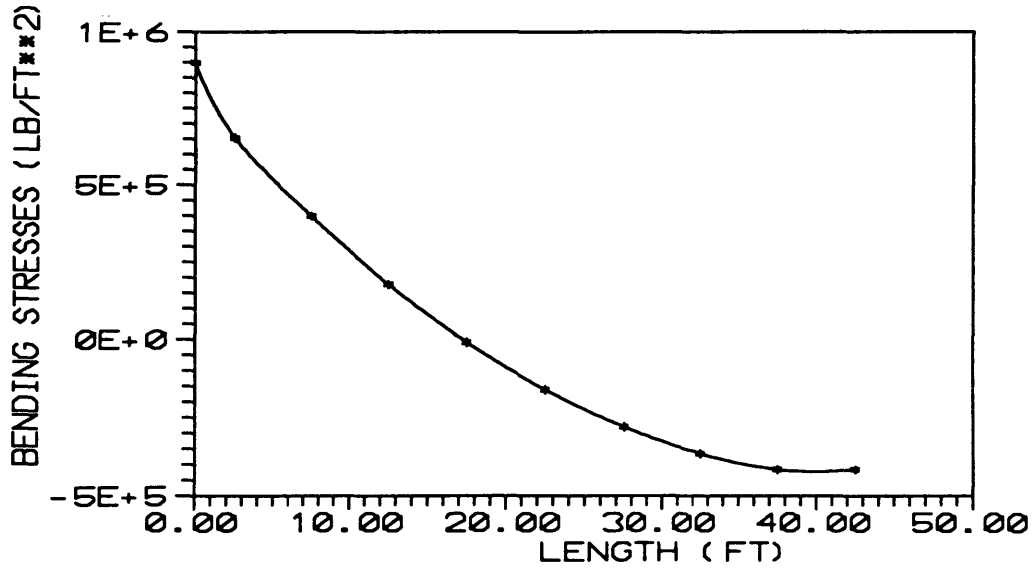

Figure 18 Bending Stresses Due to Self Weight
(Span Length =90 ft)

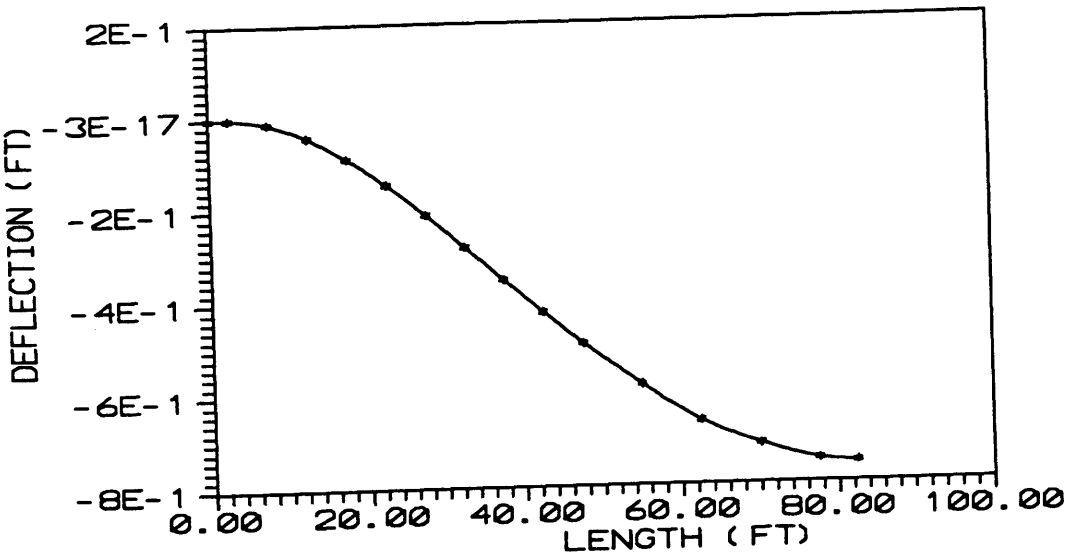

Figure 19 Pipeline Deflection Due to Self Weight
(Span Length =160 ft)

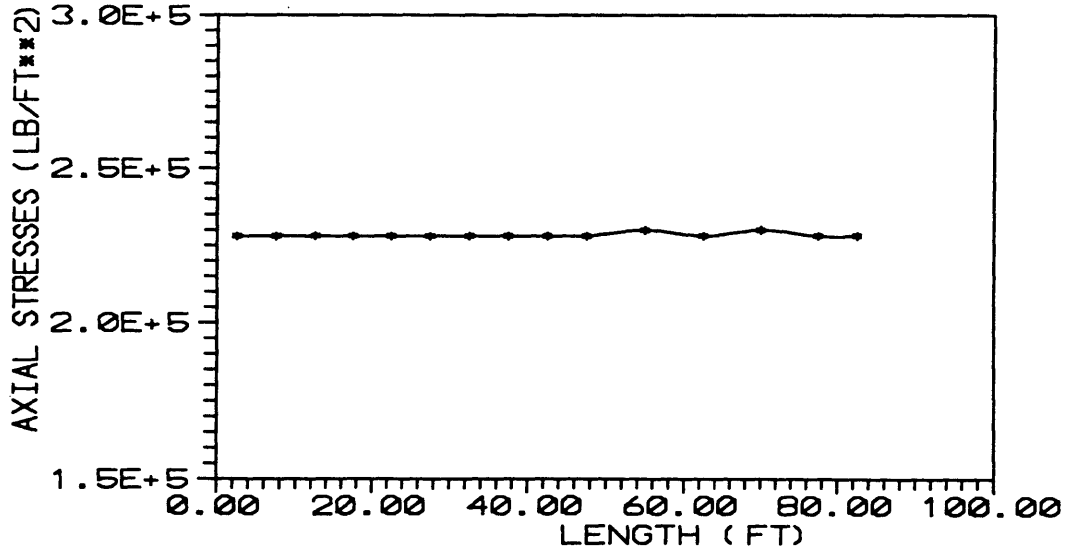

Figure 20 Axial stresses Due to Self Weight
(Span Length =160 ft)

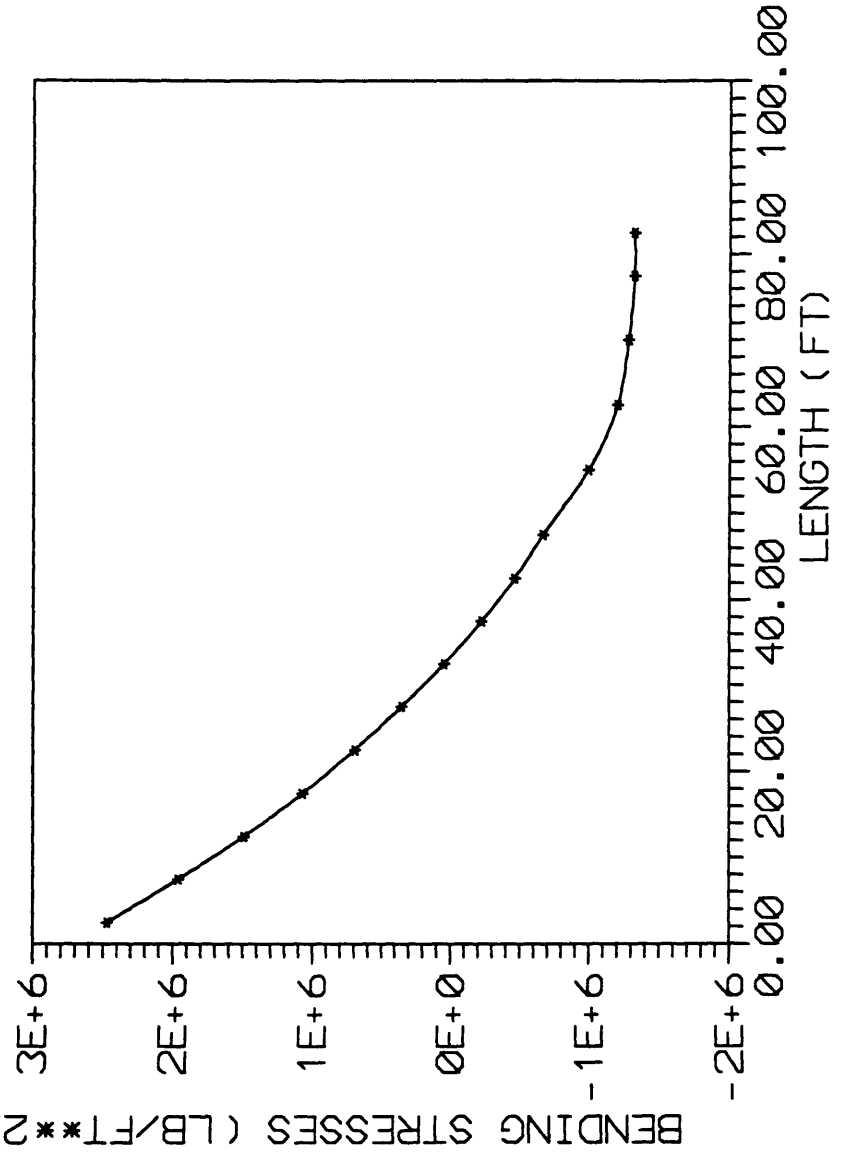

Figure 21 Bending Stresses Due to Self Weight
(Span Length =160 ft)

5.4 Dropped Anchors:

For the case of a dropped anchor, the deformation is mainly local, as the anchor, hitting the pipeline with a certain kinetic energy, will cause an inward deflection of the steel shell. In this study only global impact effects are analyzed within the elastic range. Two types of loading function were applied to the pipeline: i) impulse loading and ii) ramp loading.

5.4.1 Impulse Loading :

A triangular impact loading with a maximum value of $3x10^6$ lb (Fig. 3) is applied for a duration of t_d = 0.004 s for the three different span lengths. The resulting deflections, as well as axial and bending stresses are shown in Figs. 22-30. A time history of axial and bending stresses for the central element, where the loading functions were applied (element no. 5 for span length 45 ft, element 9 for span length 90 ft and element 15 for span length 160), are shown in Figs. 31-39. It is noted that the pipeline span begins to vibrate as soon the impact loading is applied between pipeline supports. However, the vibration decays due to the effect of water drag or damping. As the span length increased, it takes longer for the vibration to decay, which

is due to the decreasing vibrational frequency in each span.

It was noted that axial and bending stresses continue to build up in the span after the impact duration; this effect was due to the pipe vibration. The stresses reach their maximum values at time = 0.008 s. A comparison between the maximum stresses for the three different span length (Fig. 40) resulted in the conclusion that the impulse loading affects mostly the 45 ft, the shorter span. This effect is due to the higher vibrational frequencies in this span.

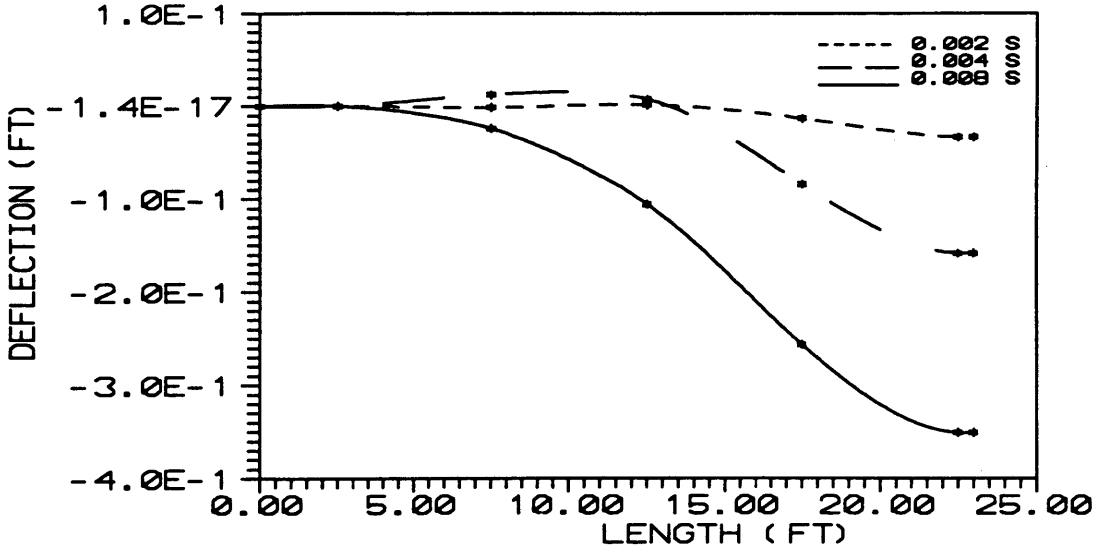

Figure 22 Pipeline Deflection Due to Impulse Loading Impact (Span Length =45 ft)

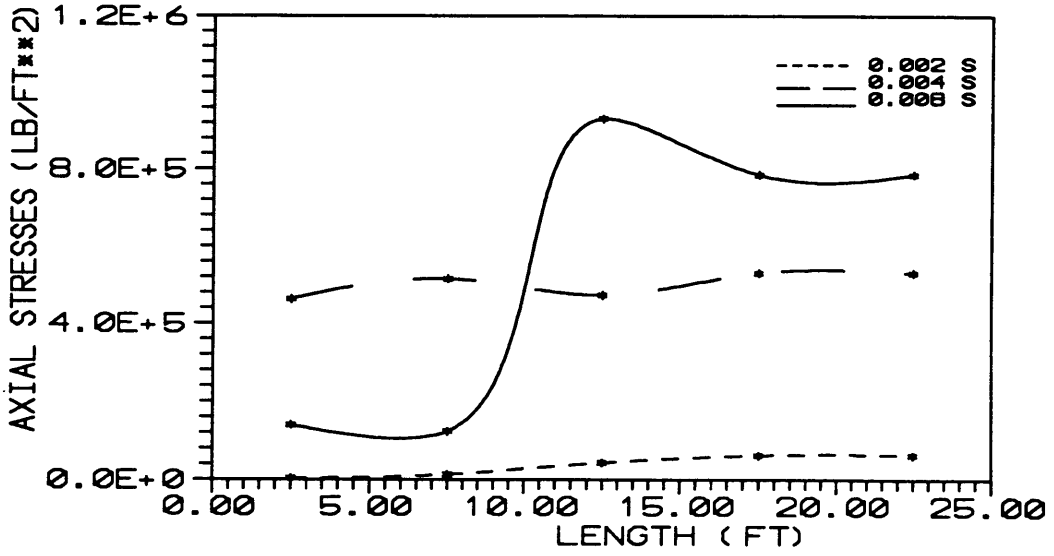

Figure 23 Axial Stresses Due to Impulse Loading Impact (Span Length =45 ft)

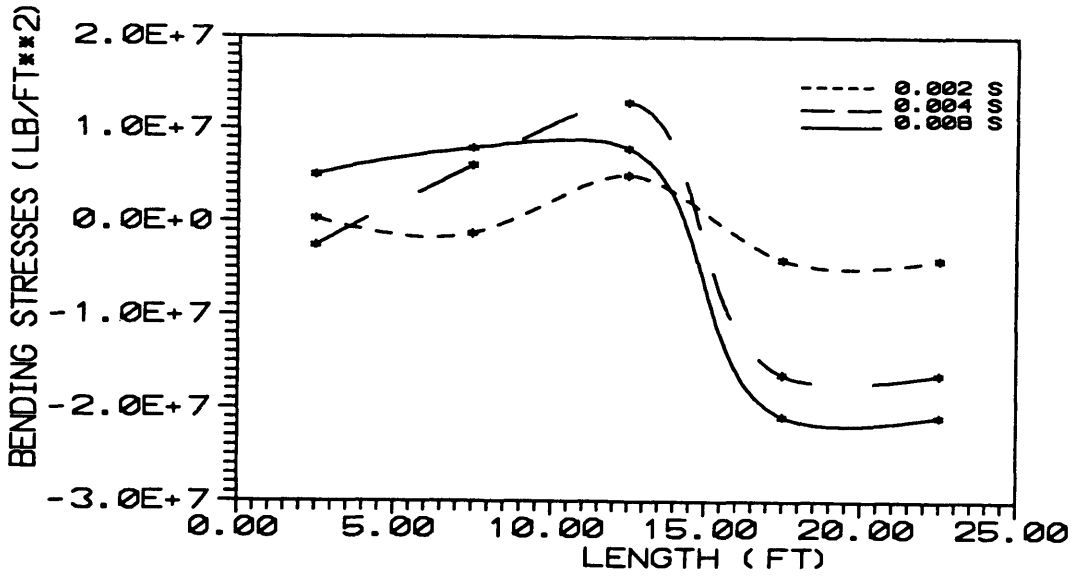

Figure 24 Bending Stresses Due to Impulse Loading Impact (Span Length =45 ft)

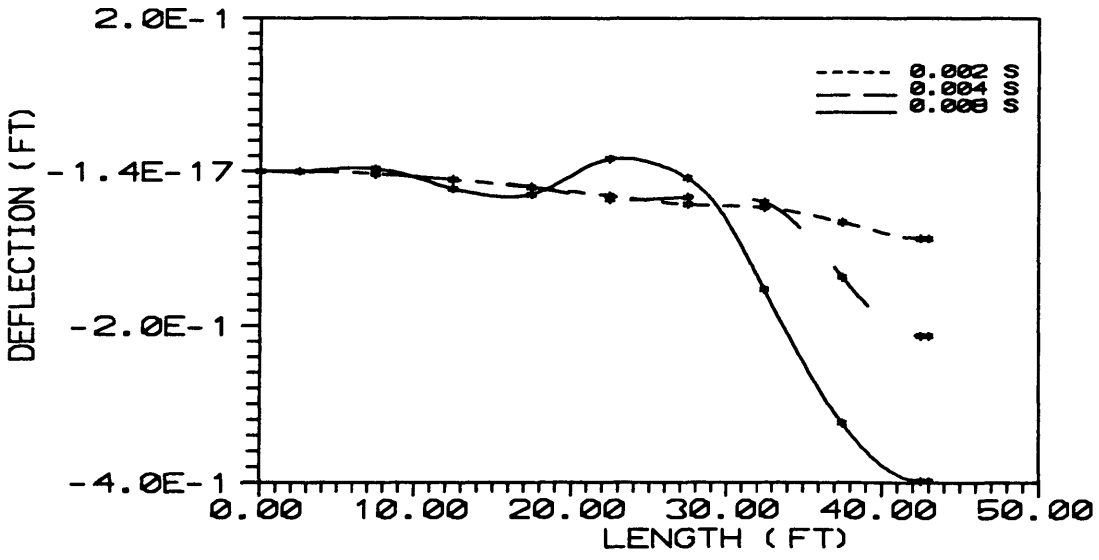

Figure 25 Pipeline Deflection Due to Impulse Loading Impact (Span Length =90 ft)

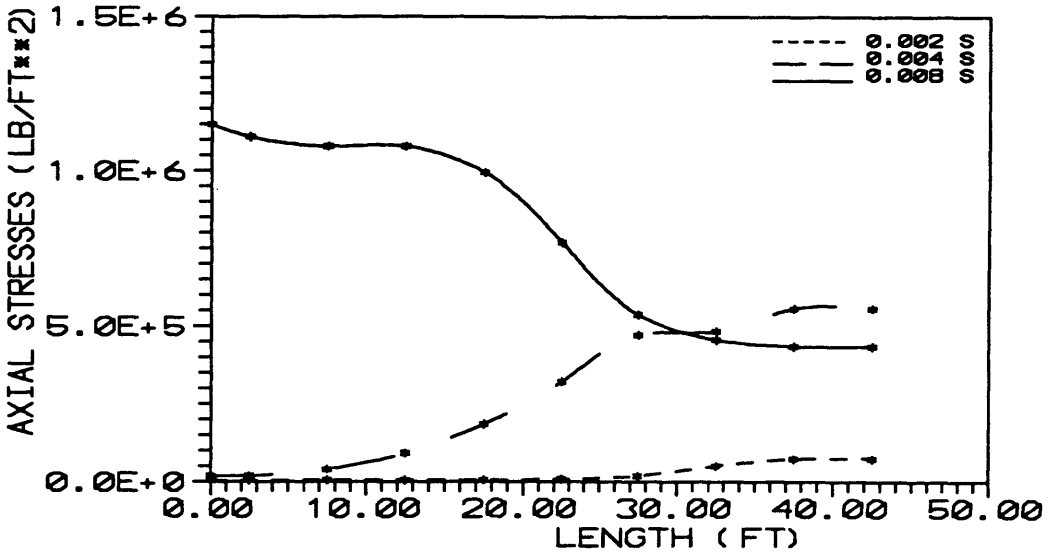

Figure 26 Axial Stresses Due to Impulse Loading Impact (Span Length =90 ft)

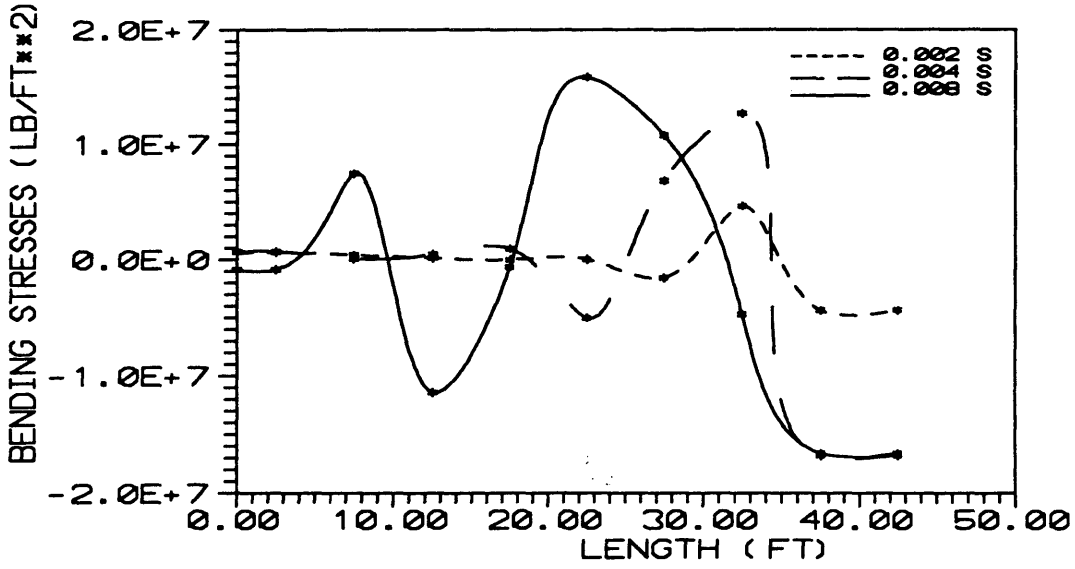

Figure 27 Bending Stresses Due to Impulse Loading Impact (Span Length =90 ft)

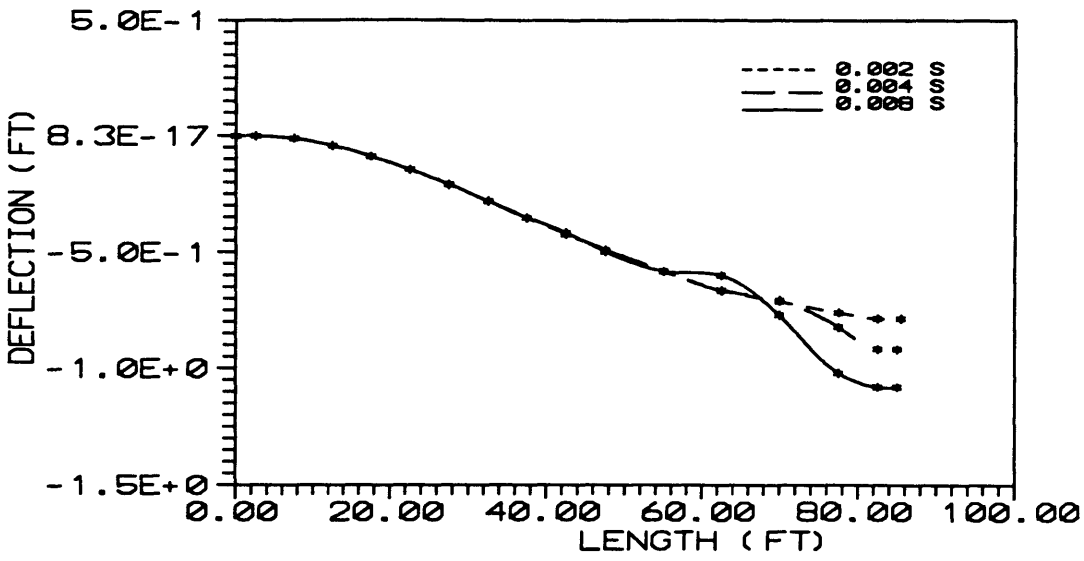

Figure 28 Pipeline Deflection Due to Impulse Loading Impact (Span Length =160 ft)

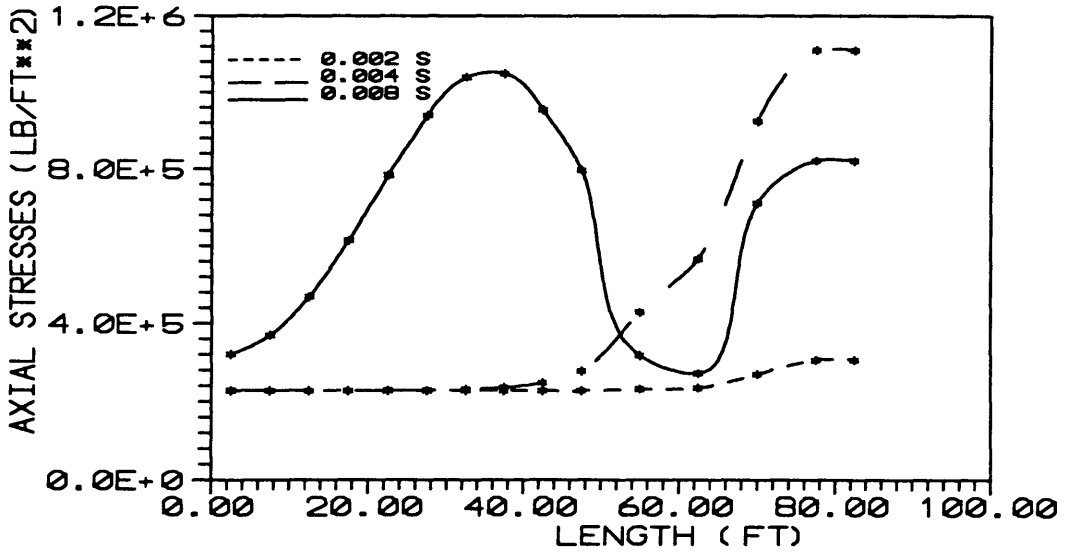

Figure 29 Axial Stresses Due to Impulse Loading Impact (Span Length =160 ft)

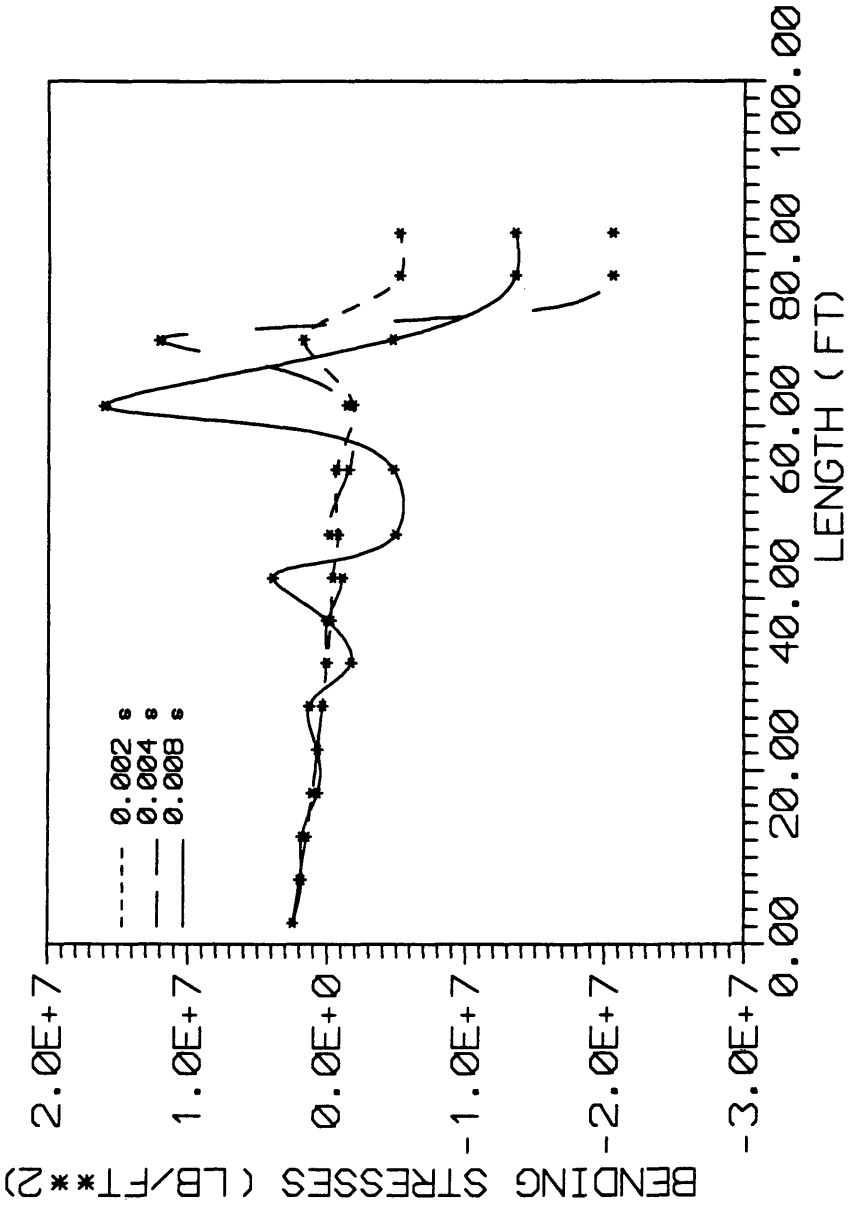

Figure 30 Bending Stresses Due to Impulse Loading Impact (Span Length =160 ft)

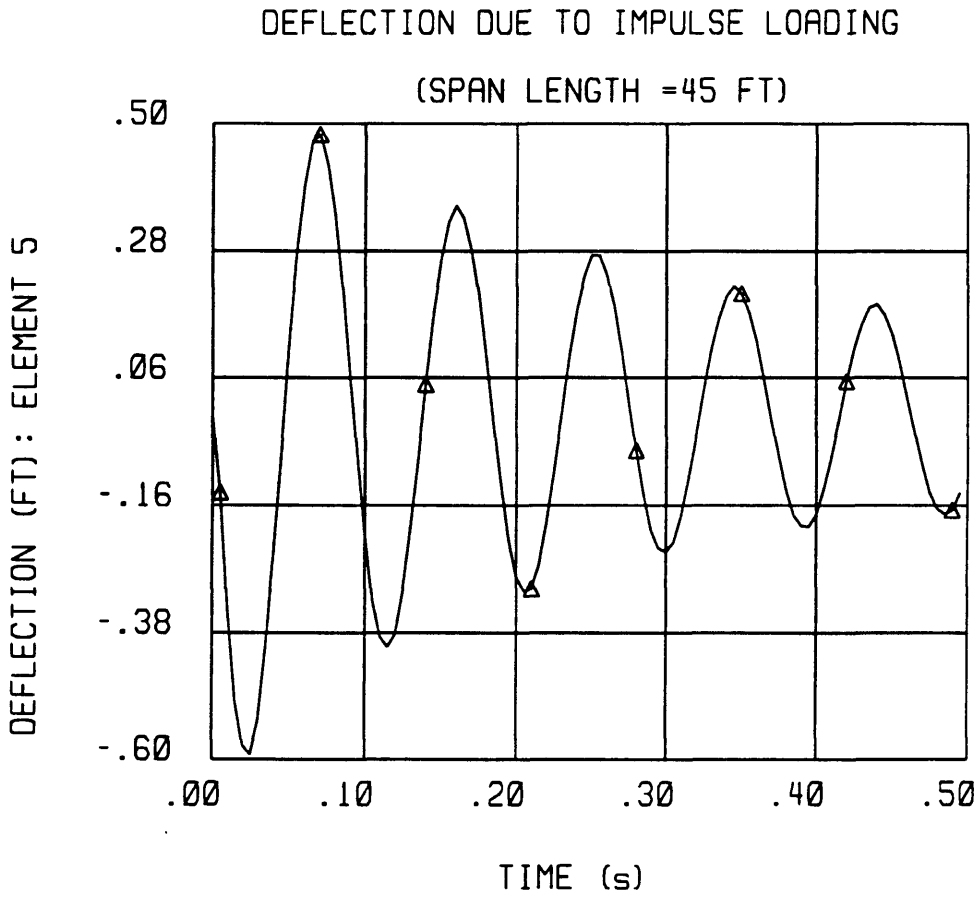

Figure 31 Time History of Pipeline Deflection Due to Impulse Loading Impact(Span Length =45 ft)

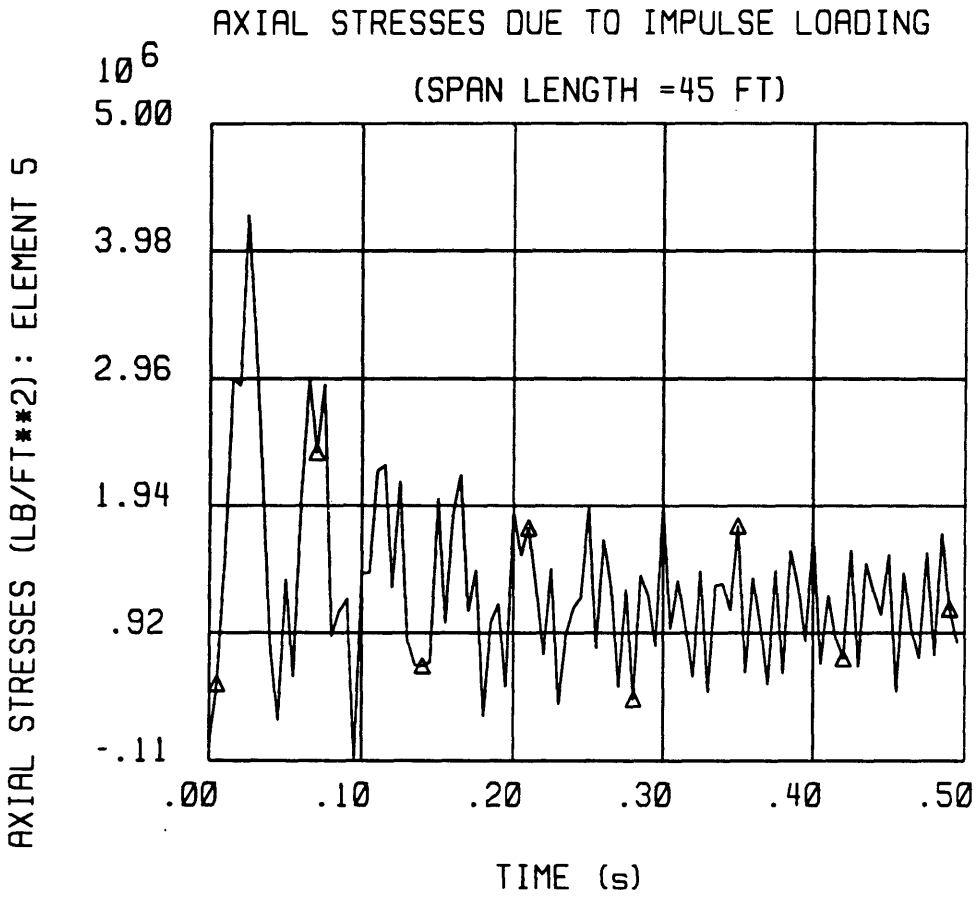

Figure 32 Time History of Axial Stresses Due to Impulse Loading Impact (Span Length =45 ft)

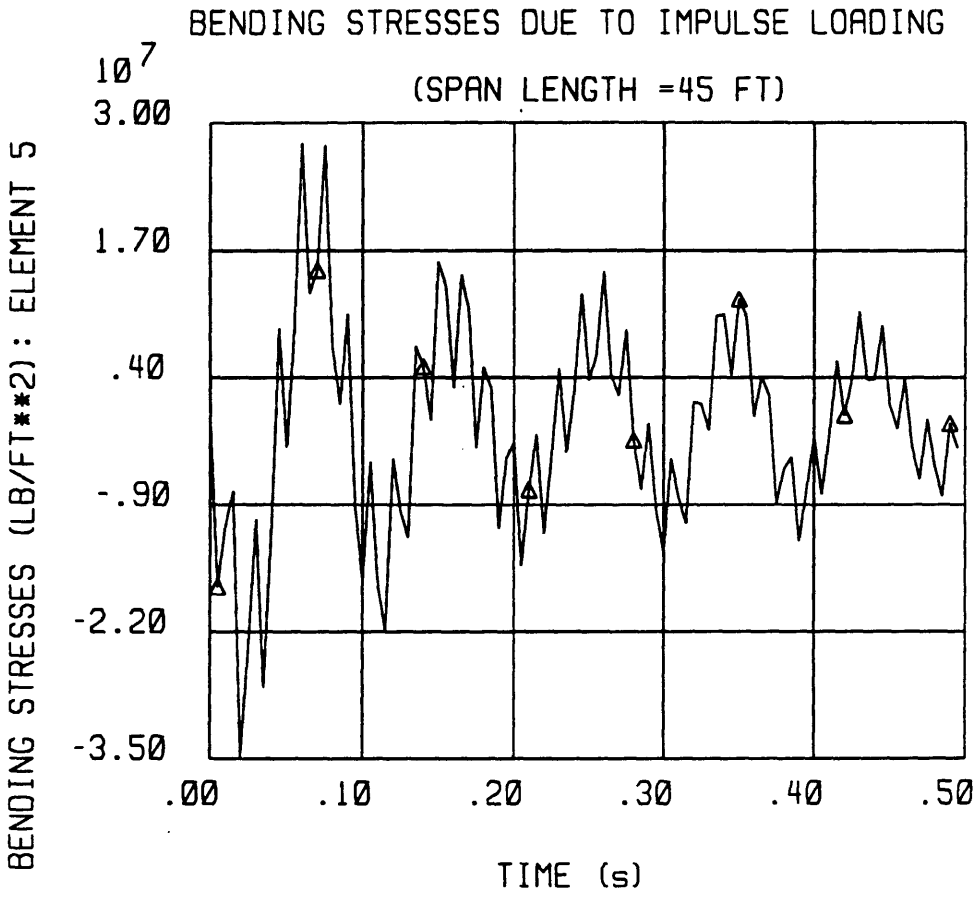

Figure 33 Time History of Bending Stresses Due to Impulse Loading Impact (Span Length =45 ft)

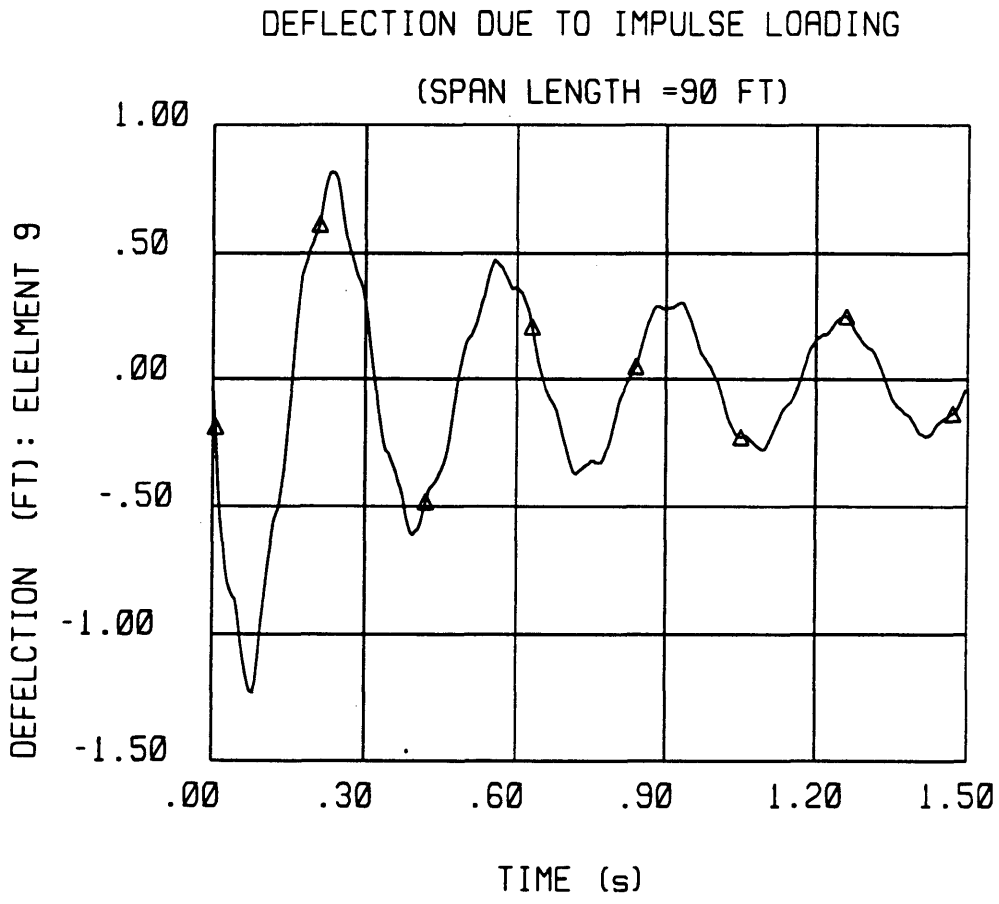

Figure 34 Time History of Pipeline Deflection Due to Impulse Loading Impact(Span Length =90 ft)

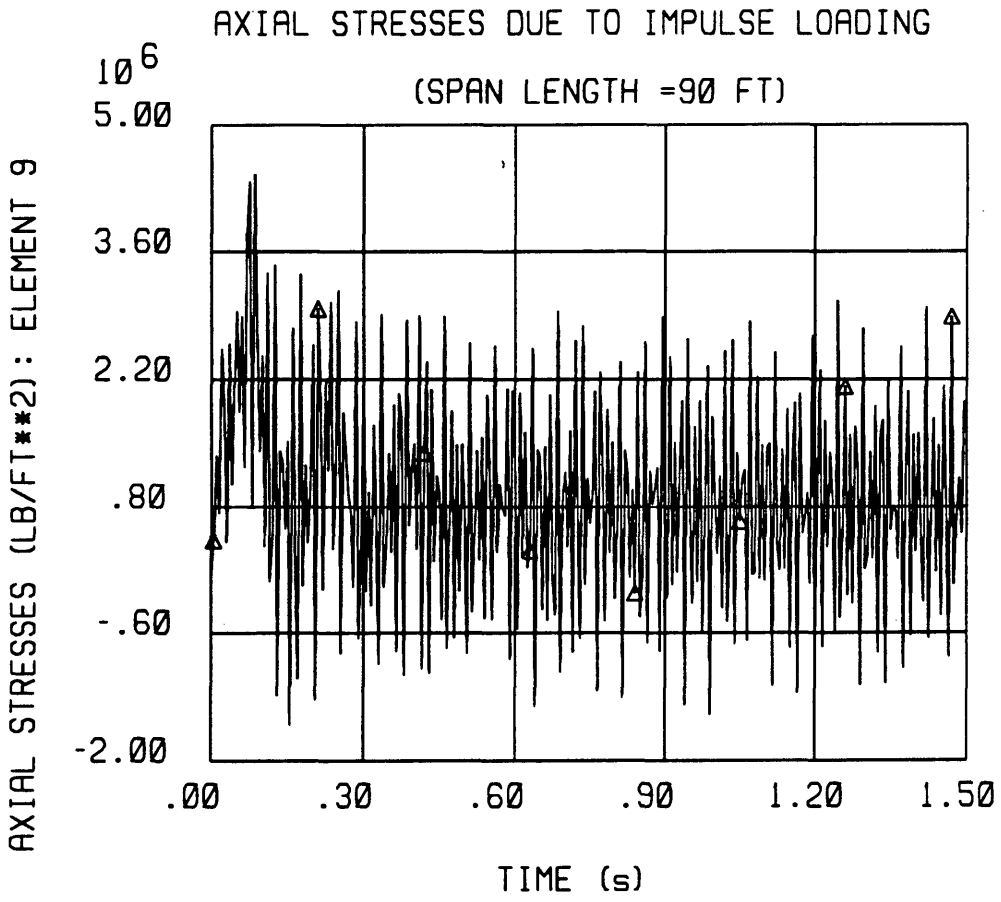

Figure 35 Time History of Axial Stresses Due to Impulse Loading Impact (Span Length =90 ft)

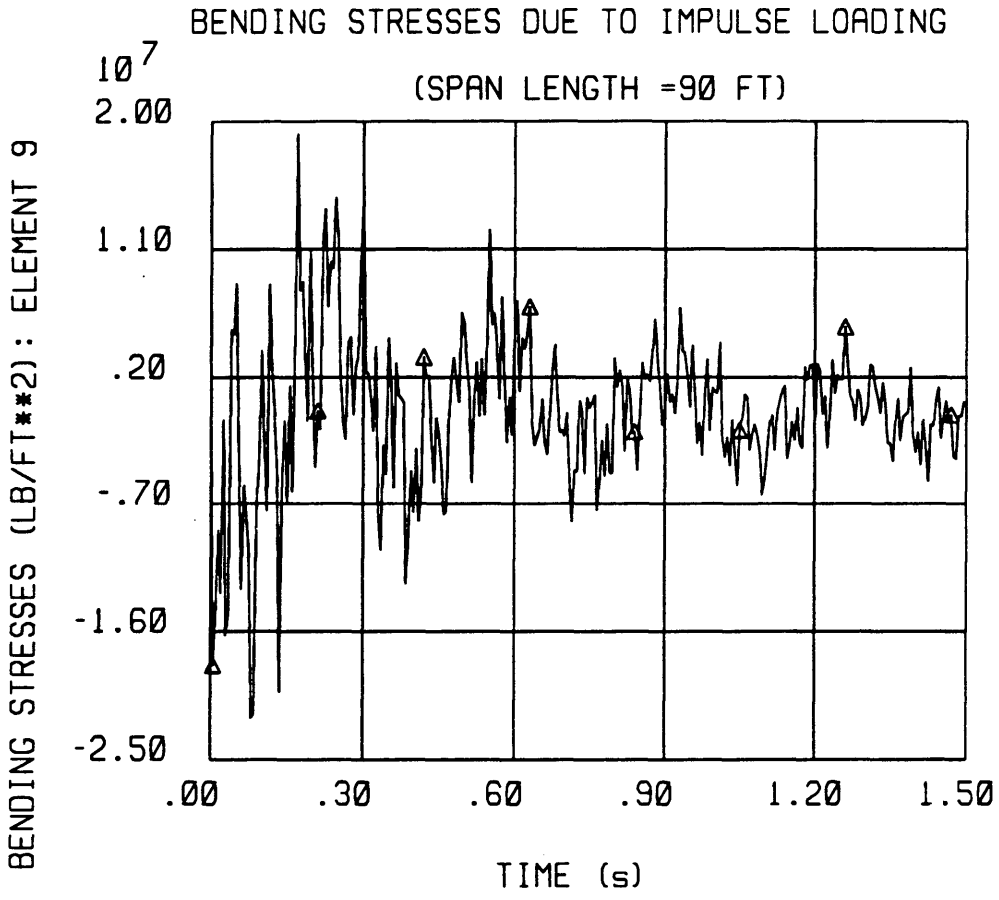

Figure 36 Time History of Bending Stresses Due to Impulse Loading Impact (Span Length =90 ft)

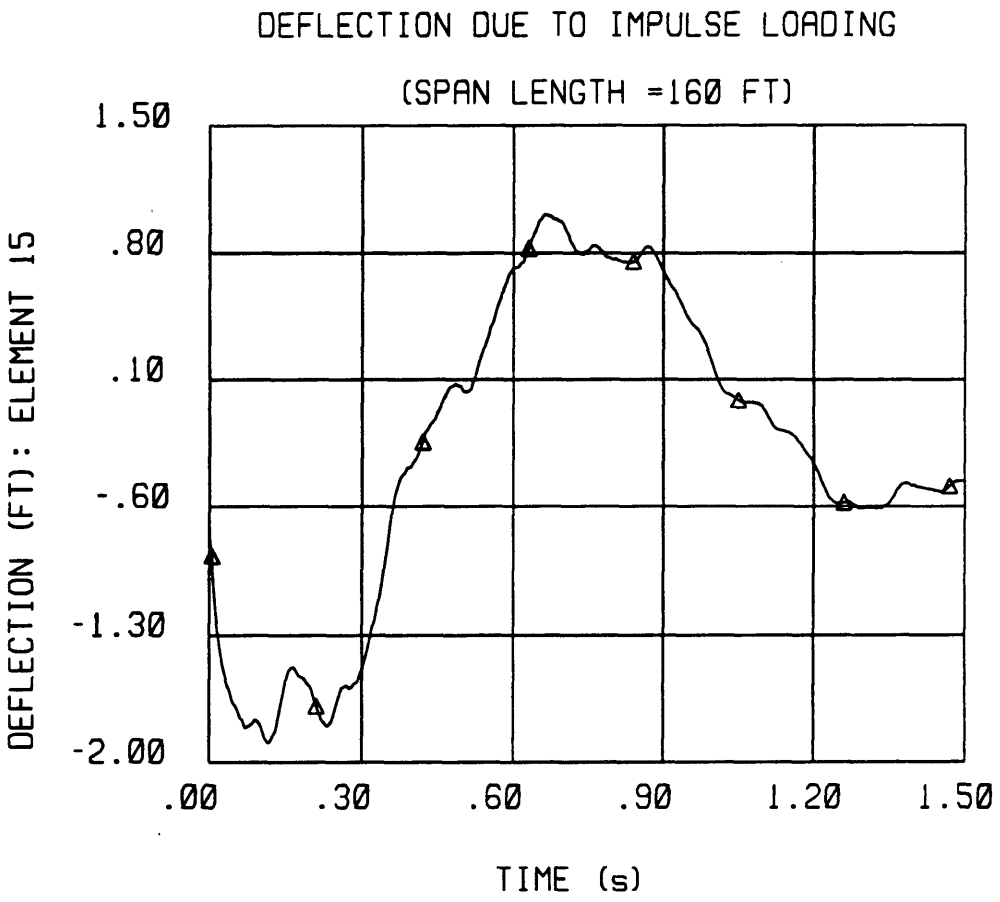

Figure 37 Time History of Pipeline Deflection Due to Impulse Loading Impact(Span Length =160 ft)

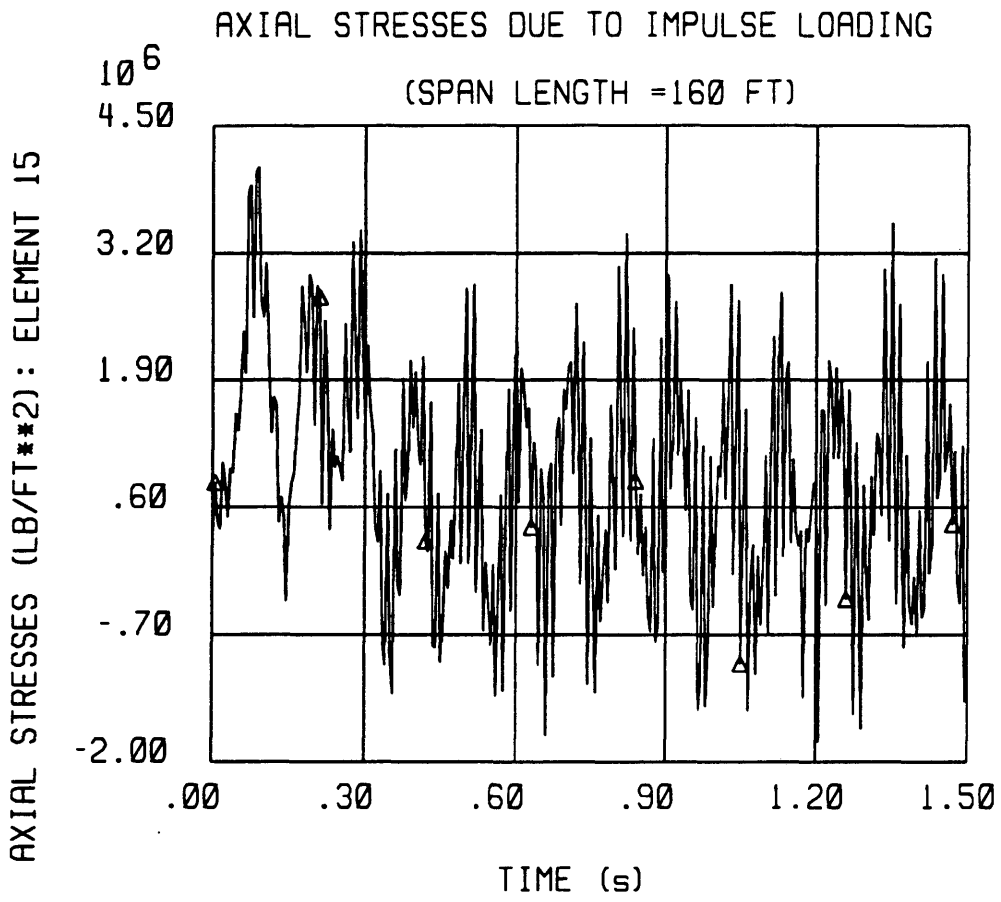

Figure 38 Time History of Axial Stresses Due to Impulse Loading Impact (Span Length =160 ft)

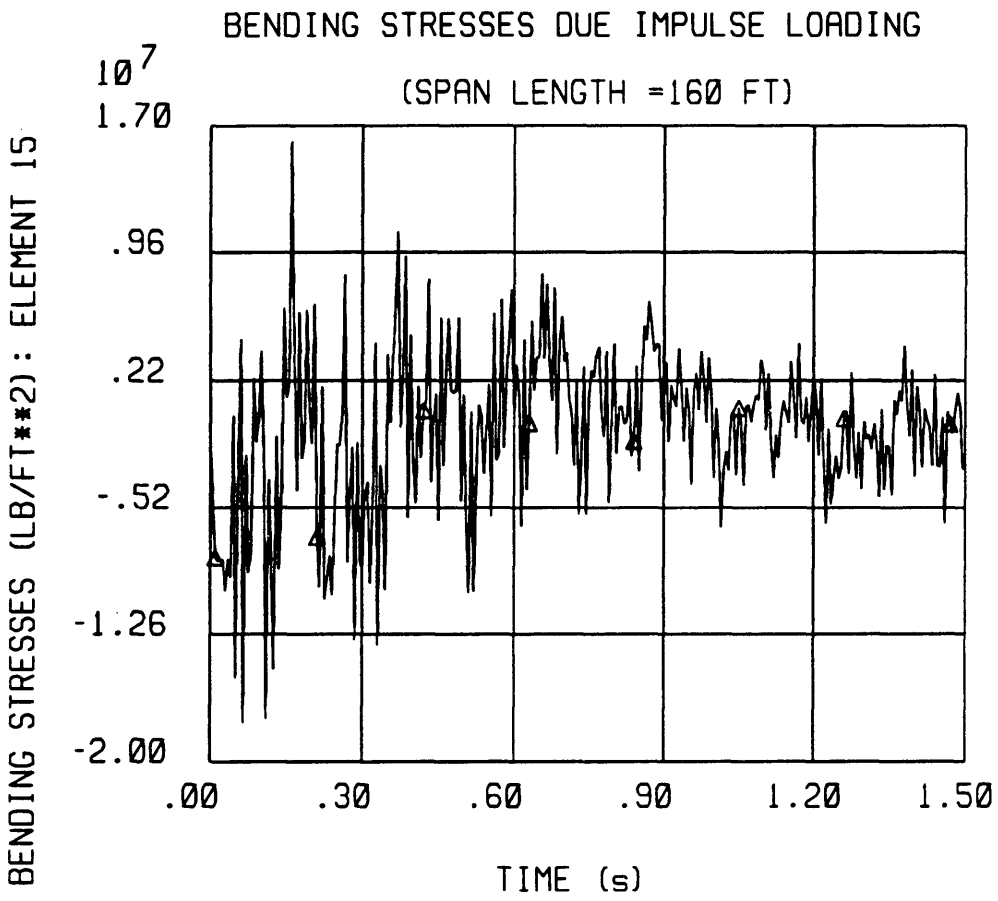

Figure 39 Time History of Bending Stresses Due to Impulse Loading Impact (Span Length =160 ft)

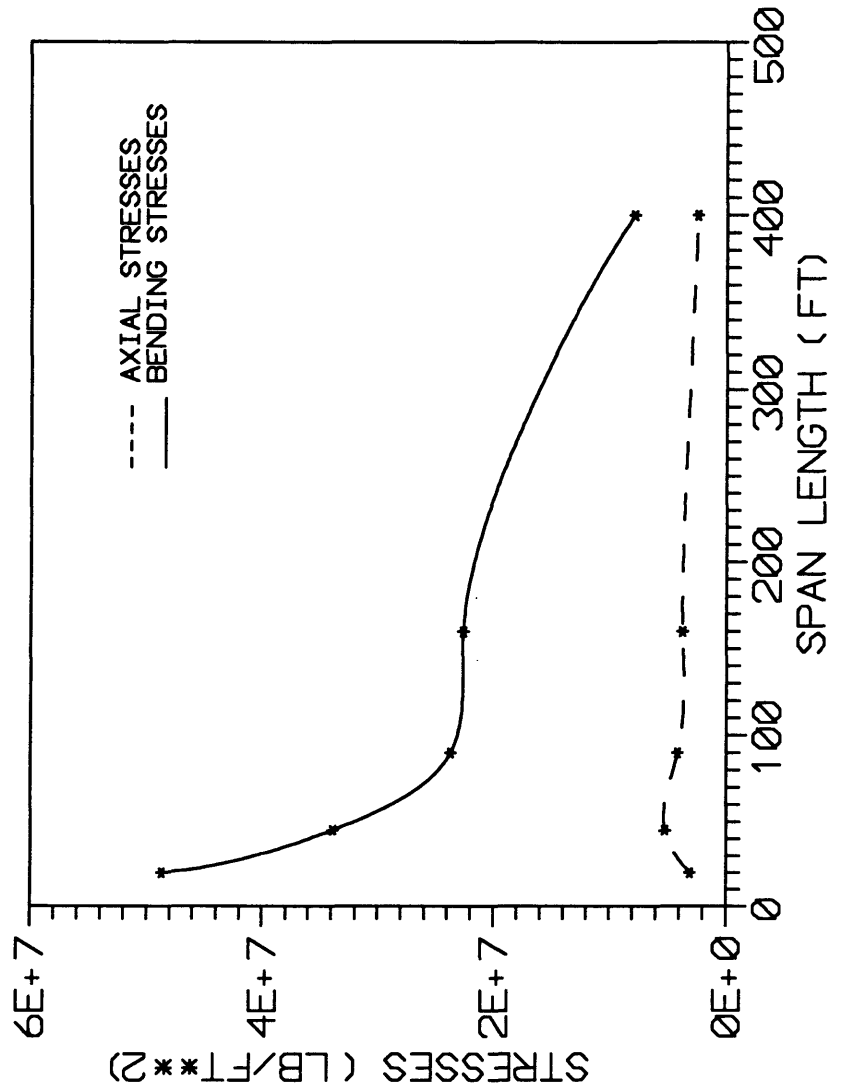

Figure 40 Maximum Stresses Versus spans length Due to Impulse Loading Impact

5.4.2 Ramp Loading:

A ramp loading function with the maximum load of 3.0×10^6 lb (Fig. 4) is applied at mid span. The load is increased linearly with a duration of 0.002 s, and then is kept constant, simulating the anchor sitting on the pipe span. As soon as the anchor hit the pipeline, it starts to vibrate for a short period of time, then the vibration decays due to hydrodynamic damping and anchor mass.

After 1 s the vibration amplitude was reduced by approximately 96 %. The resulting deflection and stresses are shown in Figs. 41-49 for the three span lengths. A time history of displacements, axial and bending stresses for the central element (element no. 5 for span length 45 ft, element 9 for span length 90 ft and element 15 for span length 160 ft), are shown in Figs. 50-58. A comparison between the maximum stresses for the three spans is shown in Fig. 59; it indicates that the bending stress increases as the span length decrease.

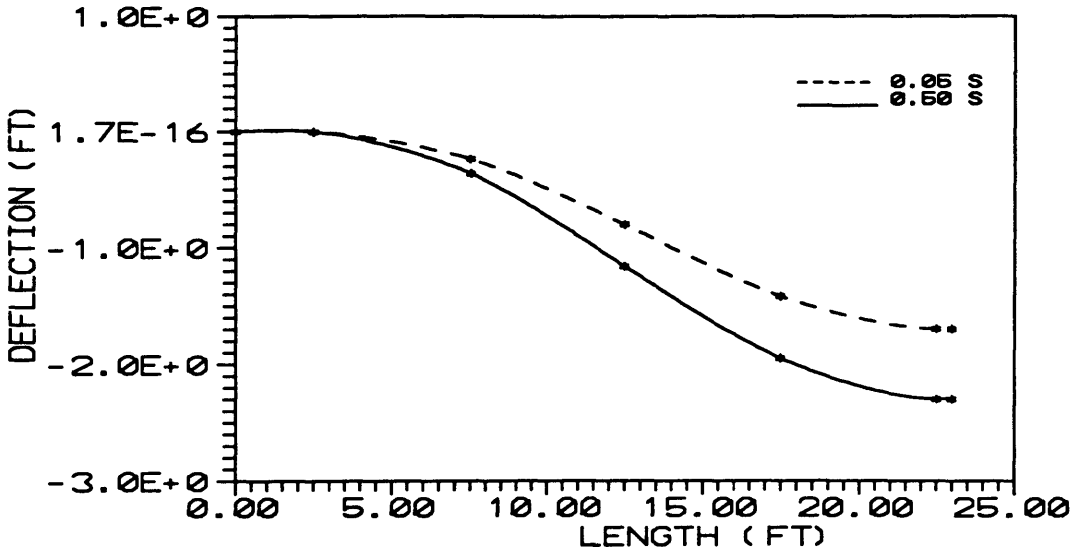

Figure 41 Pipeline Deflection Due to Ramp Loading Impact (Span Length =45 ft)

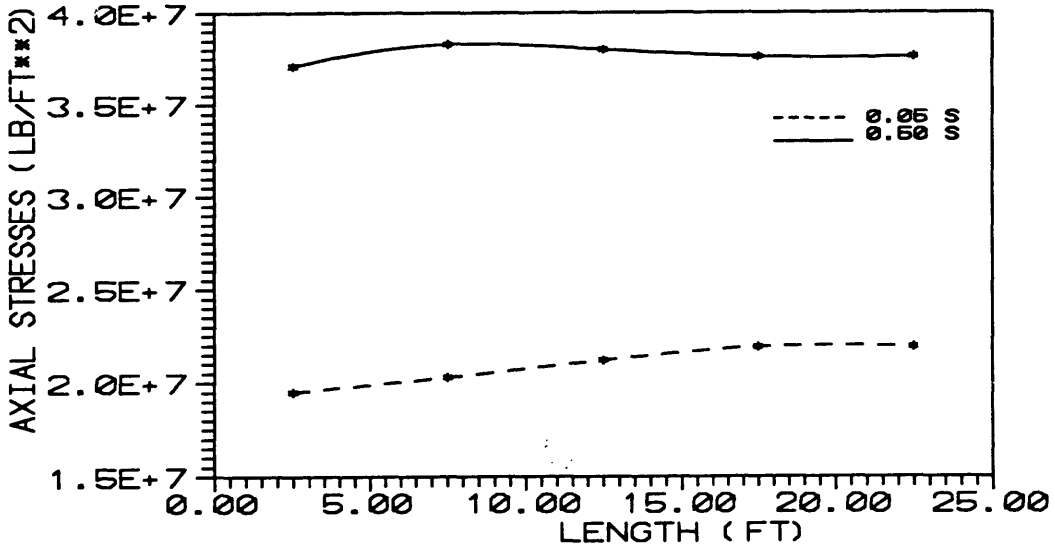

Figure 42 Axial Stresses Due to Ramp Loading Impact (Span Length =45 ft)

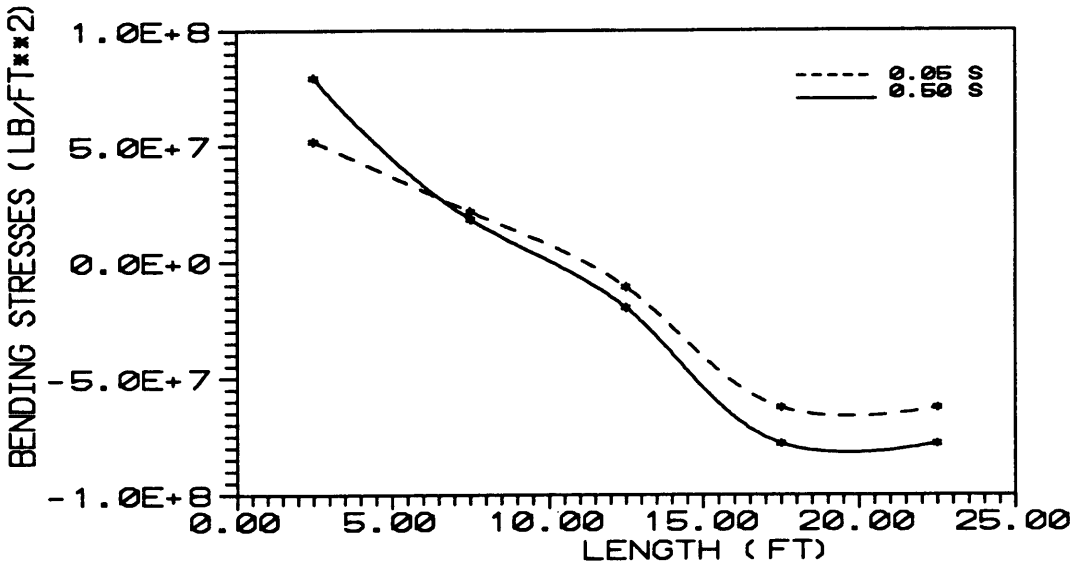

Figure 43 Bending Stresses Due to Ramp Loading Impact (Span Length =45 ft)

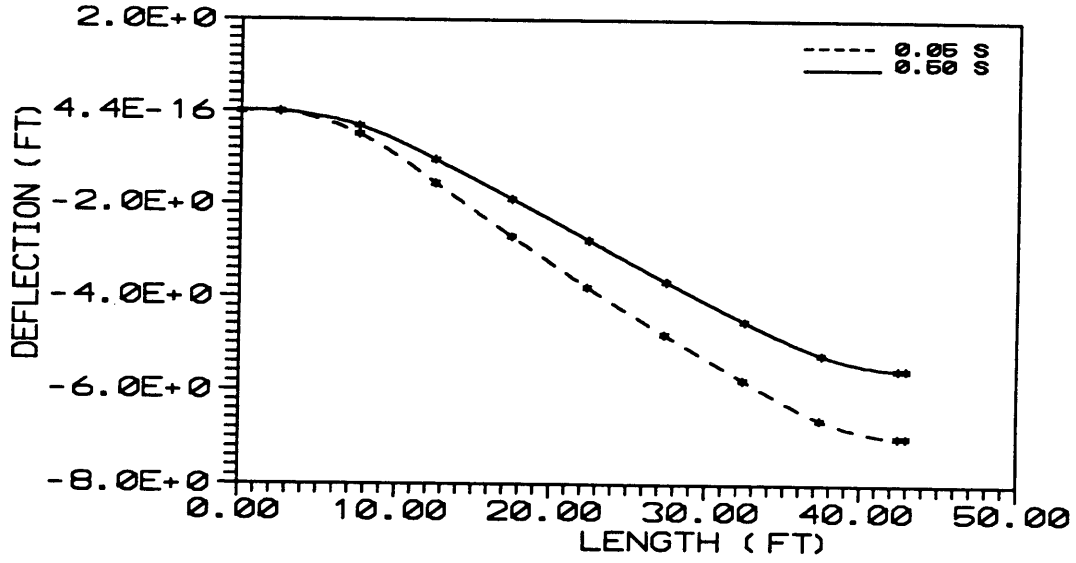

Figure 44 Pipeline Deflection Due to Ramp Loading Impact (Span Length =90 ft)

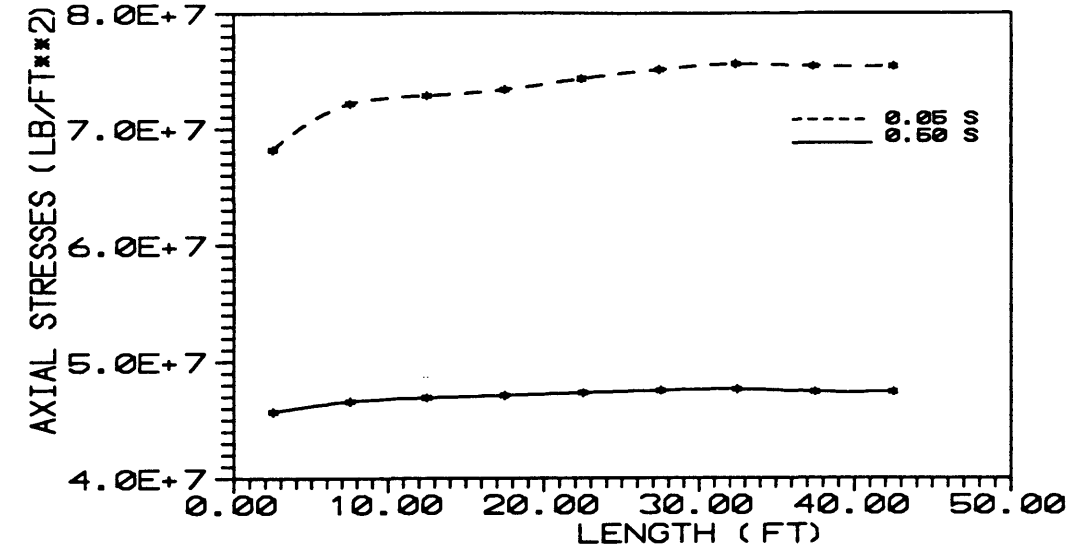

Figure 45 Axial Stresses Due to Ramp Loading Impact (Span Length =90 ft)

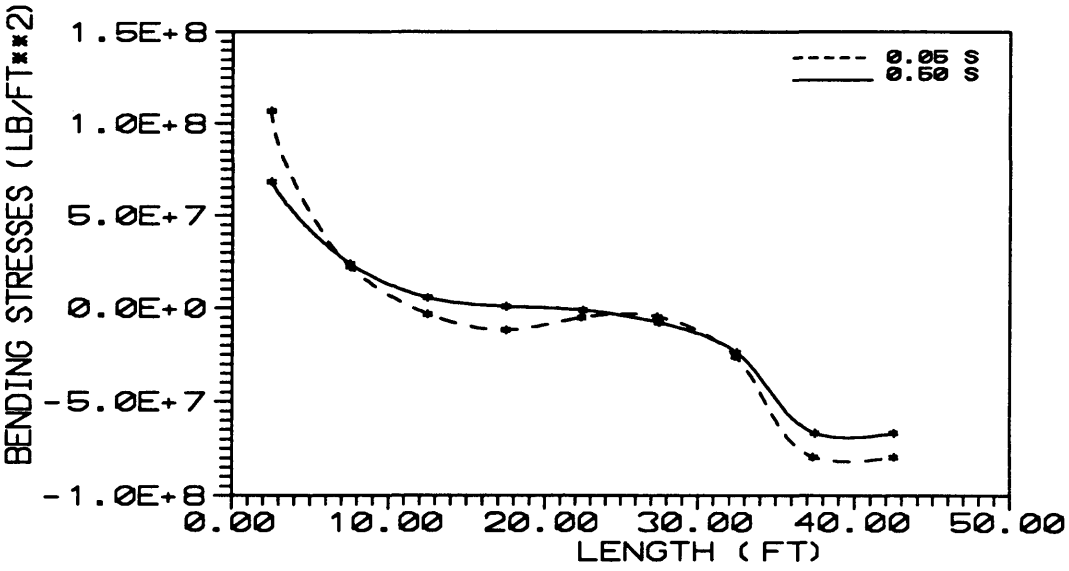

Figure 46 Bending Stresses Due to Ramp Loading Impact (Span Length =90 ft)

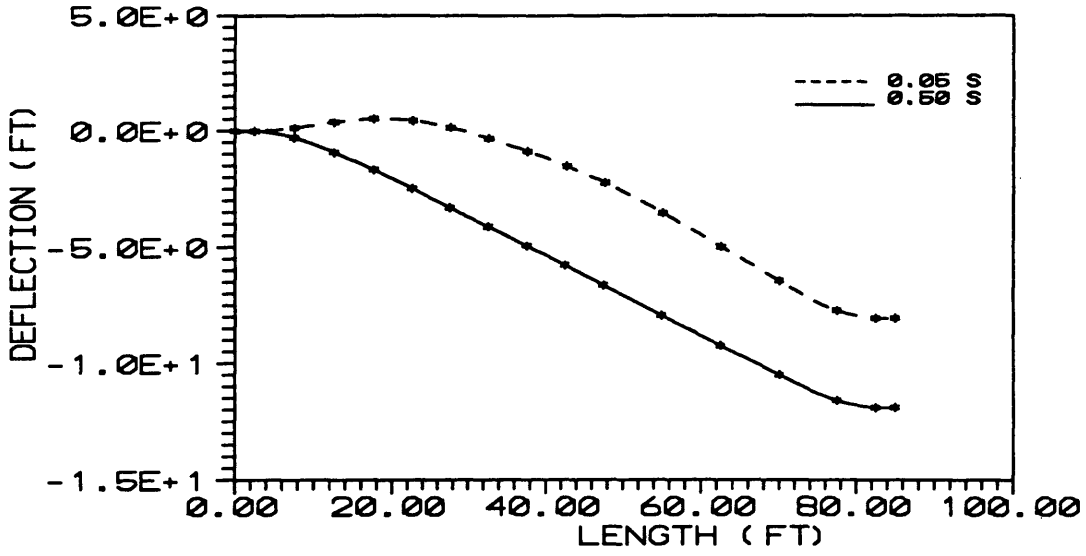

Figure 47 Pipeline Deflection Due to Ramp Loading Impact (Span Length =160 ft)

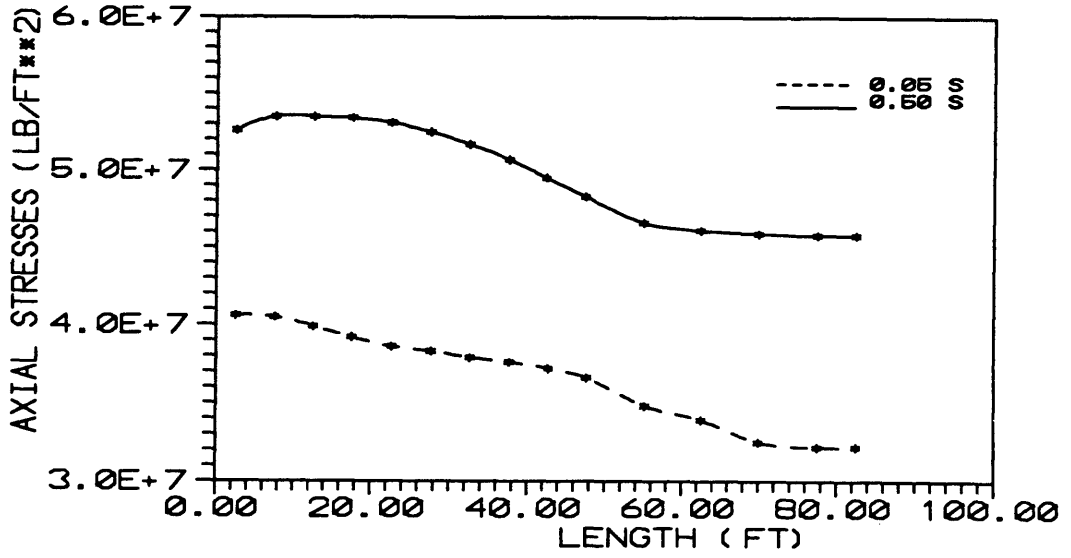

Figure 48 Axial Stresses Due to Ramp Loading Impact (Span Length =160 ft)

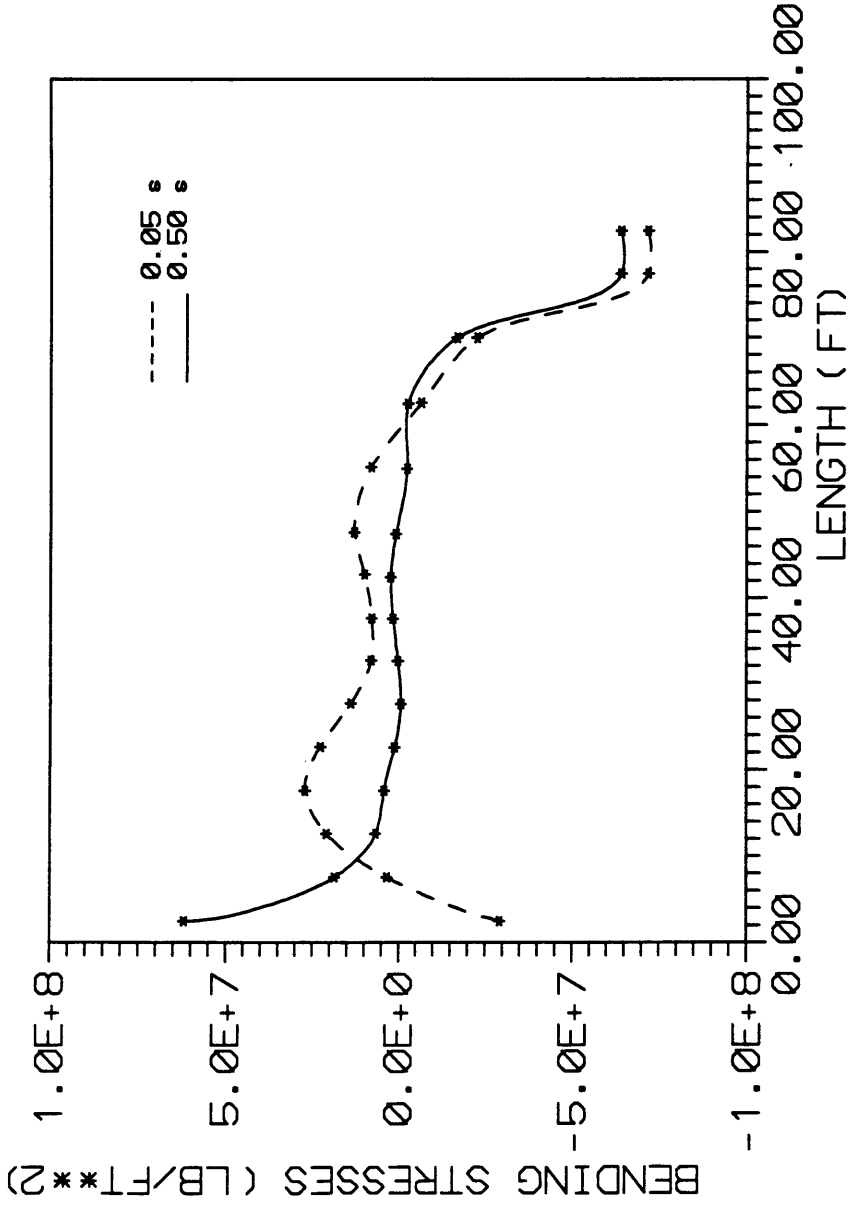

Figure 49 Bending Stresses Due to Ramp Loading Impact (Span Length =160 ft)

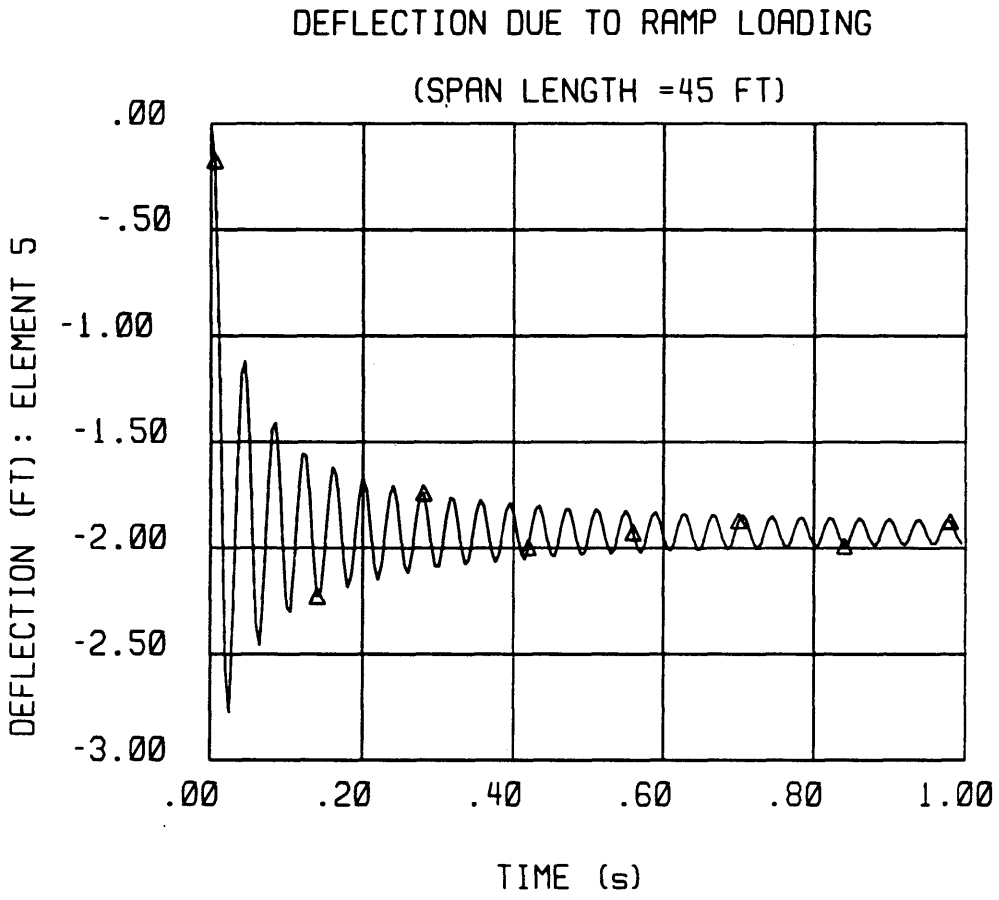

Figure 50 Time History of Pipeline Deflection Due to Ramp Loading Impact (Span Length =45 ft)

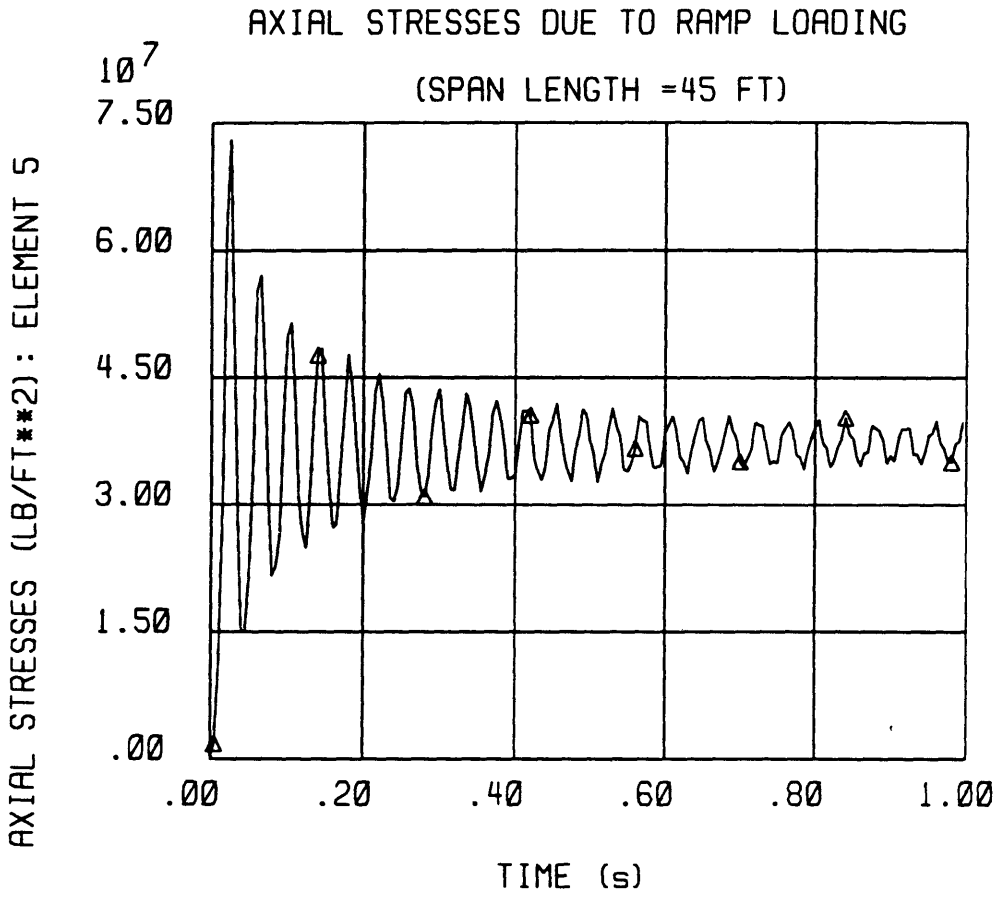

Figure 51 Time History of Axial Stresses Due to Ramp Loading Impact (Span Length =45 ft)

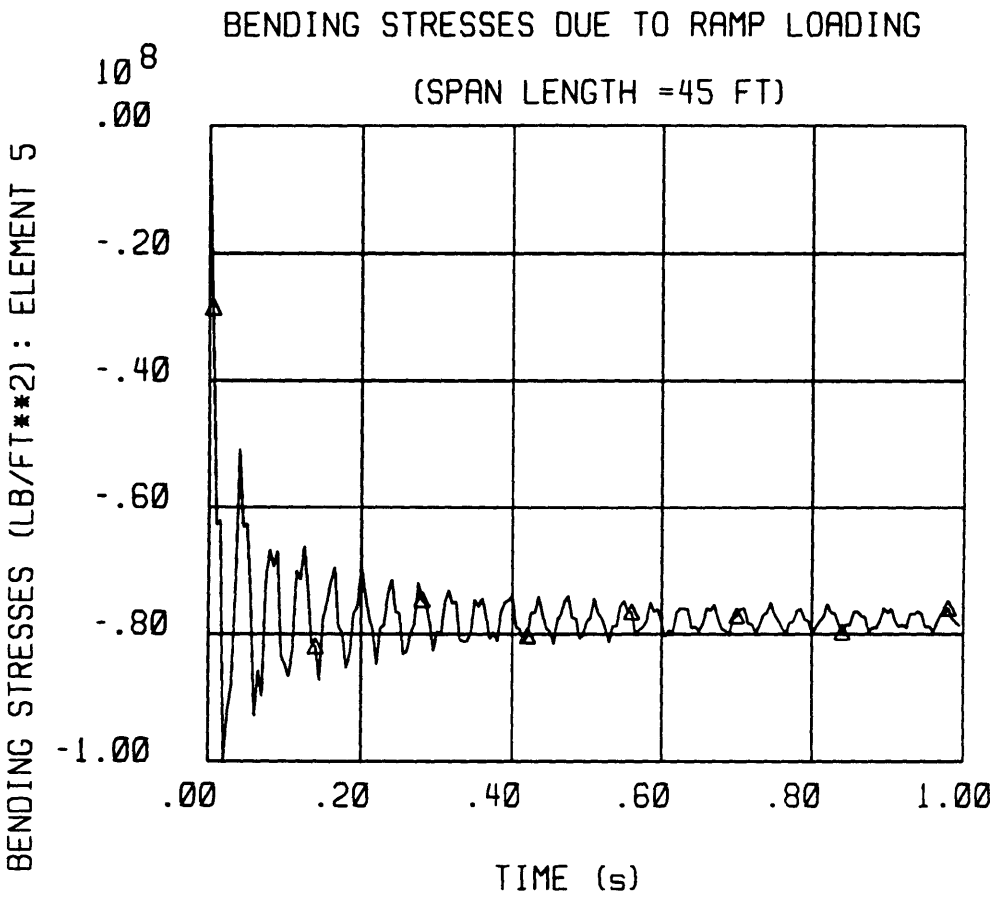

Figure 52 Time History of Bending Stresses Due to Ramp Loading Impact (Span Length =45 ft)

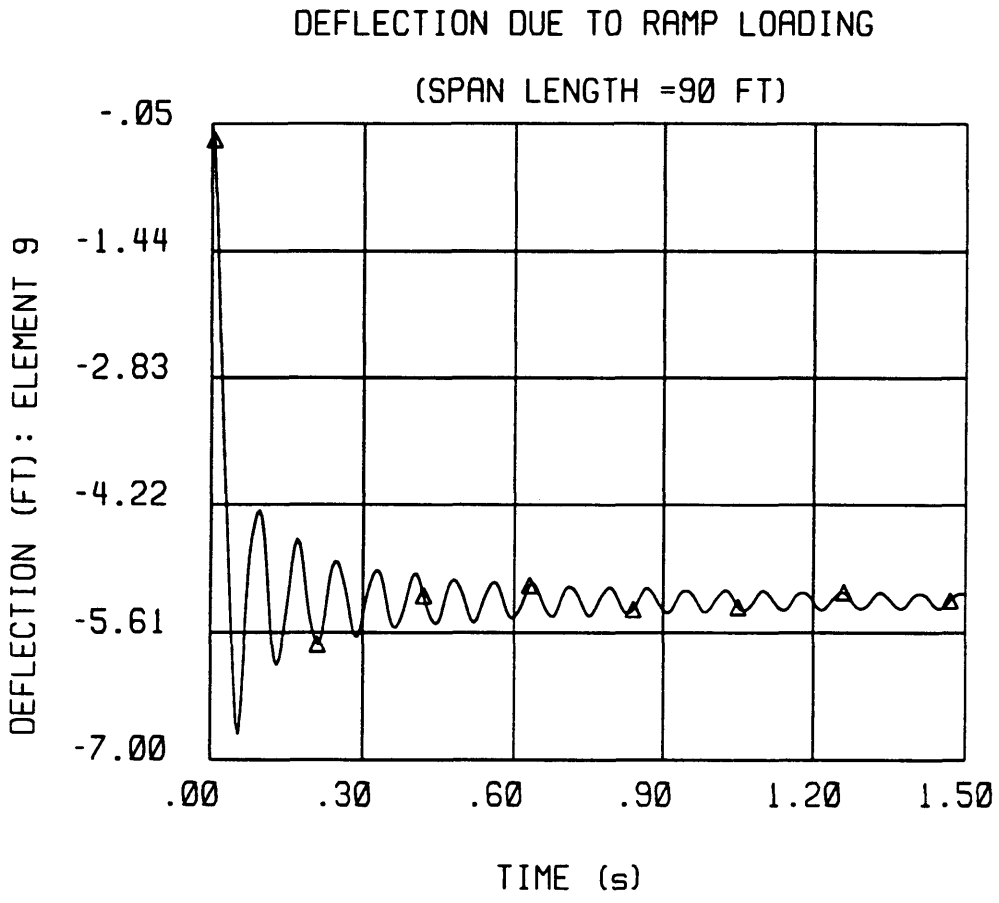

Figure 53 Time History of Pipeline Deflection Due to Ramp Loading Impact(Span Length =90 ft)

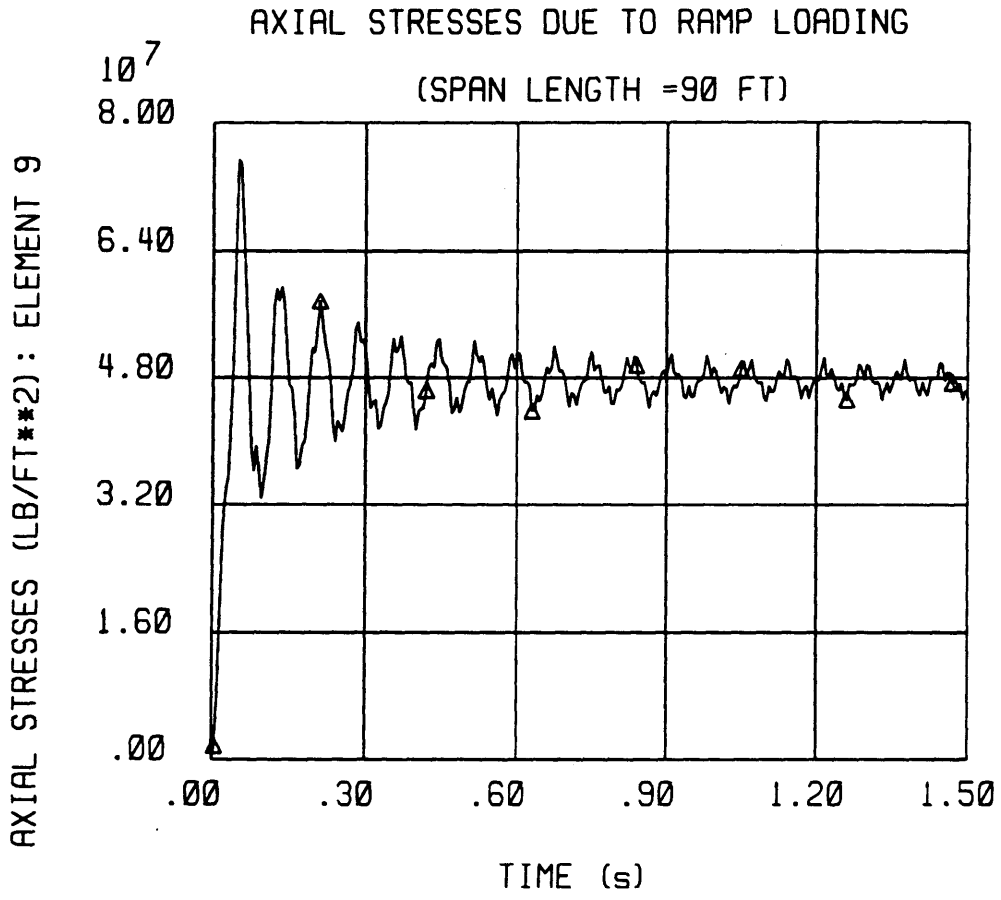

Figure 54 Time History of Axial Stresses Due to Ramp Loading Impact (Span Length =90 ft)

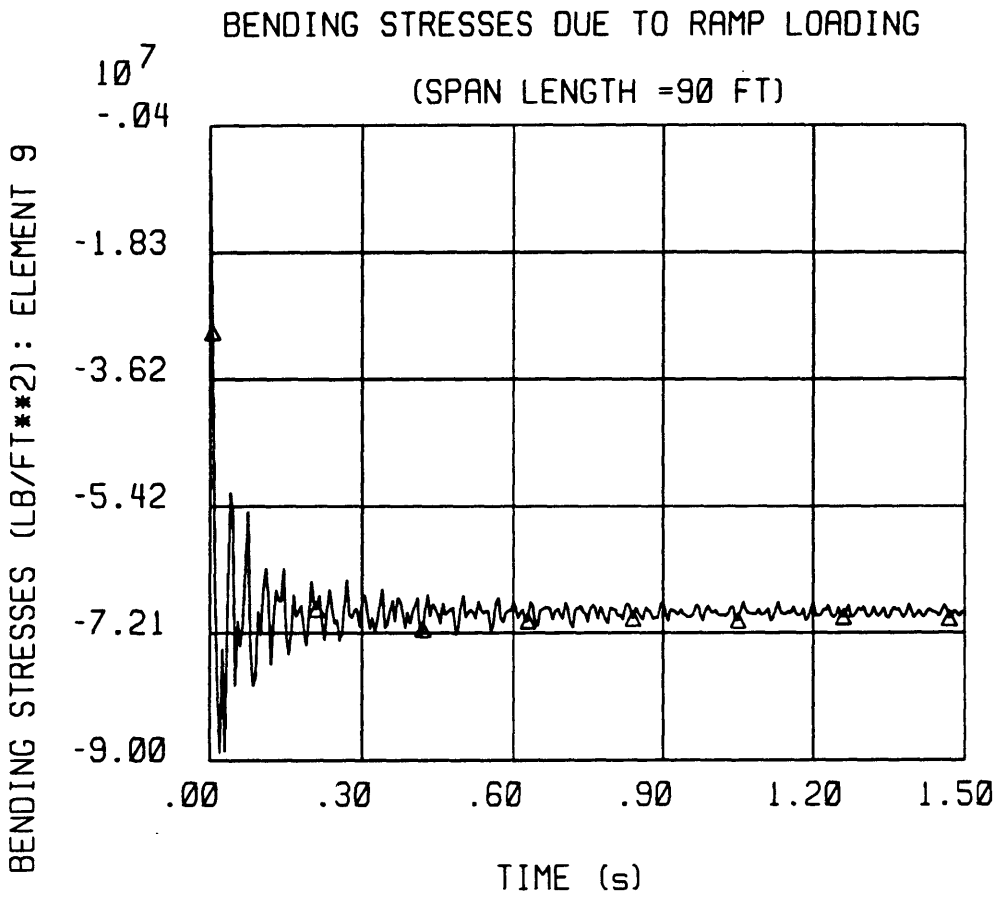

Figure 55 Time History of Bending Stresses Due to Ramp Loading Impact (Span Length =90 ft)

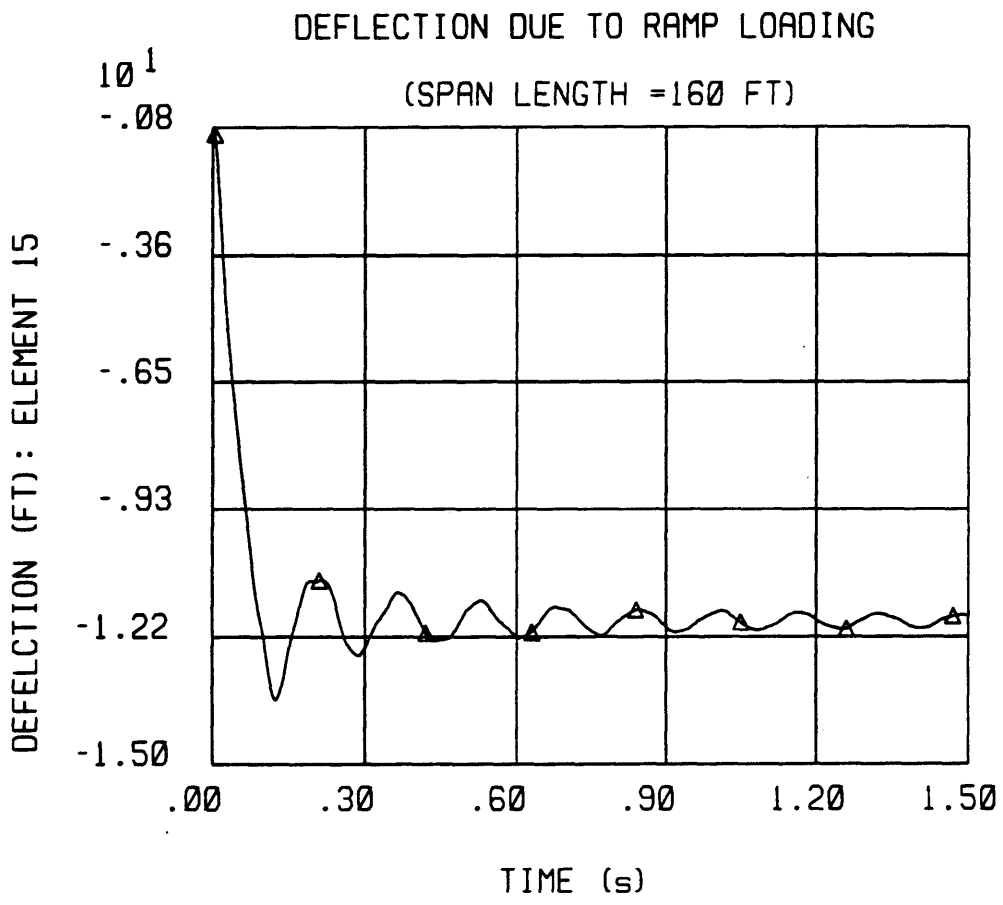

Figure 56 Time History of Pipeline Deflection Due to Ramp Loading Impact(Span Length =160 ft)

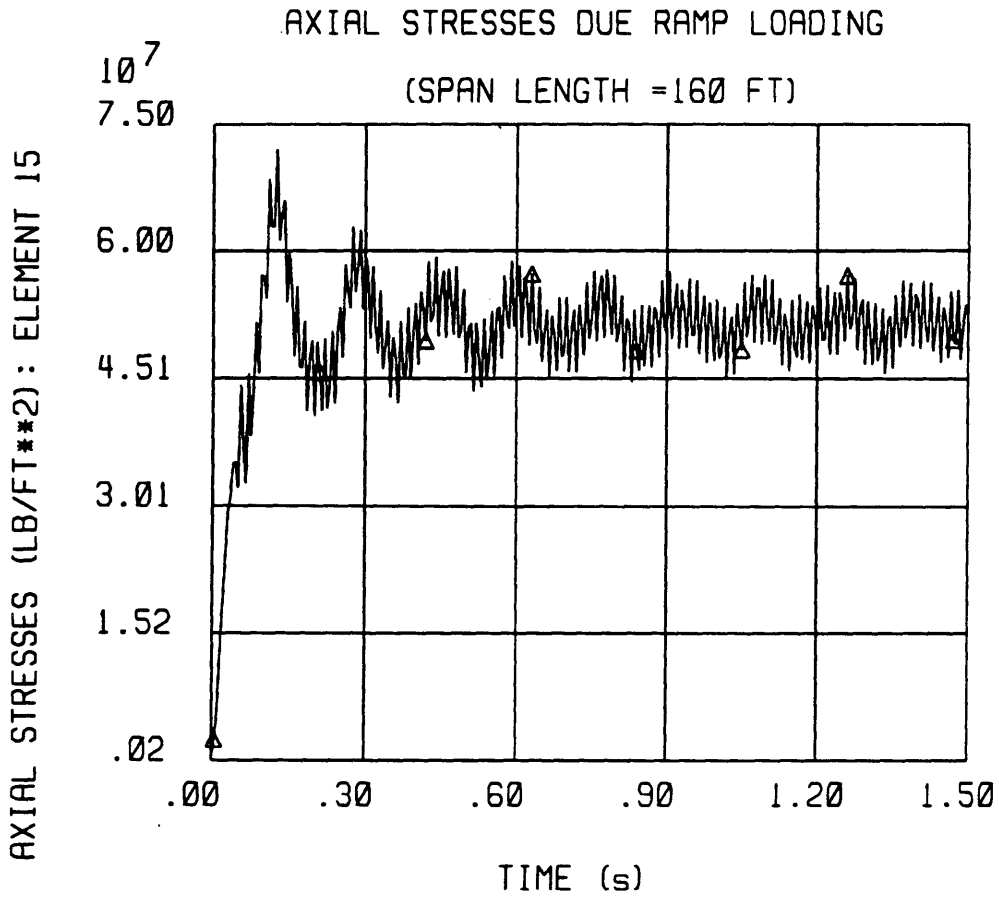

Figure 57 Time History of Axial Stresses Due to Ramp Loading Impact (Span Length =160 ft)

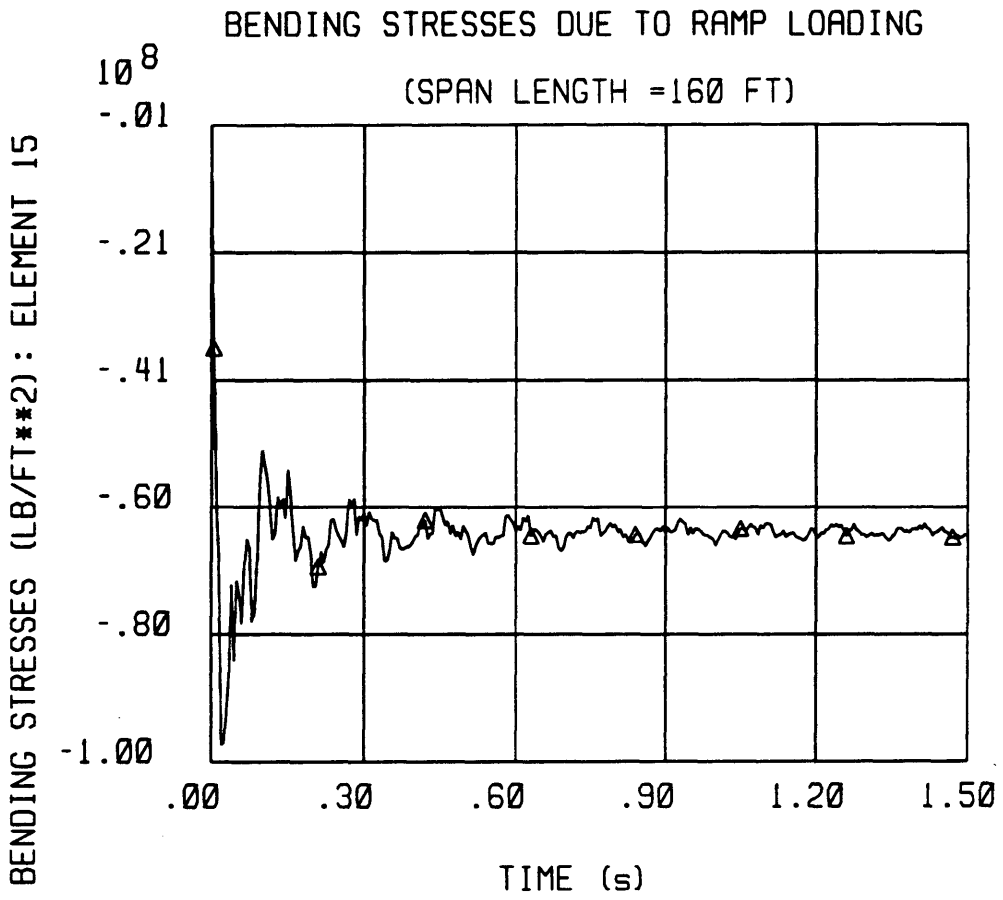

Figure 58 Time History of Bending Stresses Due to Ramp Loading Impact (Span Length =160 ft)

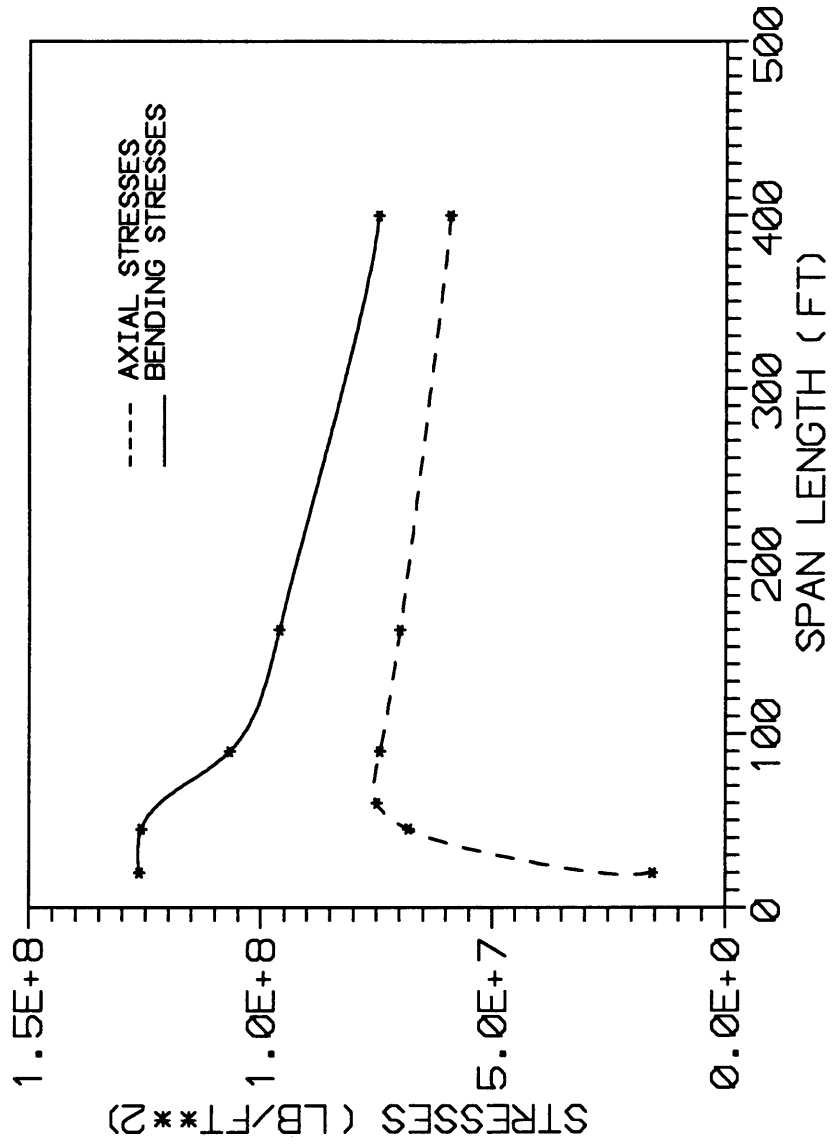

Figure 59 Maximum Stresses Versus spans length Due to Ramp Loading Impact

5.5 Anchor Hook Loading:

The anchor hook loading function with a maximum chain tension load of 3.1×10^6 lb (Fig. 6) is applied at mid span, simulating an anchor hooking to a pipeline. The applied load is due to a ship drifting caused by drag due to current and wave at a constant velocity of 1 knot, the applied load is kept constant after the anchor chain reaches its maximum length in 2 s, where it required 18 s for the chain to reach its maximum length.

The resulting pipeline displacement and stresses exerted on the three span lengths are shown in Figs. 60-68. A time history for deflection, axial and bending stresses at the mid span are shown in Figs. 69-77.

As the vessel continues to apply tension on the pipeline, the pipeline deflection, axial and bending stresses continue to build up, which could result in local pipeline buckling and plastification, if the applied tension continued to increase after 18 s.

It is noted that axial stresses increase, while the bending stresses decrease with increasing pipeline span as shown in Fig. 78.

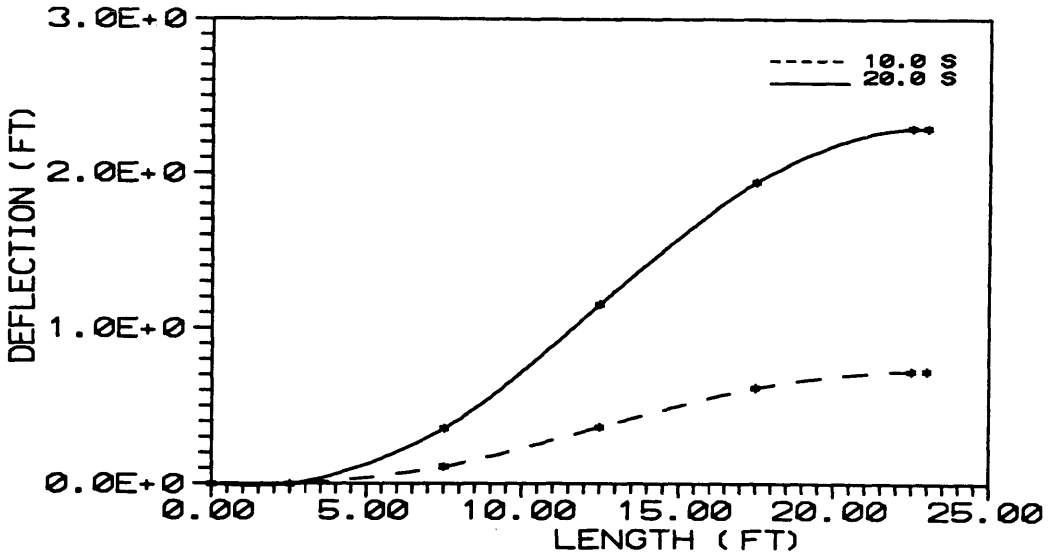

Figure 60 Pipeline Deflection Due to Hook Loading

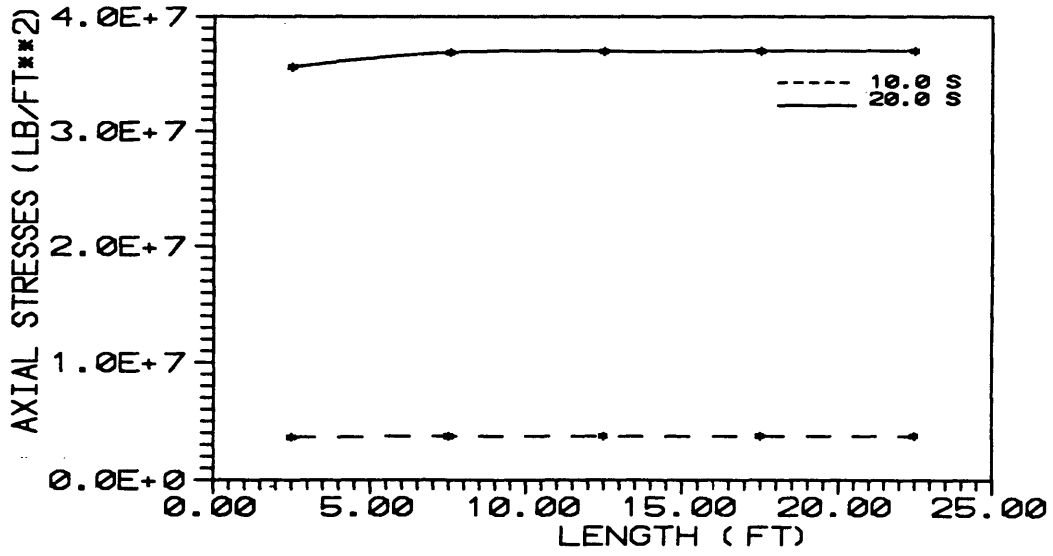

Figure 61 Axial Stresses Due to Hook Loading
(Span Length =45 ft)

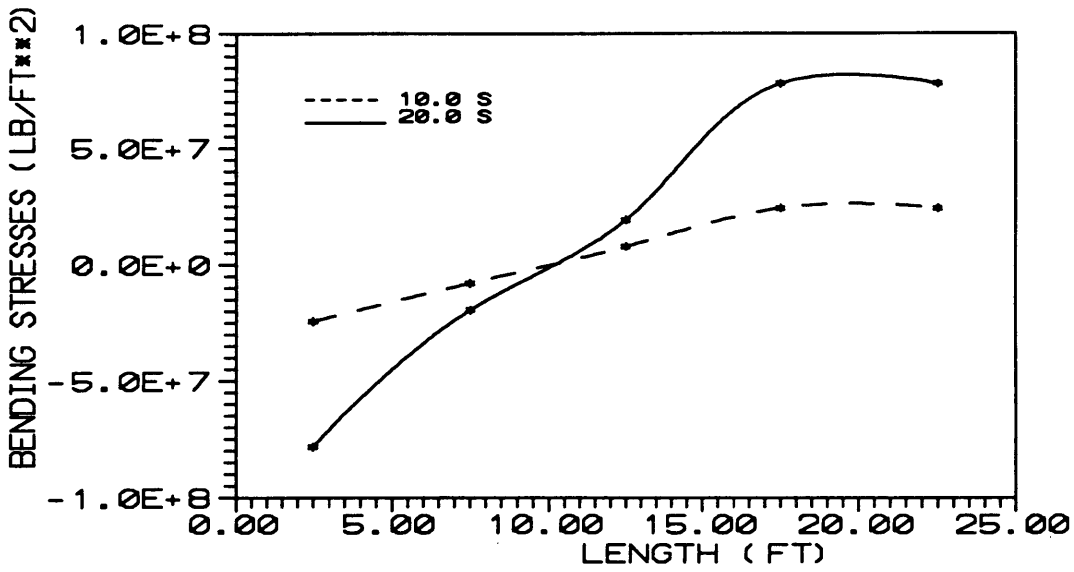

Figure 62 Bending Stresses Due to Hook Loading
(Span Length =45 ft)

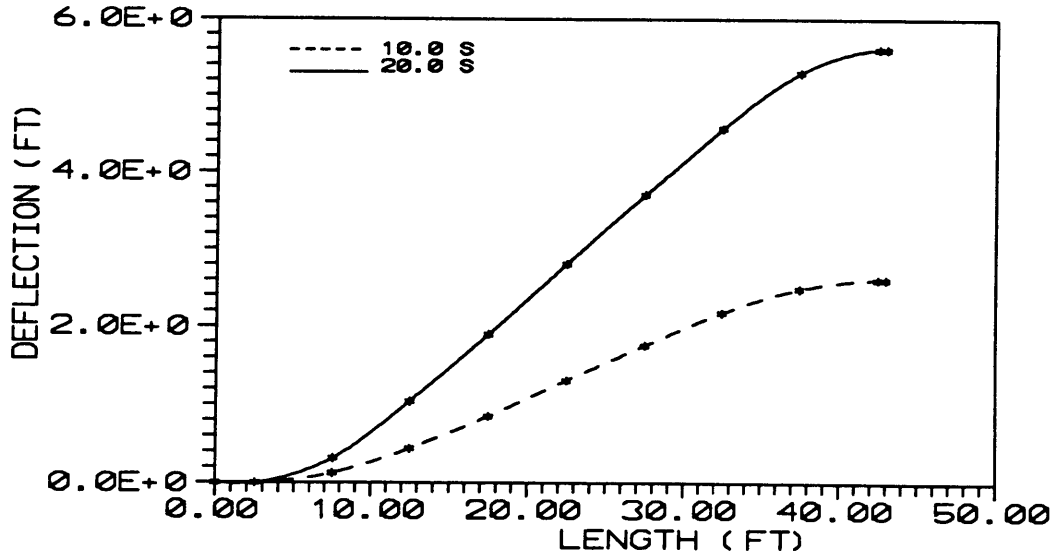

Figure 63 Pipeline Deflection Due to Hook Loading
(Span Length =90 ft)

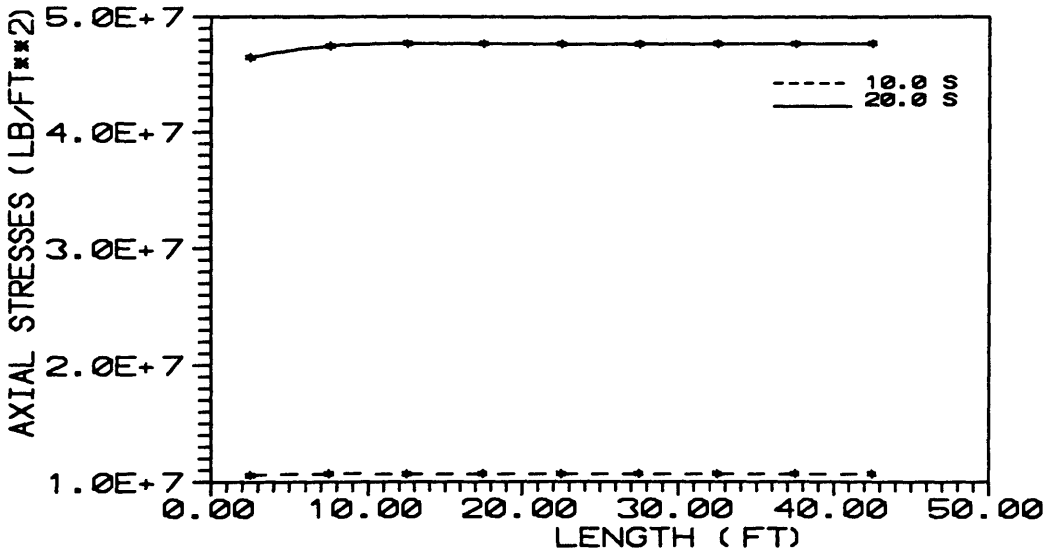

Figure 64 Axial Stresses Due to Hook Loading
(Span Length =90 ft)

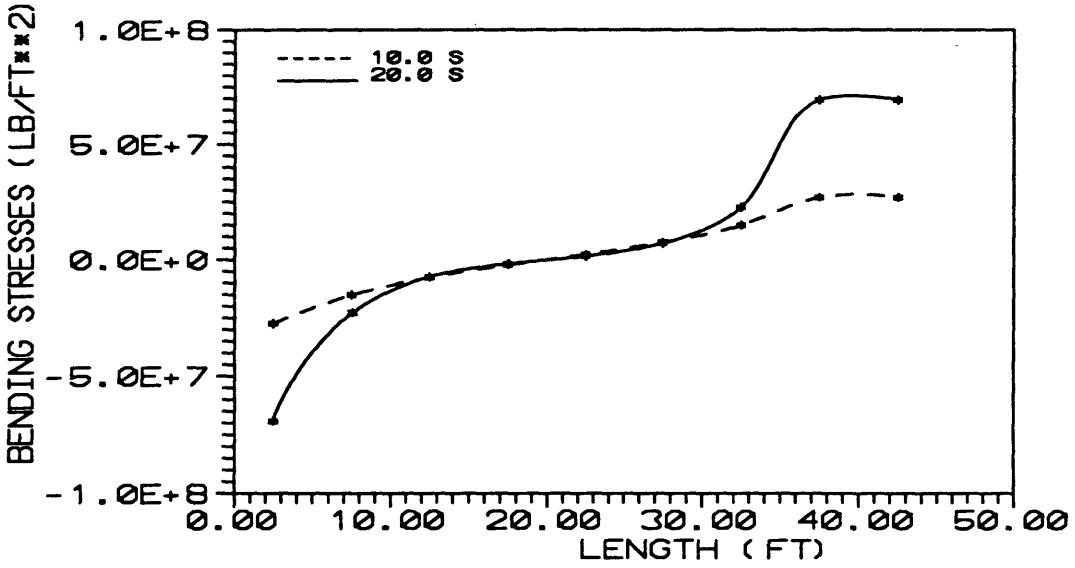

Figure 65 Bending Stresses Due to Hook Loading
(Span Length =90 ft)

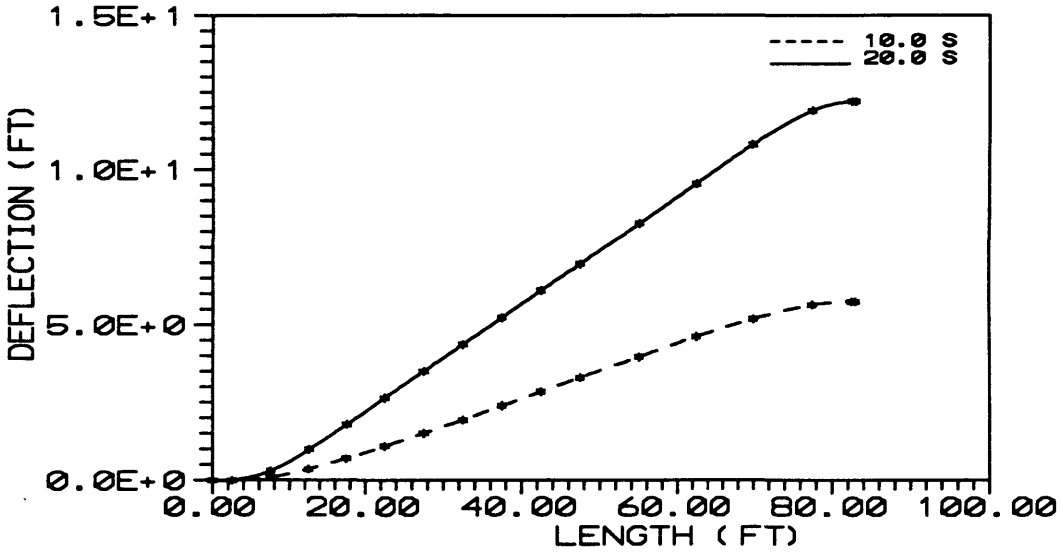

Figure 66 Pipeline Deflection Due to Hook Loading
(Span Length =160 ft)

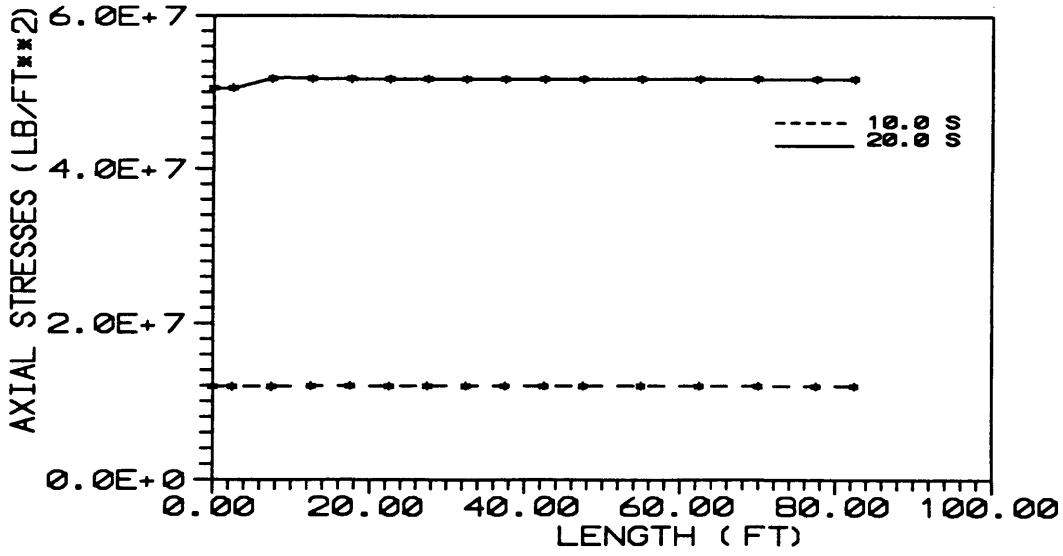

Figure 67 Axial Stresses Due to Hook Loading
(Span Length =160 ft)

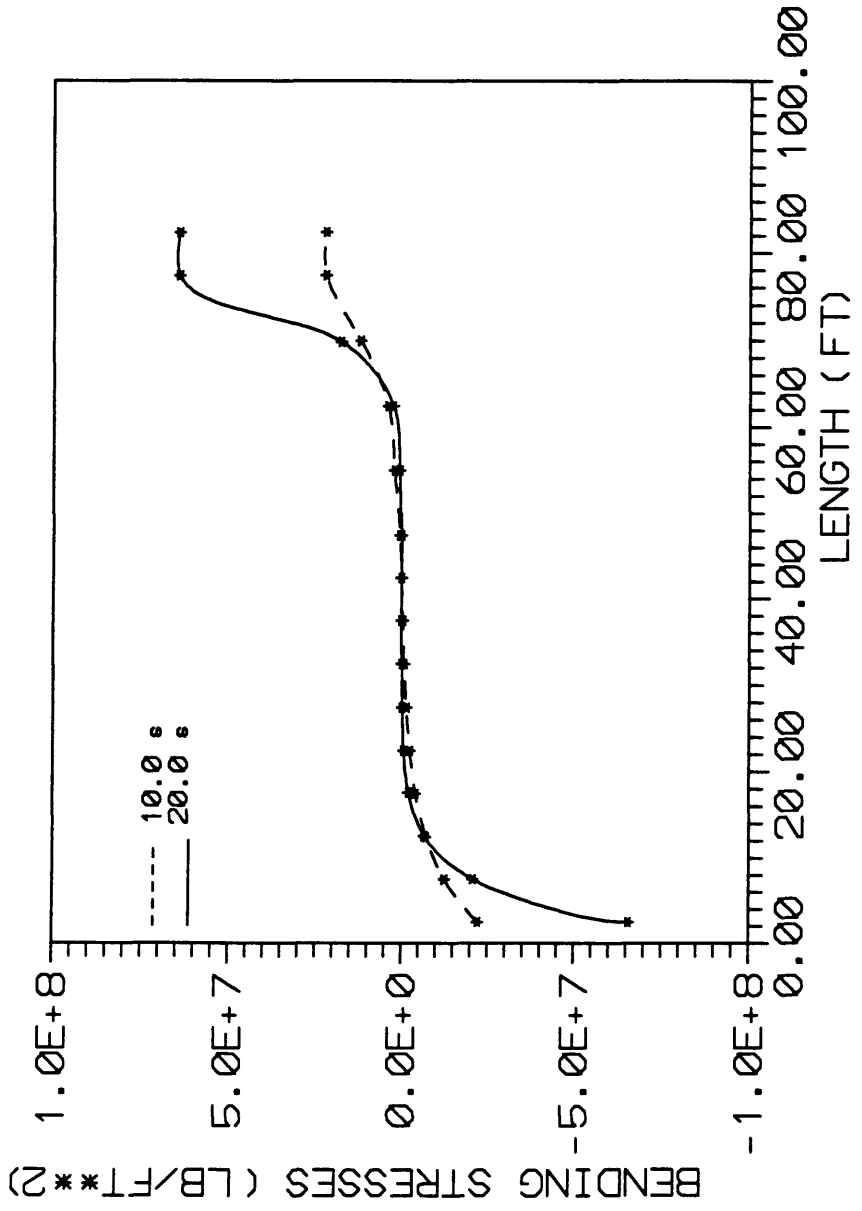

Figure 68 Bending Stresses Due to Hook Loading
(Span Length =160 ft)

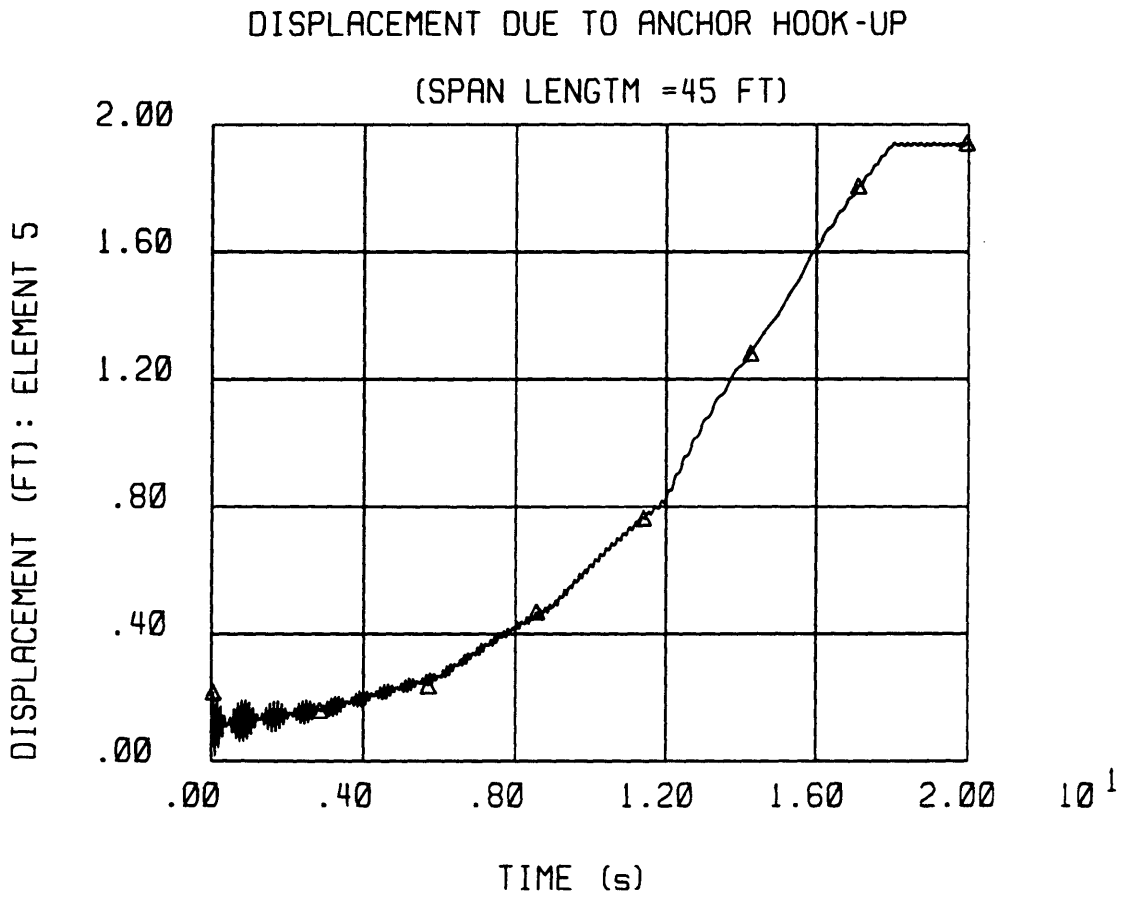

Figure 69 Time History of Pipeline Deflection Due to Hook Loading (Span Length =45 ft)

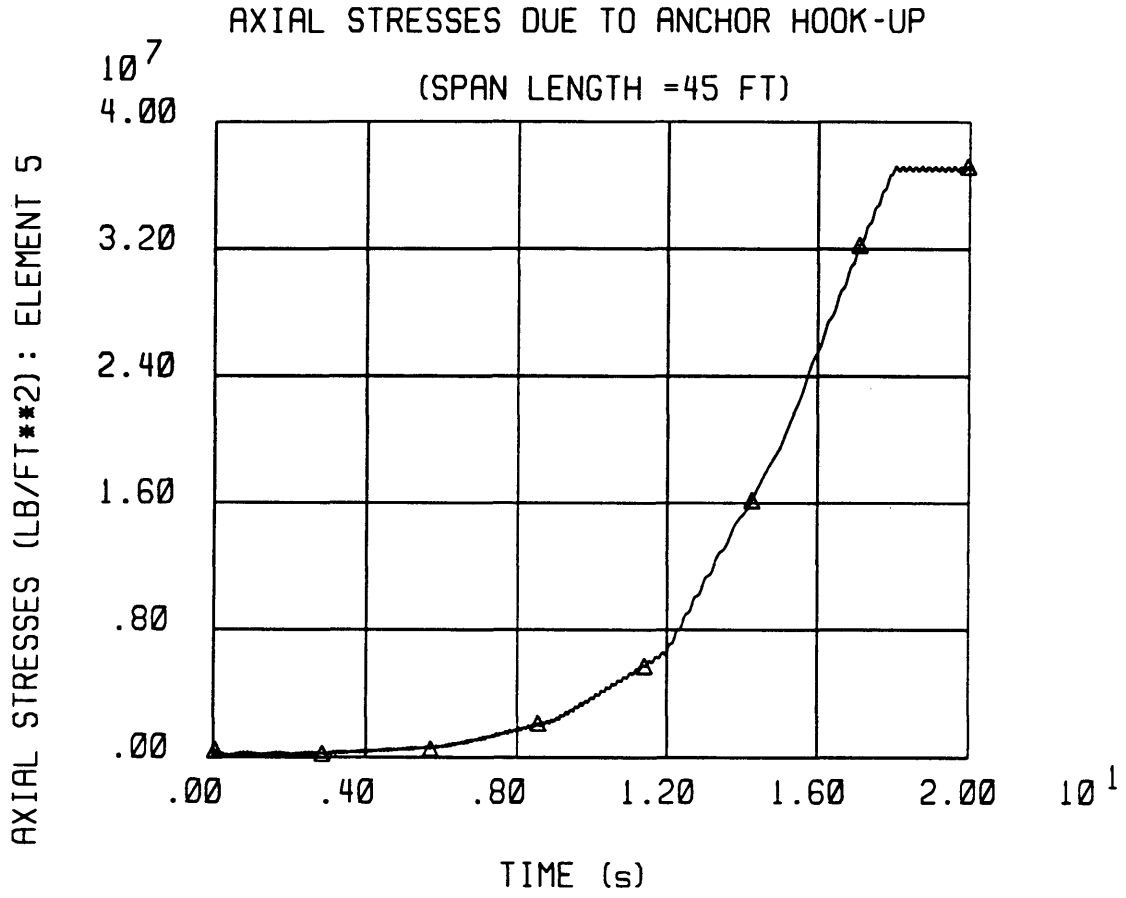

Figure 70 Time History of Axial Stresses Due to Hook Loading (Span Length =45 ft)

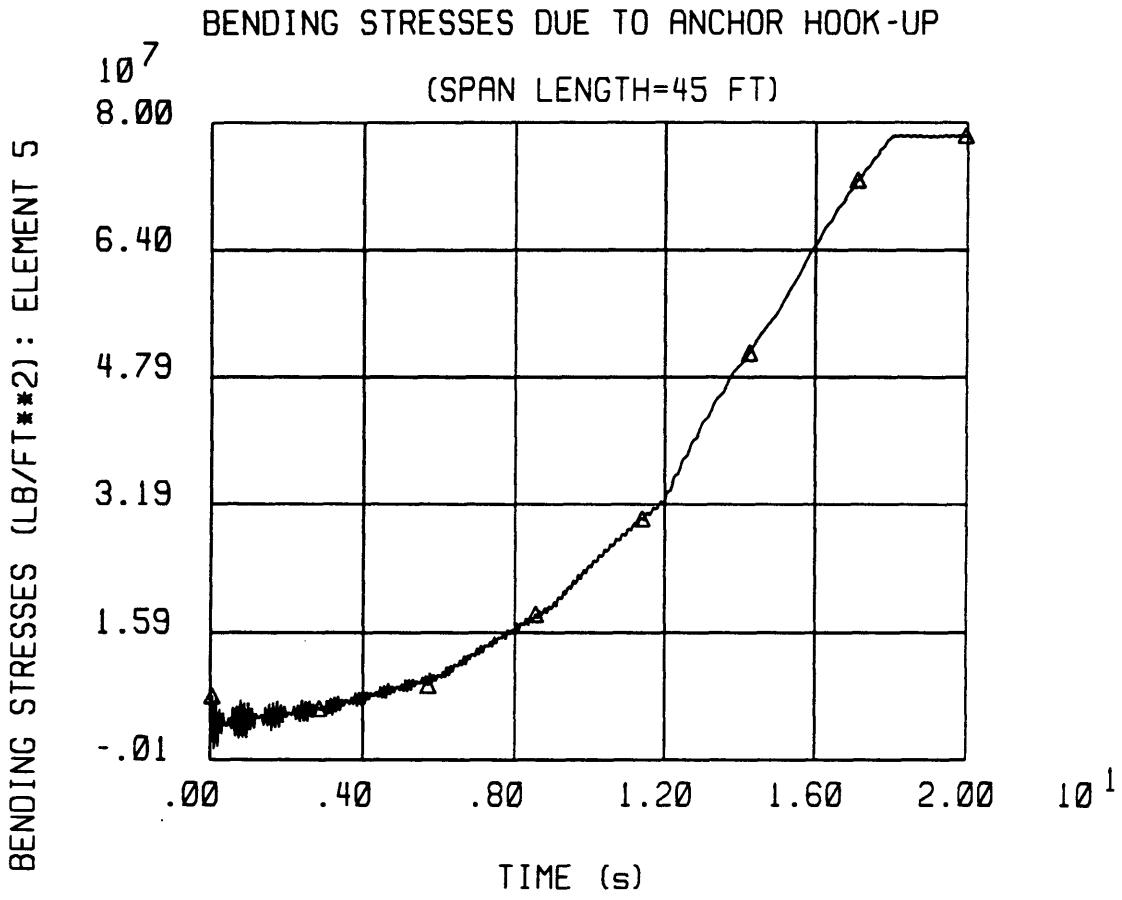

Figure 71 Time History of Bending Stresses Due to Hook Loading (Span Length =45 ft)

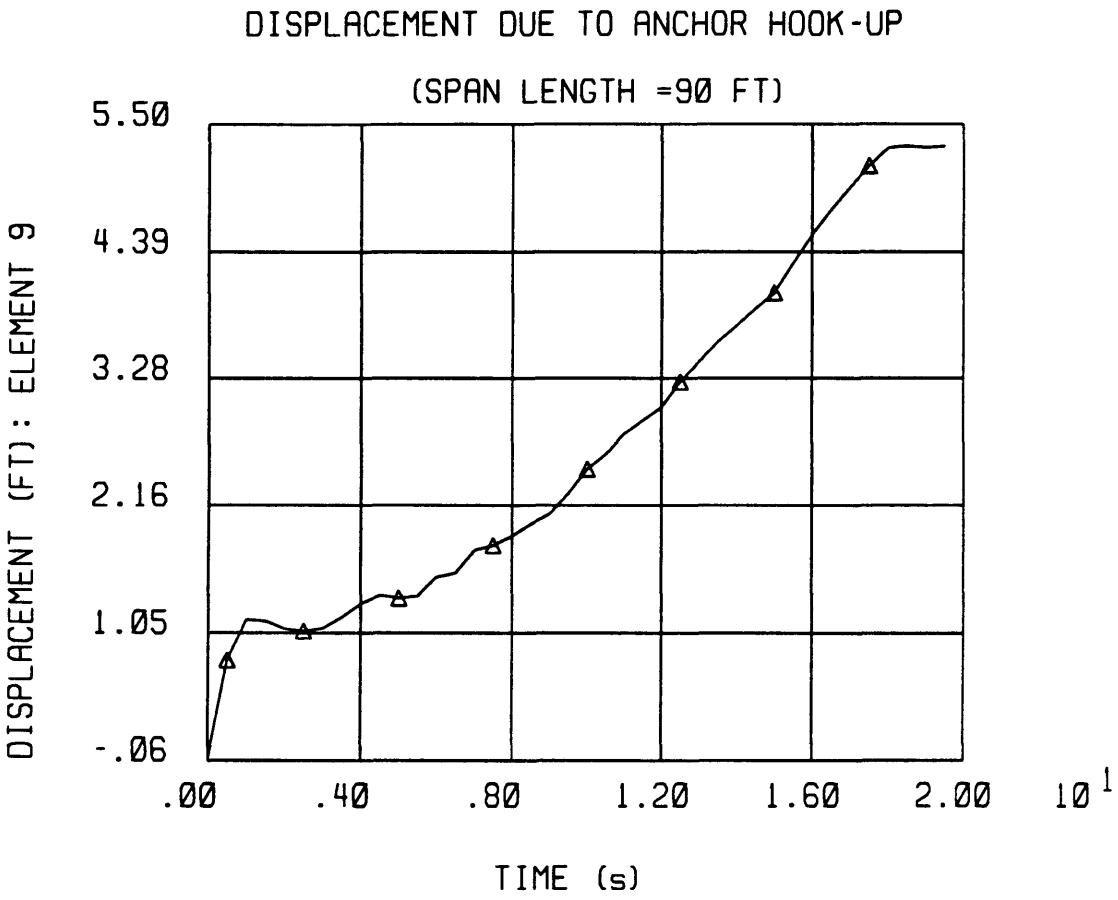

Figure 72 Time History of Pipeline Deflection Due to Hook Loading (Span Length =90 ft)

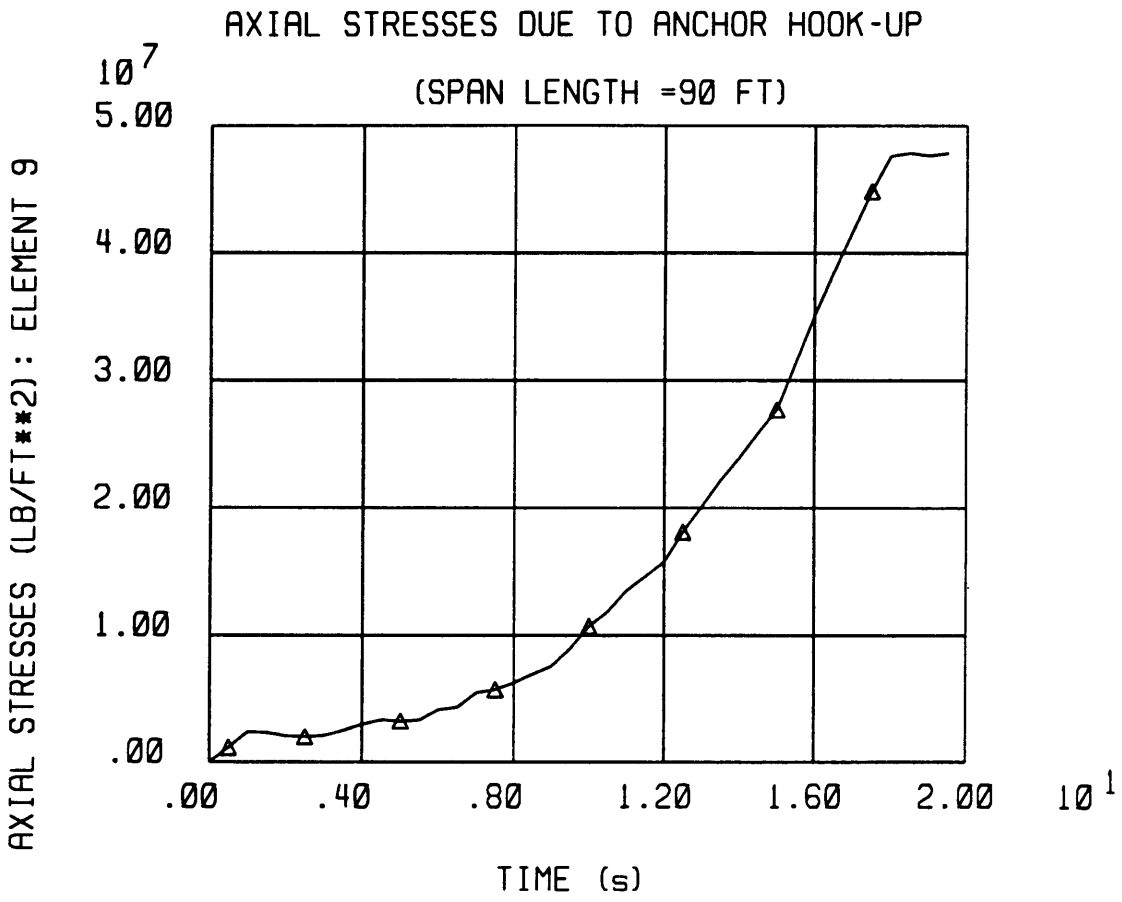

Figure 73 Time History of Axial Stresses Due to Hook Loading (Span Length =90 ft)

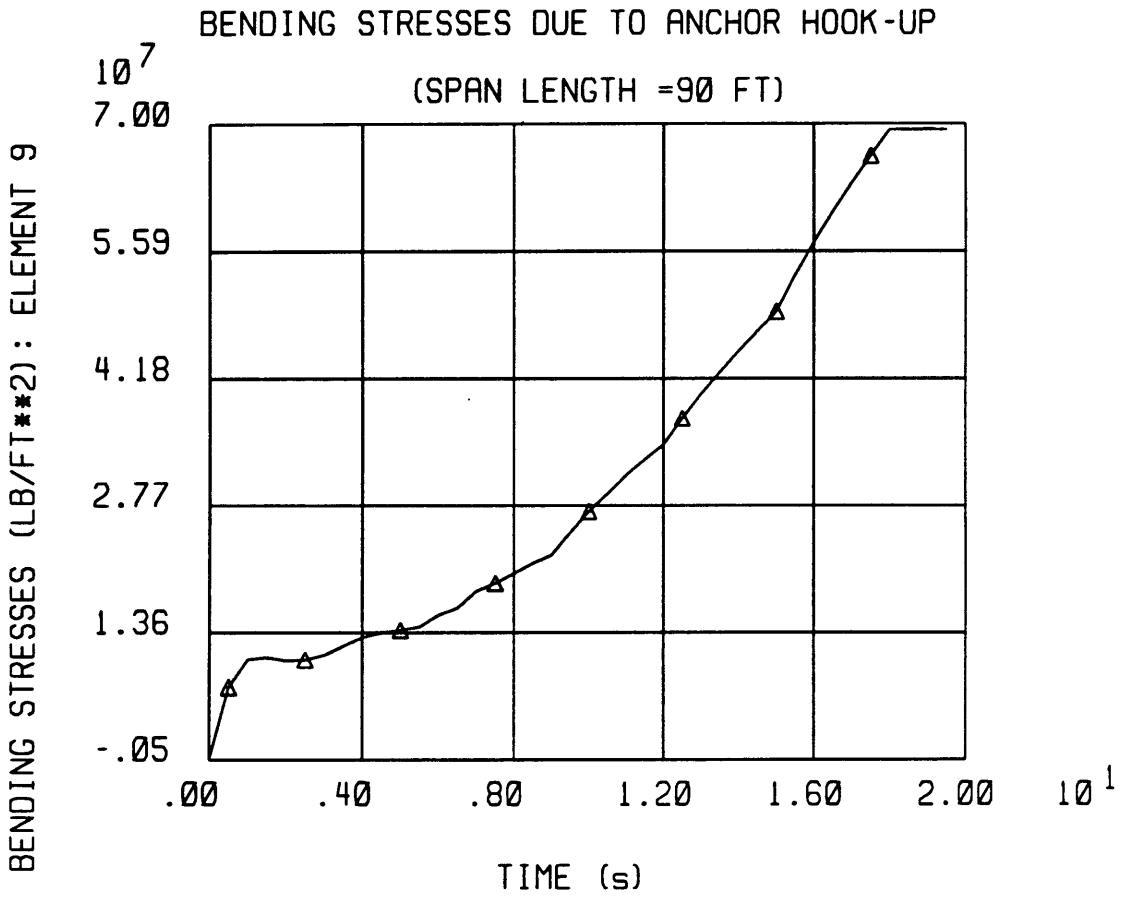

Figure 74 Time History of Bending Stresses Due to Hook Loading (Span Length =90 ft)

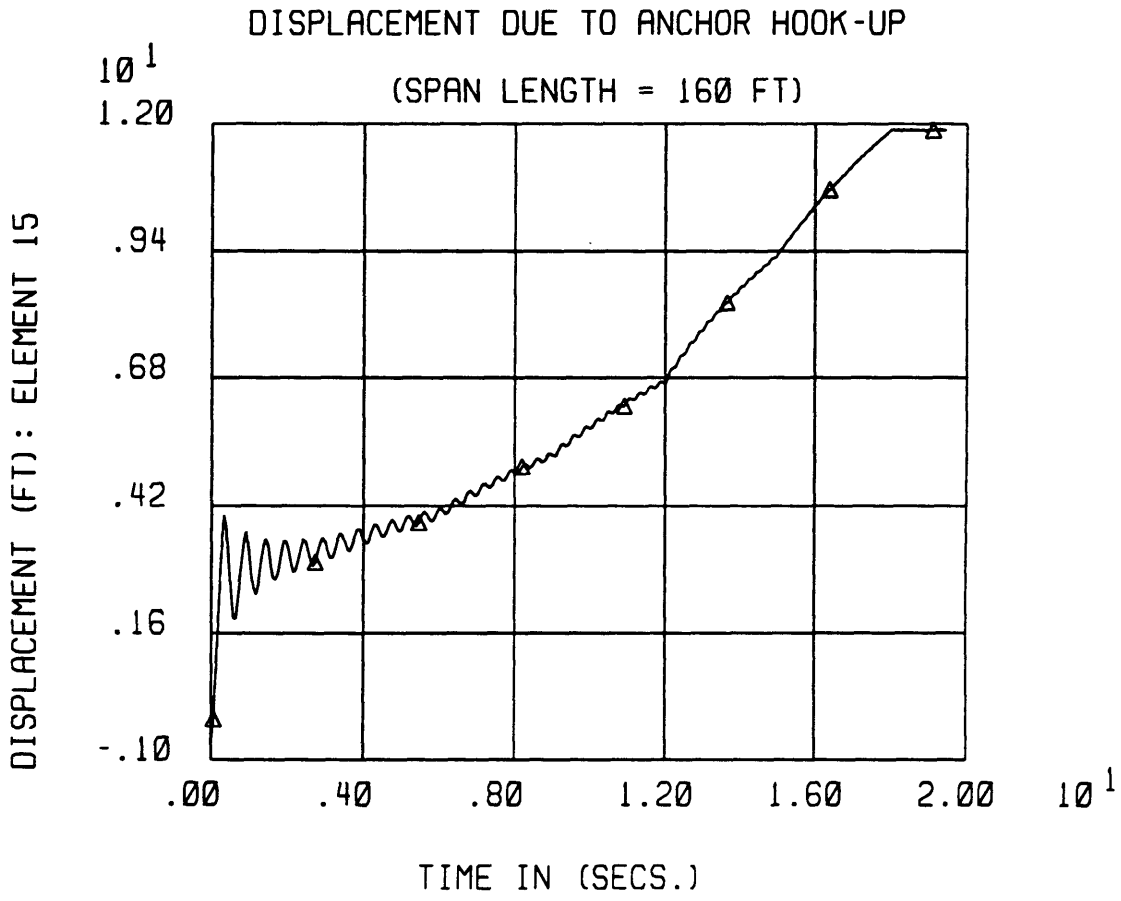

Figure 75 Time History of Pipeline Deflection Due to Hook Loading (Span Length =160 ft)

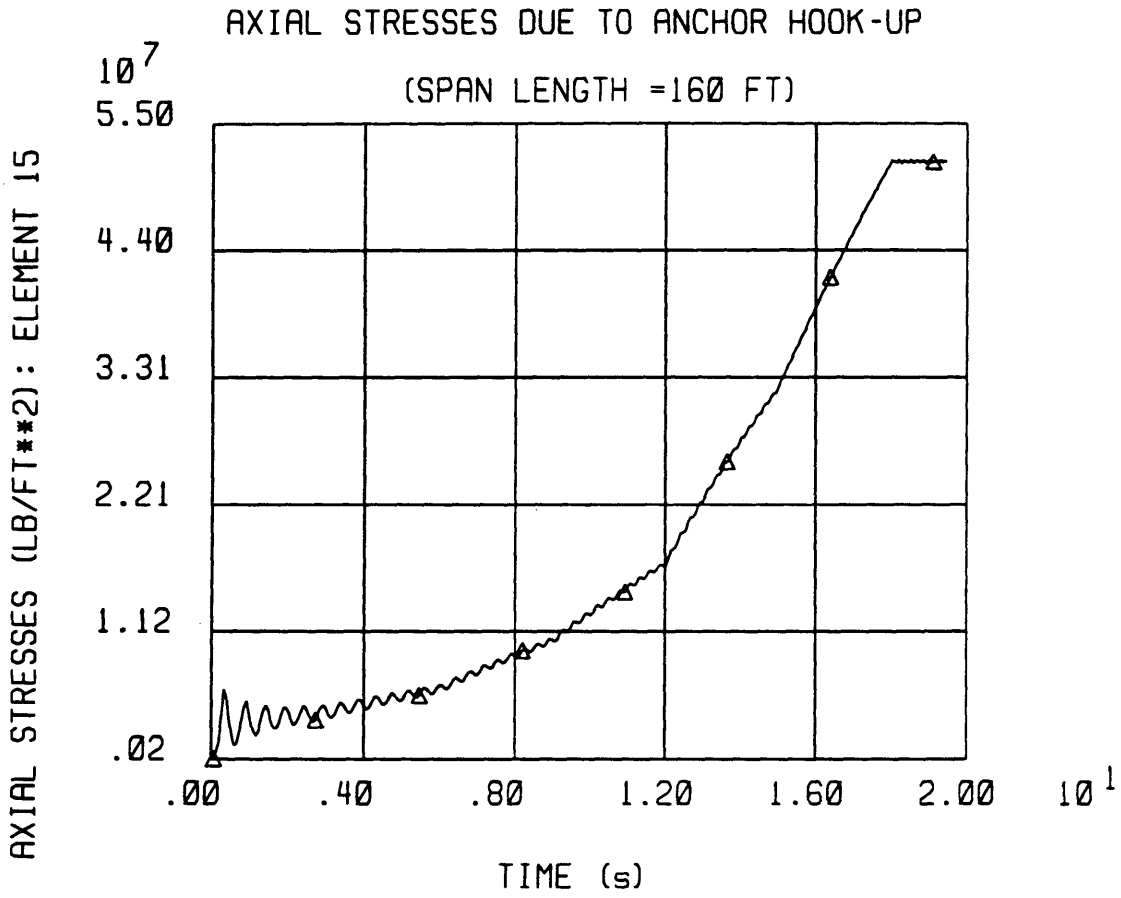

Figure 76 Time History of Axial Stresses Due to Hook Loading (Span Length =160 ft)

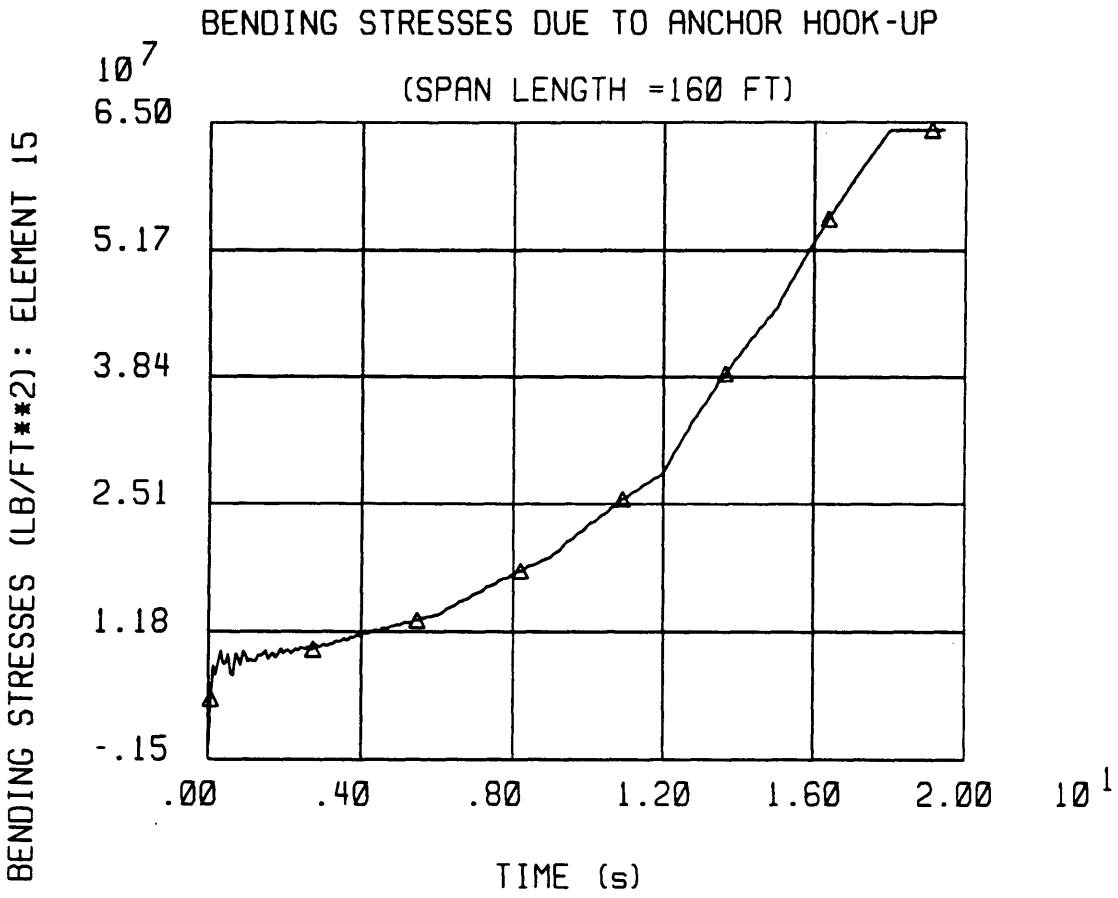

Figure 77 Time History of Bending Stresses Due to Hook Loading (Span Length =160 ft)

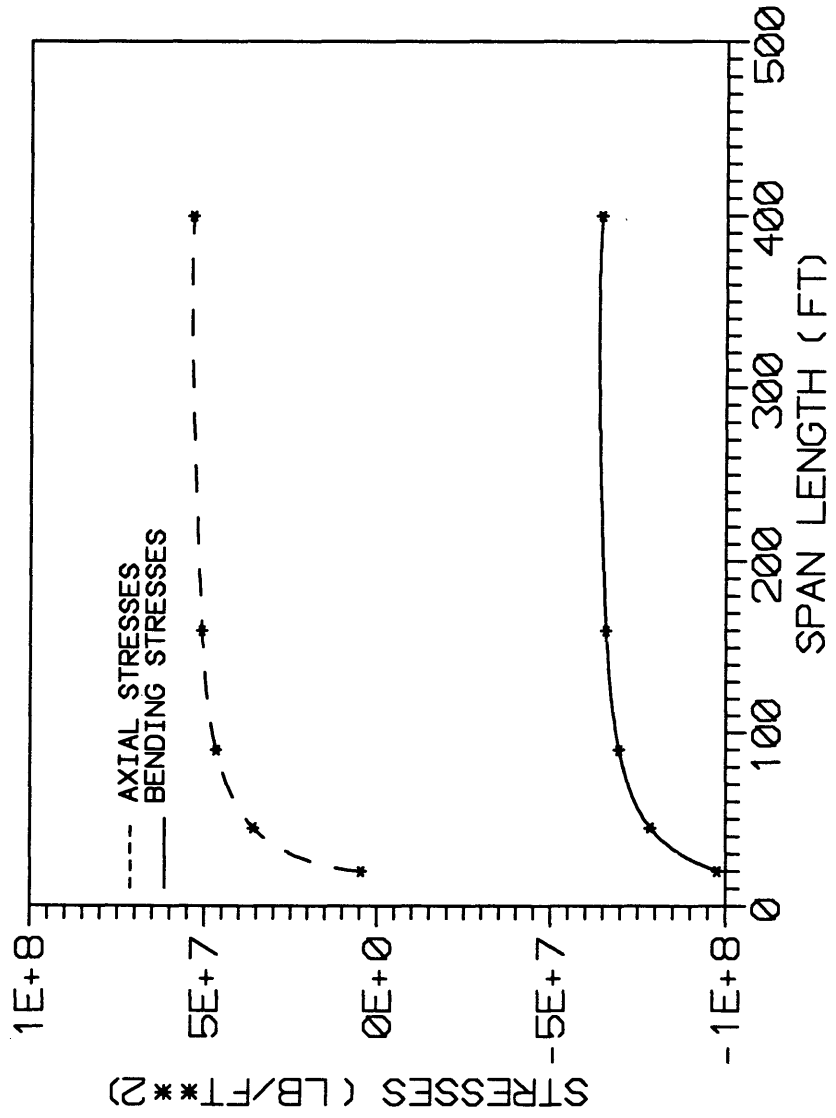

Figure 78 Maximum Stresses Versus Spans Length Due to Hook Loading

5.6 Discussion of Results:

From the analyses of the three different loading functions applied to the three span lengths, it is noted that the maximum stresses exerted in each span were due to ramp loading. A comparison between the maximum stresses resulting from the different types of loading function are shown in Figs. 79-81.

The analyses of effects of span length with respect to stresses exerted by different loading functions (Figs. 40, 59,78) led to the conclusion, that, as the span length increases, bending stresses decrease. Therefore, these types of loading functions, with the size of anchor used, affect mostly the short pipeline spans.

Comparison of the stresses resulting from the anchor impulse loading and ramp loading with a pipeline grad API x 60 showed that these stresses exceed the yield stress. Stresses due to the hook loading reached yield after 4 s from anchor hook-up with a chain excursion of 6.756 ft.

A further investigation was carried out to identify the maximum anchor weight that can operate safely in the pipeline vicinity. This anchor weight was found to be 805 lb, which is a typical anchor used in a vessel with 2000 ton displacement. The resulting deflection, axial and bending

stresses, caused by applying impulse and ramp loading on the three span lengths, are shown in Figs. 82-99.

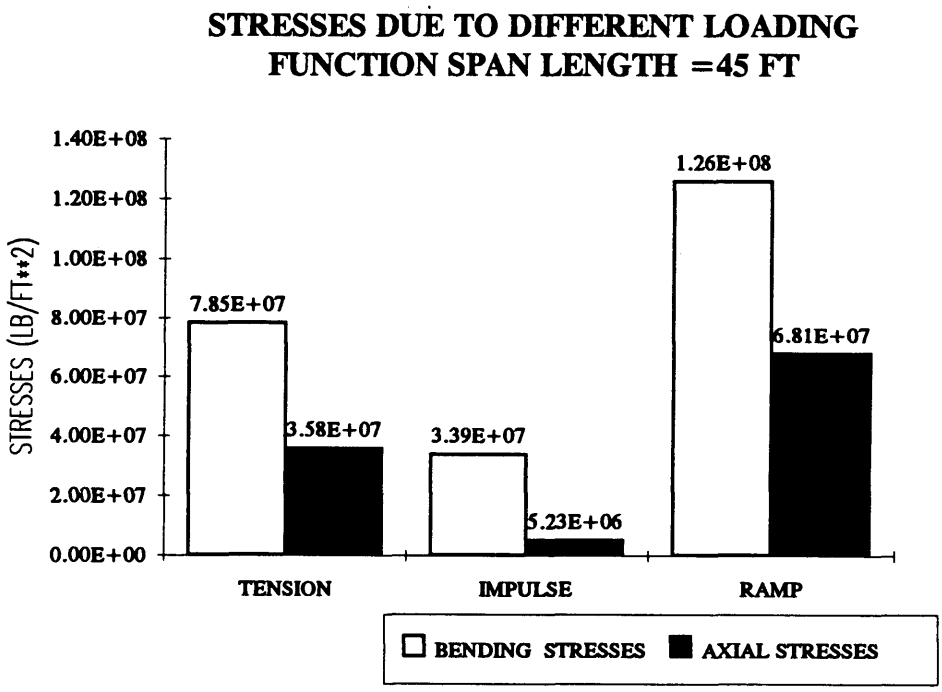

Figure 79 Maximum Stresses Due to Different Loading Functions (Span Length = 45 ft)

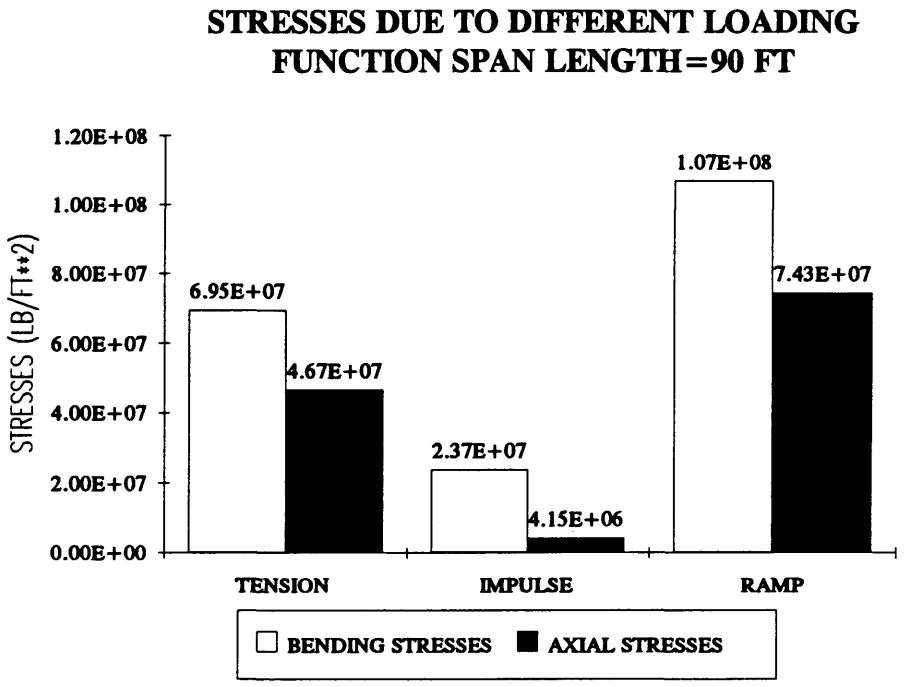

Figure 80 Maximum Stresses Due to Different Loading Functions (Span Length = 90 ft)

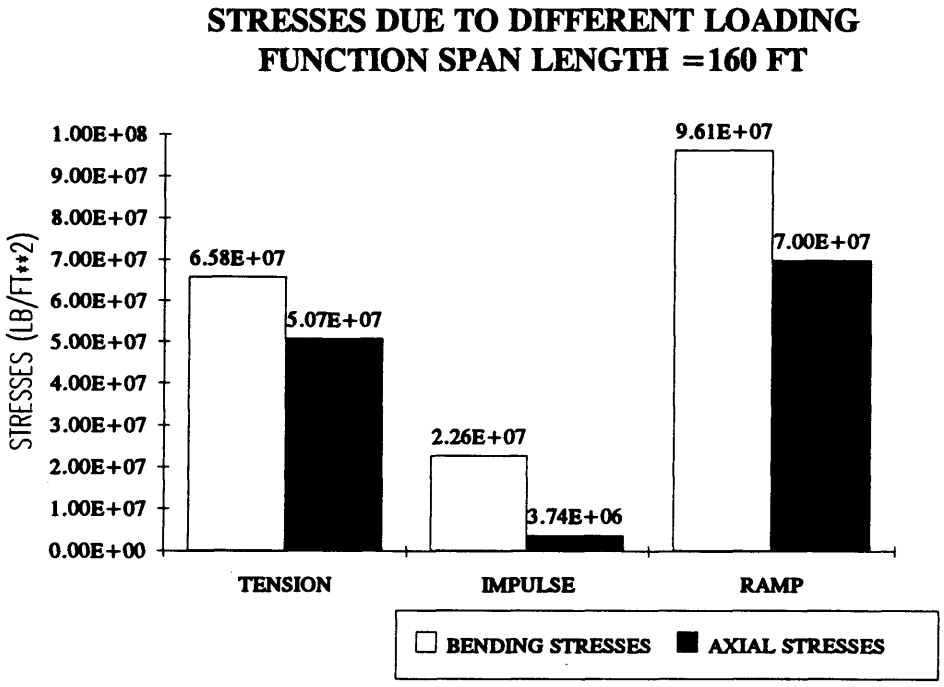

Figure 81 Maximum Stresses Due to Different Loading Functions (Span Length = 160 ft)

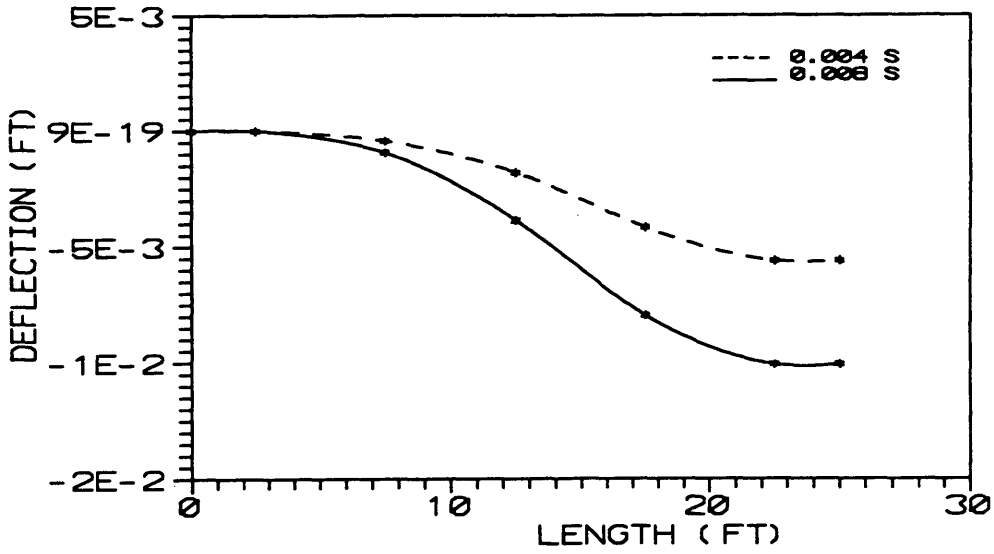

Figure 82 Pipeline Deflection Due to Impulse Loading Impact (Span Length =45 ft)

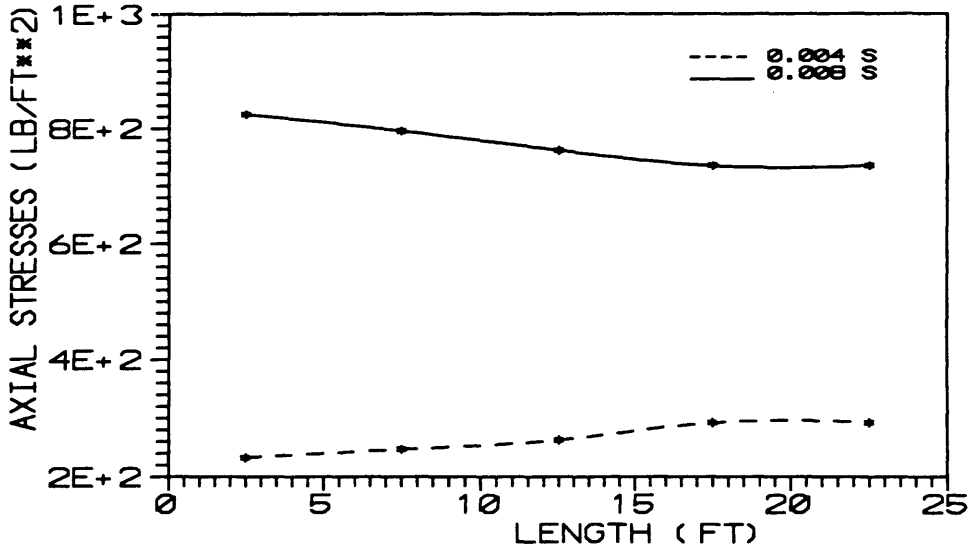

Figure 83 Axial Stresses Due to Impulse Loading Impact (Span Length =45 ft)

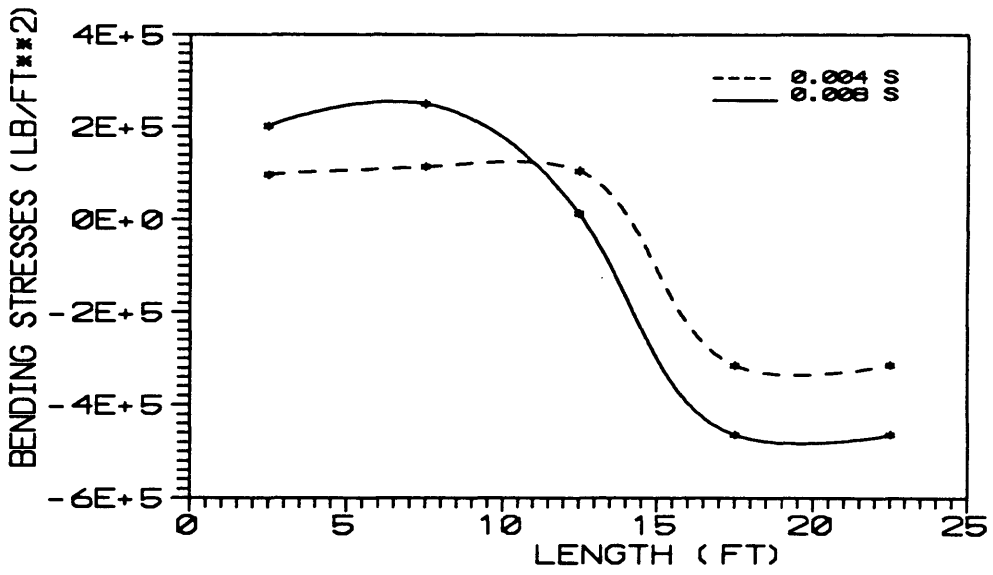

Figure 84 Bending Stresses Due to Impulse Loading Impact (Span Length =45 ft)

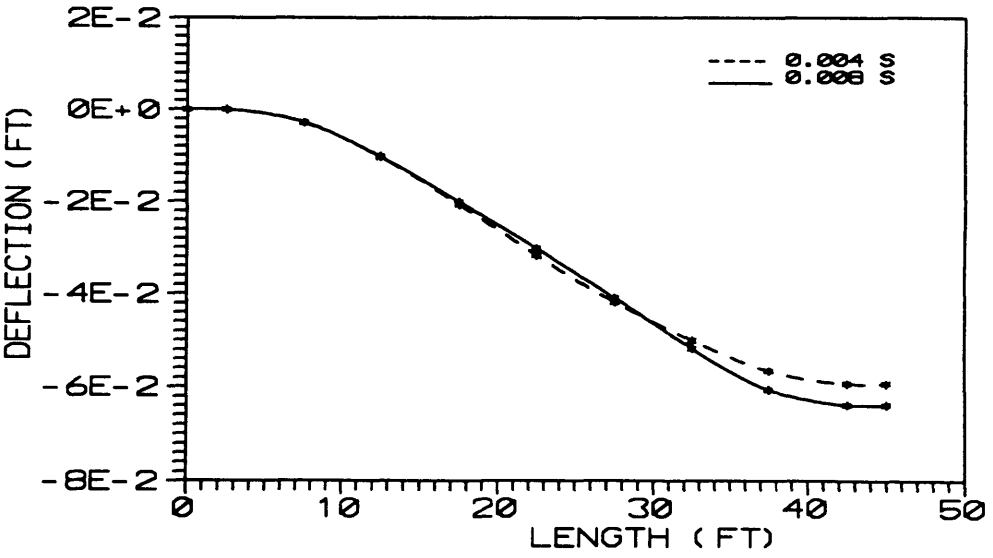

Figure 85 Pipeline Deflection Due to Impulse Loading Impact (Span Length =90 ft)

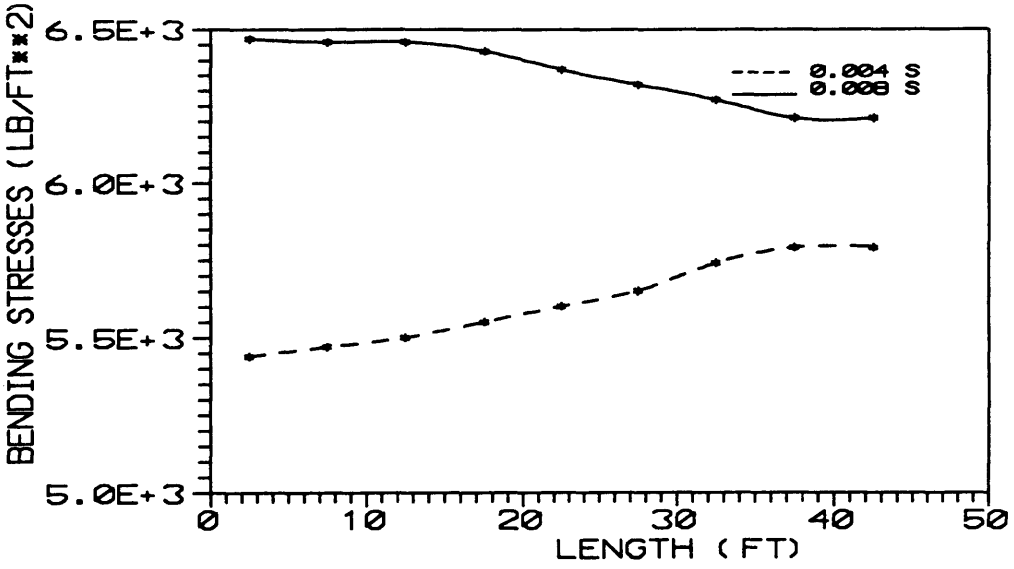

Figure 86 Axial Stresses Due to Impulse Loading Impact (Span Length =90 ft)

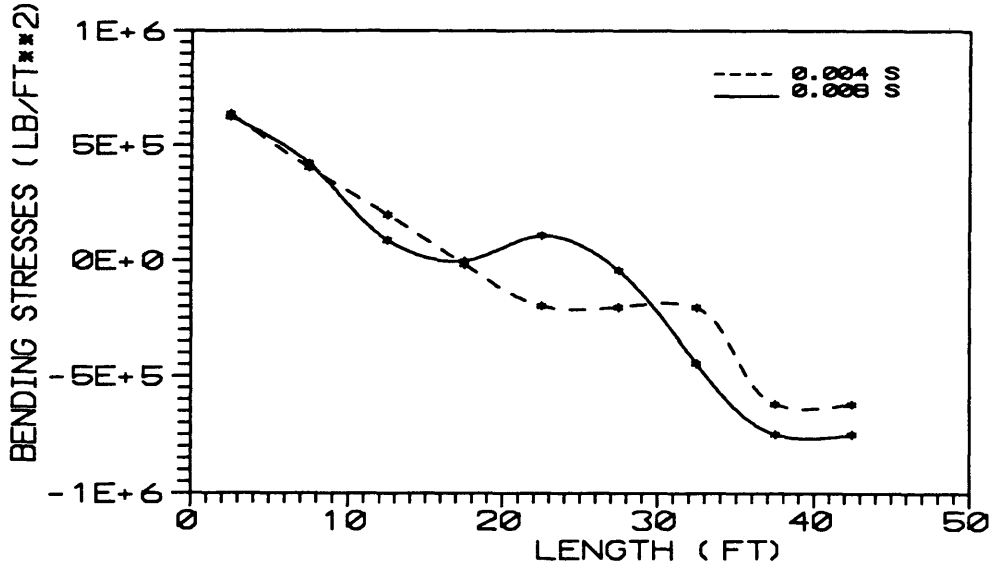

Figure 87 Bending Stresses Due to Impulse Loading Impact (Span Length =90 ft)

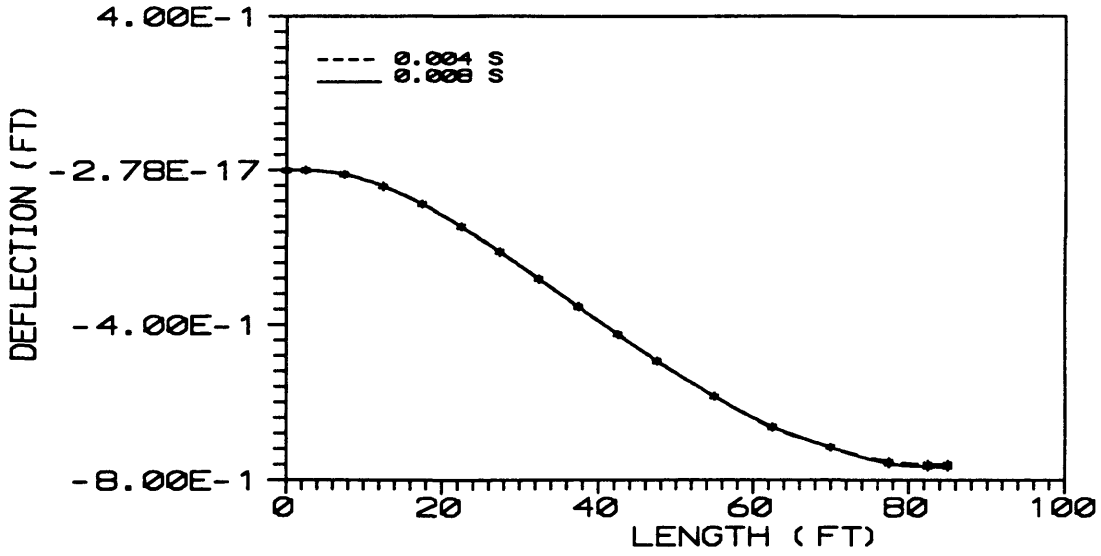

Figure 88 Pipeline Deflection Due to Impulse Loading Impact (Span Length =160 ft)

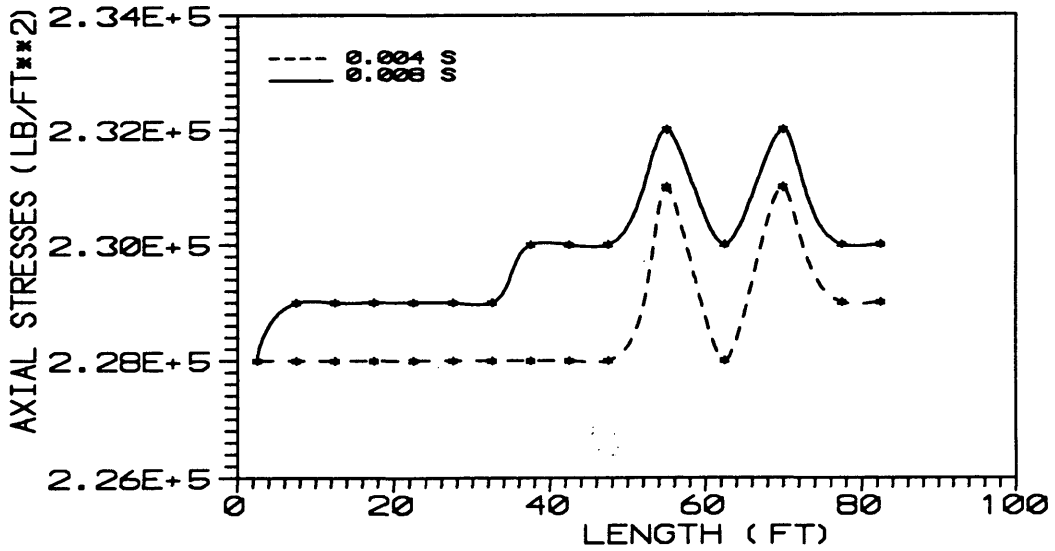

Figure 89 Axial Stresses Due to Impulse Loading Impact (Span Length =160 ft)

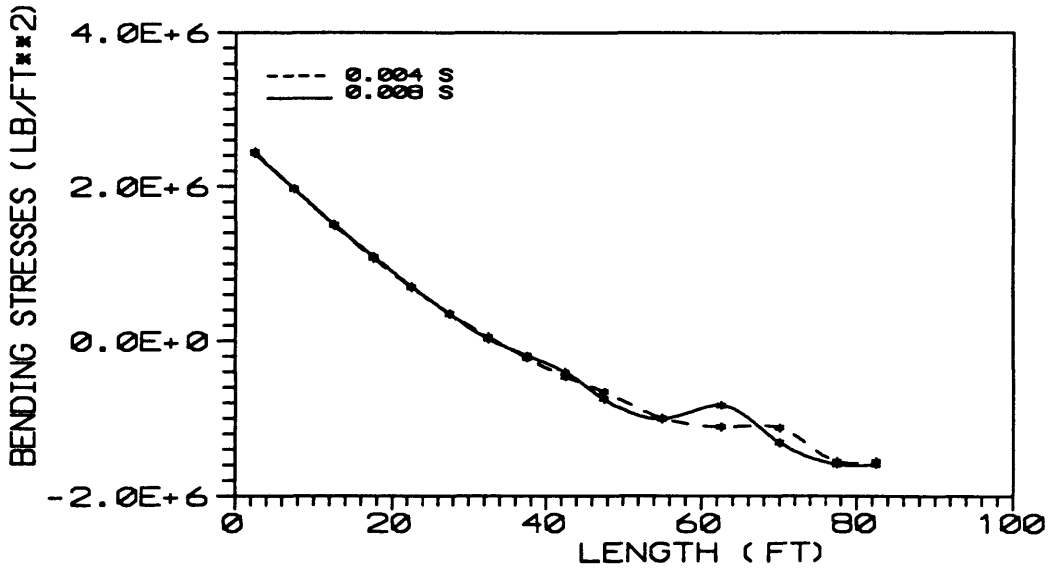

Figure 90 Bending Stresses Due to Impulse Loading Impact (Span Length =160 ft)

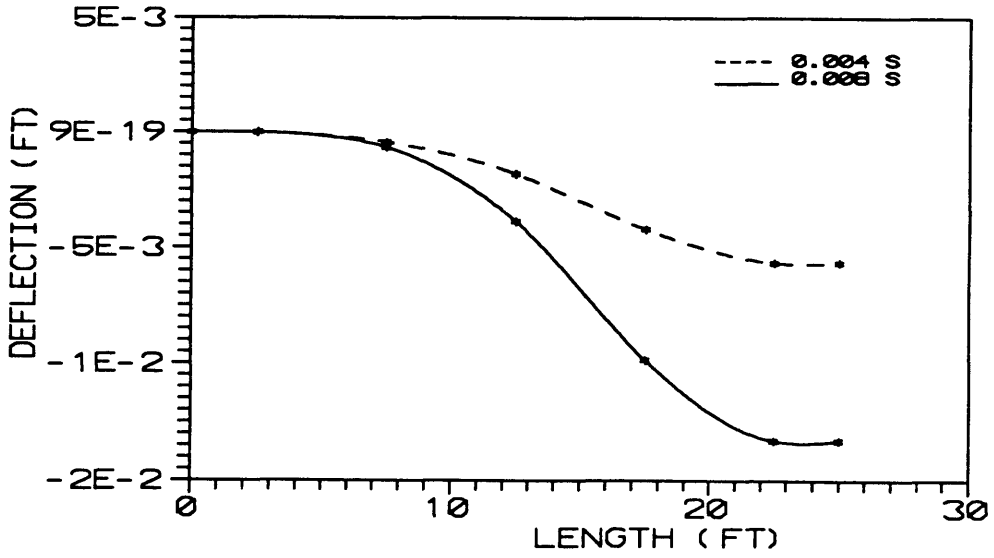

Figure 91 Pipeline Deflection Due to Ramp Loading Impact (Span Length =45 ft)

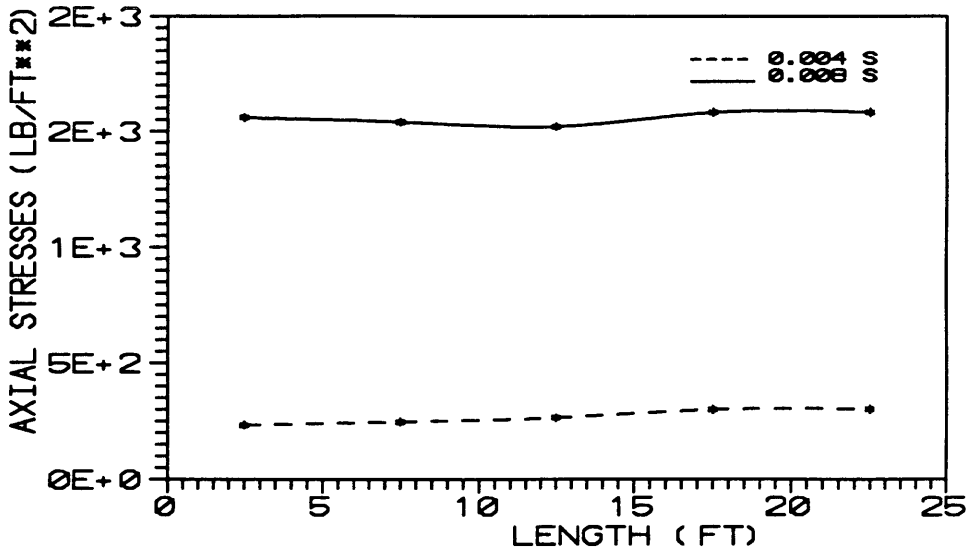

Figure 92 Axial Stresses Due to Ramp Loading Impact
(Span Length =45 ft)

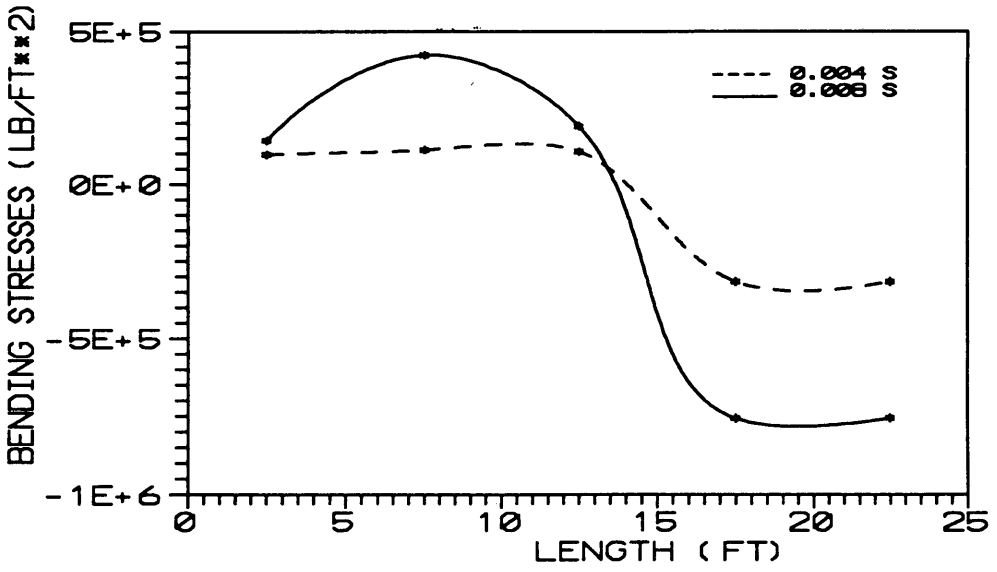

Figure 93 Bending Stresses Due to Ramp Loading Impact
(Span Length =45 ft)

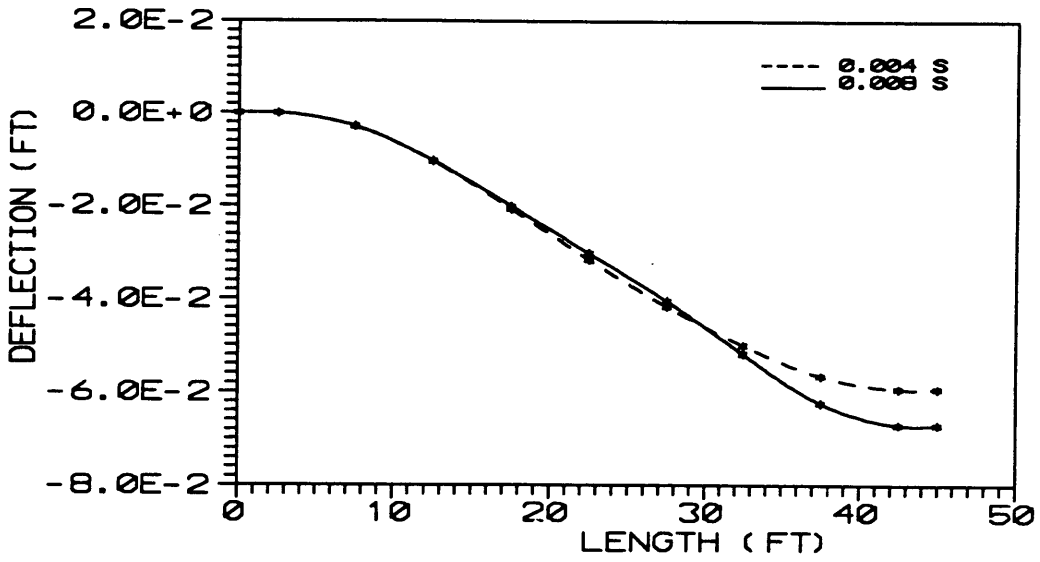

Figure 94 Pipeline Deflection Due to Ramp Loading Impact (Span Length =90 ft)

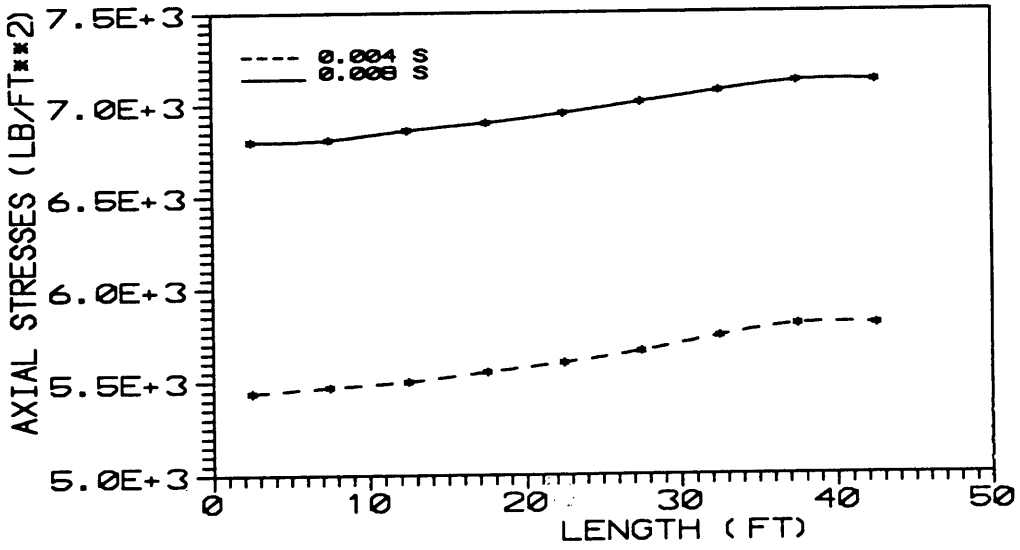

Figure 95 Axial Stresses Due to Ramp Loading Impact (Span Length =90 ft)

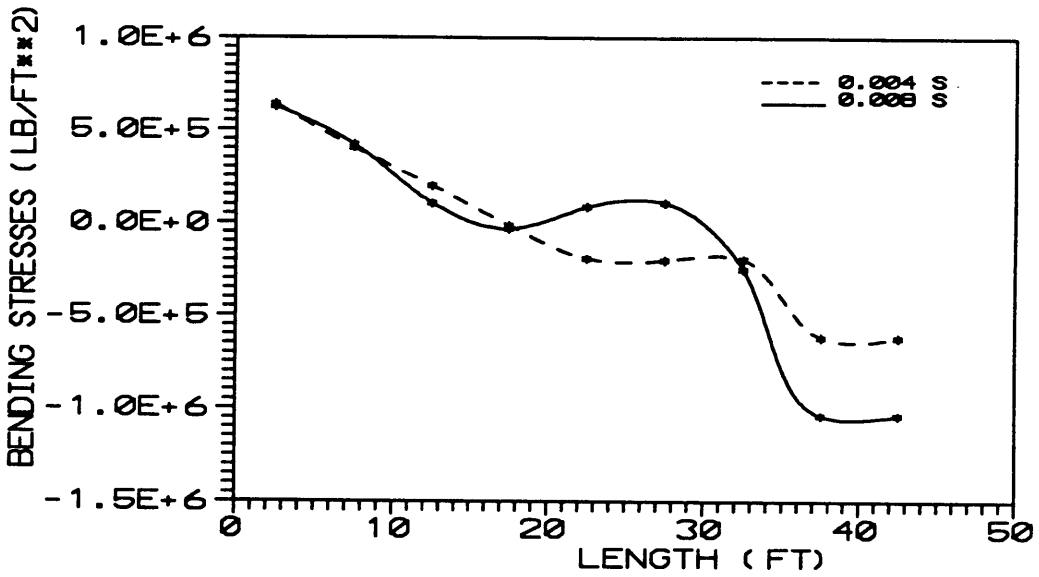

Figure 96 Bending Stresses Due to Ramp Loading Impact (Span Length =90 ft)

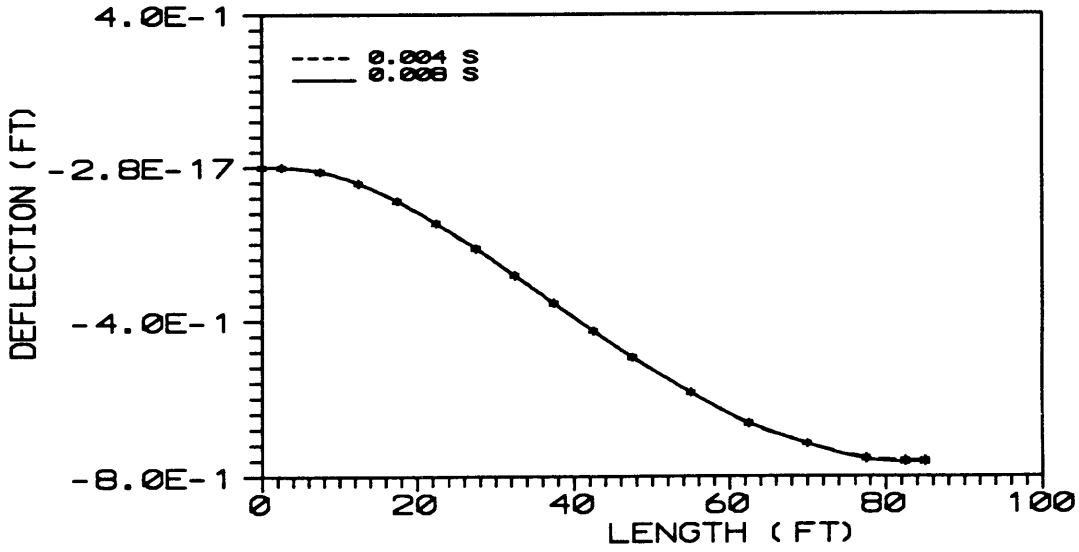

Figure 97 Pipeline Deflection Due to Ramp Loading Impact (Span Length =160 ft)

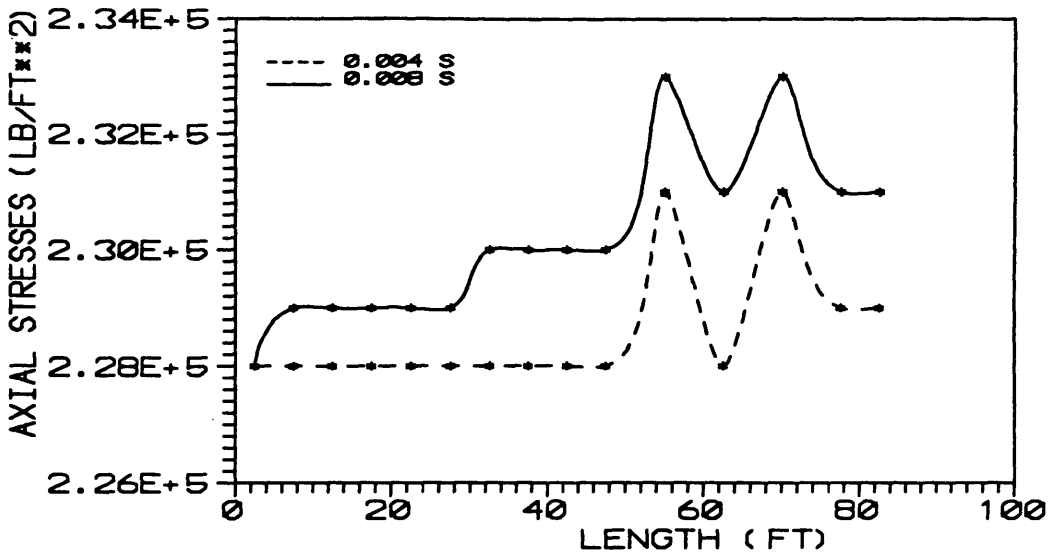

Figure 98 Axial Stresses Due to Ramp Loading Impact
(Span Length =160 ft)

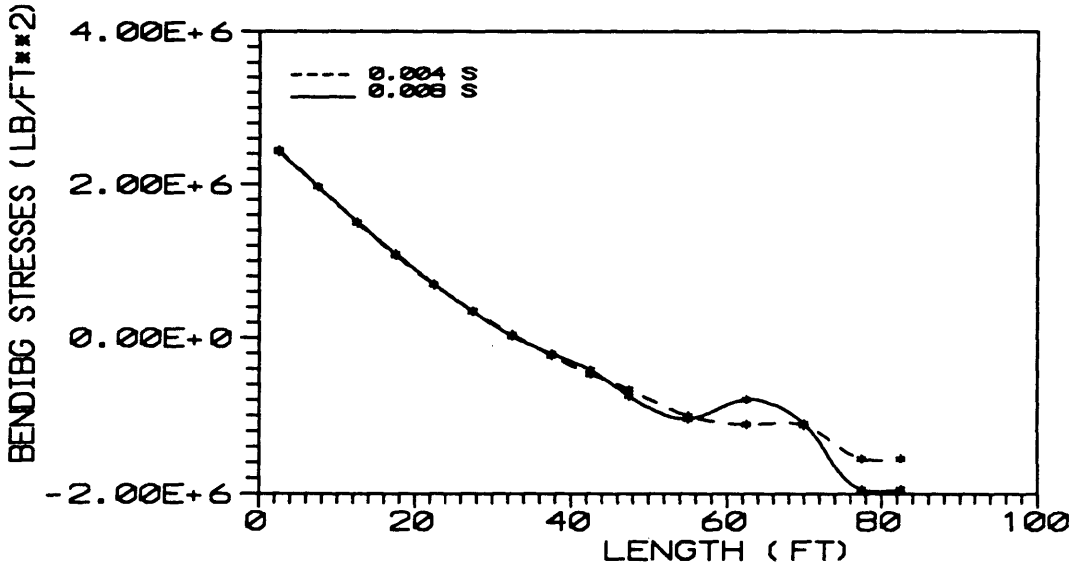

Figure 99 Bending Stresses Due to Ramp Loading Impact
(Span Length =160 ft)

CHAPTER 6

PROTECTION METHODS

The most commonly used method of protecting offshore pipelines from external accident is trenching and pipe burying. However, dropped and dragged anchors tend to penetrate the seabed; Mousseli (1978) had analyzed the protection of anchoring for these cases. An anchor weight of 10,000 lb can penetrate up to 16 ft into a clay seabottom (Fig. 100). Therefore, a normal burial is not sufficient for the pipeline protection. It may not be feasible to try to provide the required depth with normal construction equipment.

The penetration of an anchor in the seabed depends upon the type of seafloor condition. For example, an anchor does not penetrate through a hard surface. Therefore, a feasible method to protect pipelines from anchor hooking/impact would be by covering the pipeline with a shell-like structure with a hard surface.

Recently an experimental result was presented by Hvam (1990) where the author performed extensive model and prototype tests with respect to pipeline protection. These test results show that pipelines can be protected

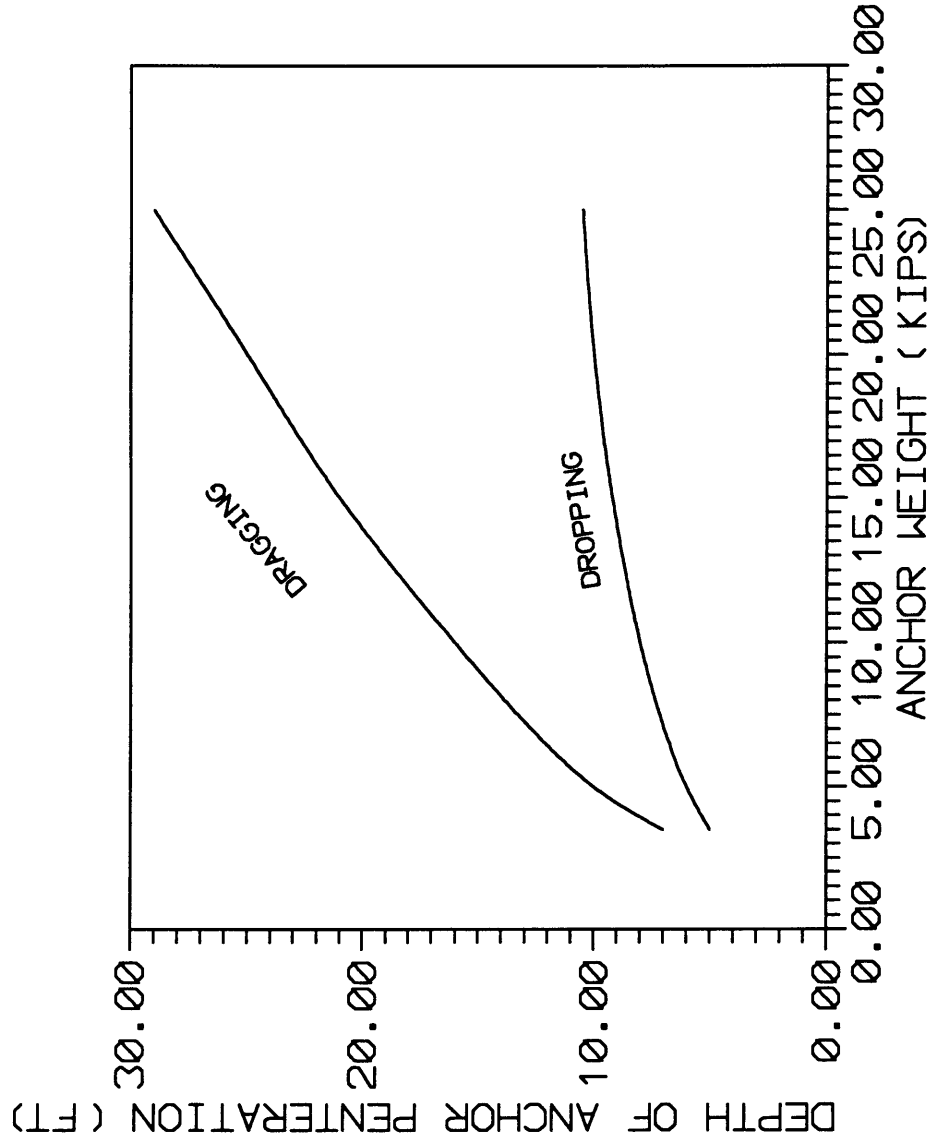

Figure 100 Depth of Anchor Penetration in Seafloor

against damage from dragged and/or dropped anchors with a protection layer of stone or coarse gravel. Three feet of cover fill with 20-120 lb rocks as illustrated in Fig. 101, over a 45 foot width give a sufficient protection against all types of anchors up to 30,000 lb in weight.

It is not cost effective to maintain this type of cover on the whole pipeline length. The pipeline route could be divided to two areas: i)tie-in locations (near platforms or loading unloading terminals) and ii) sections in between the tie in locations where the major pipeline length lies.

The possibility of pipeline/anchor interaction is mostly near the tie-in locations. Therefore it is recommended to use this coarse gravel cover at the tie-in locations.

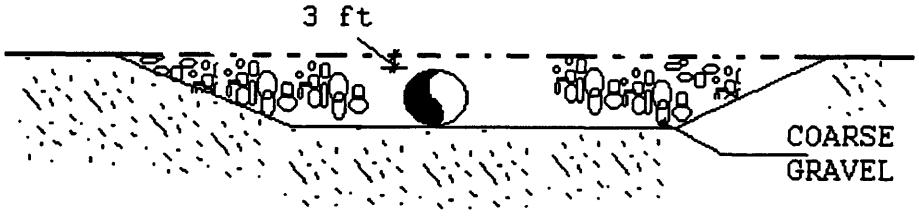

Coarse gravel protection

Figure 101 Protection Methods

CHAPTER 7

CONCLUSION AND RECOMMENDATION

7.1 CONCLUSION:

A study of stresses resulting from pipeline interaction with tanker anchors as a function of span lengths, was presented. This could be used as a model in designing offshore pipelines for anchor impact. From the analysis in this study it is noted that the maximum stresses were due to a ramp loading function on a 45 ft span. These stresses should be considered in designing a pipeline in the areas where there exists a significant probability of interaction with ship anchors, such as the loading/unloading terminals or close to an offshore platform, where a tanker is present.

7.2 RECOMMENDATION:

Having analyzed that effect of anchor interaction with offshore pipelines, it is noted that as a result of this interaction, the pipeline encounters a large amount of axial and bending stresses which exceed the yield stresses for the most commonly used pipeline grad API X-60. It was concluded that such interaction would result in yielding the

pipeline and would create local buckling which would put the pipeline out of operation. Therefore these interactions should be considered during offshore pipeline design. Also, it is necessary to include a protection system, that would prevent occurrence of pipeline/anchor interactions thus reducing drastically the probability of environmental damages.

REFERENCES CITED

Baker E. 1953. Interaction to Steel Shipbuilding. New York: McGraw-Hill Book company

Bergan, P. G, and Mollestad, E. 1981. Impact Response of Offshore Pipeline. Proceeding of Offshore Technology Conference (OTC 4065), Houston

Brown, R.J. 1972. Pipeline Can be Designed to Resist Impact From Dragging Anchors and Fishing Boards. Proceeding of Offshore Technology Conference (OTC 4065), Houston

Brown, R.J. 1971. How Deep Should an Offshore Pipeline be Buried for Protection. The Oil and Gas Journal 90-98

Carpanterto, R. 1991. Risk Analysis of Subsea Pipelines Hazards Induced by Human Offshore Activities. Proceeding of the Second International Offshore and Polar Engineering Conference, vol 2 ISOPE, San Francisco

Chung, J. S. 1992. Class notes Introduction to Offshore Technology. Department of Engineering Colorado School of Mines

Chung J.S, Whitney, A.k. and Loden, W.A. 1980-1981. Nonlinear Transient Motion of Deep Ocean Mining Pipe. Proceeding of Offshore Technology Conference, Houston

Fredsϕe, J. and Hansen, E.A. 1986. Three-Dimensional Scour Below Pipelines. Proceeding of International Offshore Mechanics and Arctic Engineering Symposium, Tokyo

Guijt, J., and Horenberg, J. A. 1987. Recent Investigations Concerning The Effect of Trawl Gear Crossing On Submarine Pipeline Integrity. Proceeding of Offshore Technology Conference (OTC 5616), Houston

Guijt, J., and Horenberg, J. A. 1987. An Analytical and Experimental Analysis of Trawl Gear-Pipeline Interaction. Proceeding of Offshore Technology Conference (OTC 5617), Houston

Guoyang J., Skallerud, B. and Rorrbjorn S. 1991.Safety and Integrity of Submarine Pipelines/Flowlines Under Interaction Of Fishing Trawl Doors. Proceeding of Int. Offshore and Polar Engineering Conference ISOPE-91, Edinburgh, Scotalnd

Hunter, S. C. 1957. Energy Absorbed by Elastic Waves During impact. Journal of Mechanics and Physics of Solids. vol. 5: 162-171

Hvam, C. 1990. Risk of Pipe Damage from Dragging Anchors. Proceeding of the First European Offshore Mechamics Symposium, ISOPE, Trondheim Norway

Jensen, J.J. 1990. Impact Strength of Concrete Coating on Pipelines. Proceeding of the 3rd International Symposium on Offshore Engineering

Love, A. E. H. 1927. A Treatise on the Mathematical Theory of Elasticity, New York, Dover Publication

Moshagen, H., and Kjeldsen, S. P. 1980. Fishing Gear Loads and Effects on Submarine Pipeline. Proceeding of Offshore Technology Conference (OTC 3782), Houston

Mousselli, A. and Basu, R. 1978. Risk Studies Analyze Anchor Damage to Offshore Pipelines. The Oil and Gas Journal 90-101

Mustoe, G.W., Huttelmaier, H.P. and Chung, J. S. 1992. Dynamic Coupling Bending-Axial Analysis of Two Dimensional Deep-Ocean Pipes by the Discrete Element Method. Proceeding of the Second International Offshore and Polar Engineering Conference, ISOPE, San Francisco

Mustoe G.W. and Williams J. R. 1989. Educational Workshop on Discrete Element Methods. National Science Foundation and Colorado School of Mines

Strating, J. 1981. A Survey of Pipeline in the North Sea Incidents During Installation, Testing and Operation. Proceeding of Offshore Technology Conference (OTC 4069), Houston

Tϕrum, A., Bostrom, B., and Sandoy, A. B. 1989. On the Damping Of and Forces on a Current Induced Vibrating Pipeline. Proceeding of Int. conf. Offshore Mechanics and Arctic Engineering, The Hague

Verley, R. L. P., Moshagen, B. H., and Moholdt, N. C. 1991. Trawl Forces On Free Spanning Pipelines. Proceeding of International Offshore and Polar Engineering Conference (ISOPE-91), ISOPE Edinburgh, Scotland

Williams, A. J. 1990. Hazard Assessment and Pipeline Design. Advances in Subsea Pipeline Engineering and Technology, Society for Under water Technology, 263-278

APPENDIX A

Program Structure

The program structure of the research code OCEAN, is given below. A short description of each subroutine used attached.

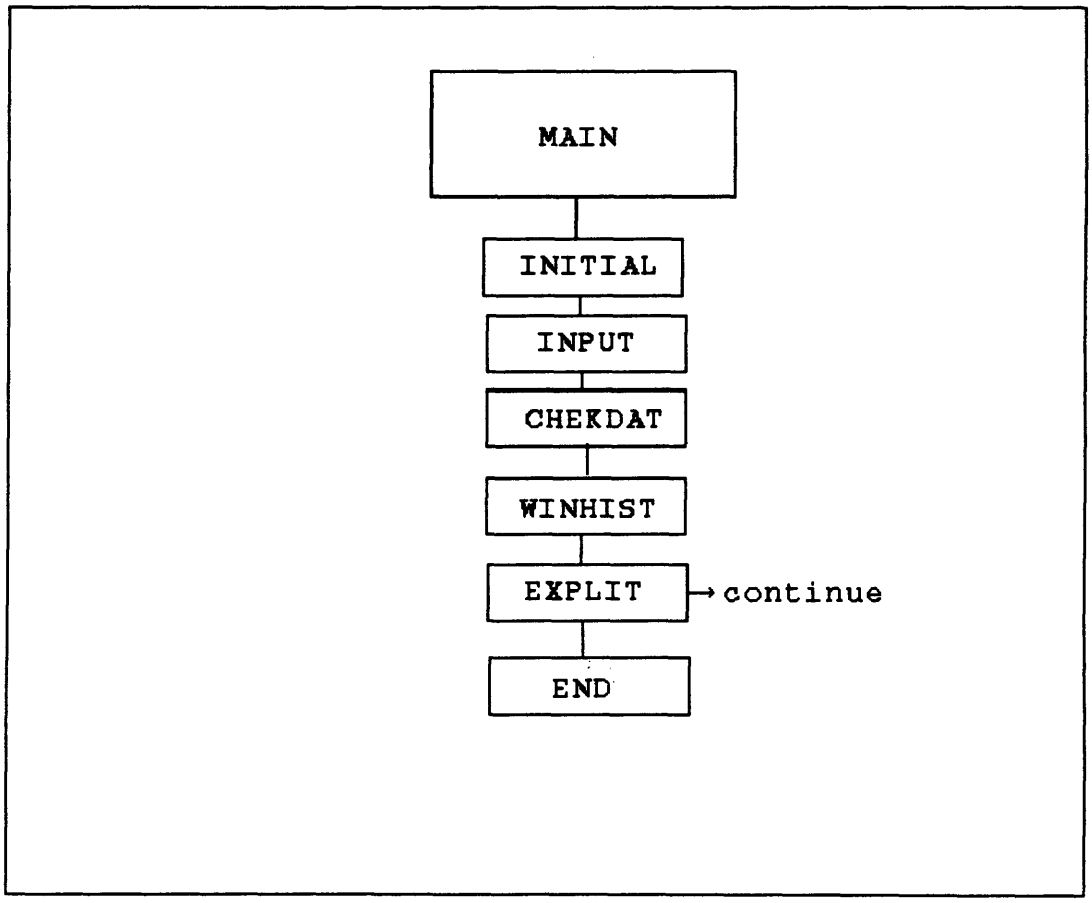

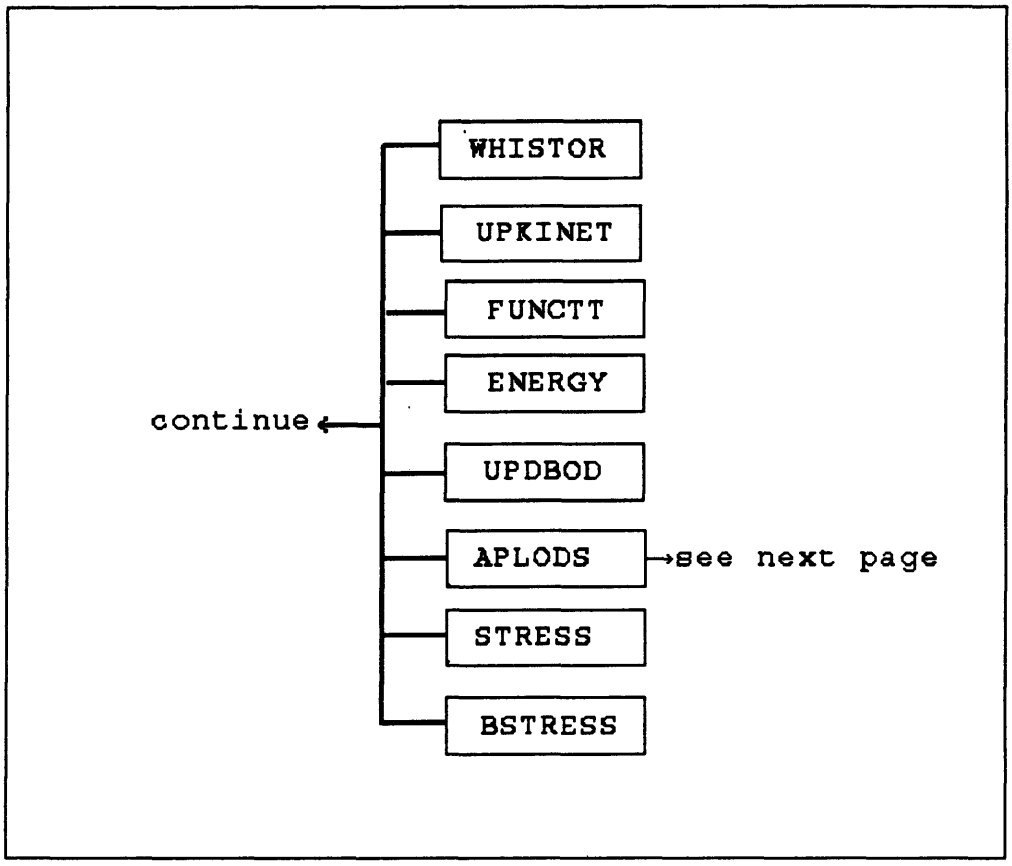
WHISTOR
UPKINET
FUNCTT
ENERGY
continue
UPDBOD
APLODS
see next page
STRESS
BSTRESS

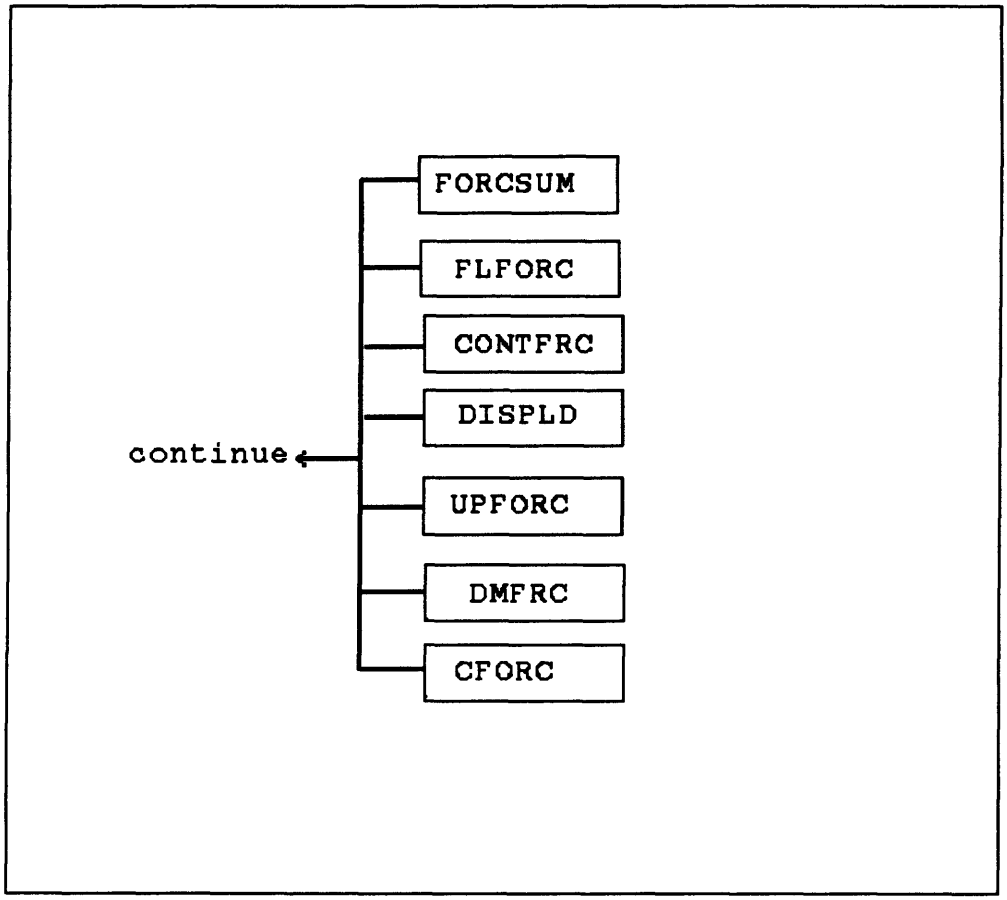
FORCSUM
FLFORC
CONTFRC
DISPLD
continue
UPFORC
DMFRC
CFORC

Program Description

The following is the list of the subroutine used in the program OCEAN. This includes and a brief description of each subroutine.

MAIN - Main drive

INITIAL - Initialize element data structure and set up names of element variables in the main data structure

INPUT - Read input data from data file

CHECDAT - Compute and check the allowable time step

WINHIST - Write initial history data into history file

EXPLIT - Perform time stepping algorithm

PRTOUT - Print selected output data to output file

WHISTOR - Write element history data on to history file

FUNCTION - Compute scale factor on applied loads and velocity at certain times

APLODS - Compute applied loads at certain time and calculate forces and moment sum

DISPLD - Apply a displacement at boundary

CFORCE - Compute the incremental applied loads on element

UPFORCE - Update the contact forces between locked elements

FLFORCE - Calculate the hydrodynamic forces

ENERRG - Compute system energies from element energies at every time step

CONFRC - Compute the contact force acting on the centeroied of an element

DMPFRC - Compute the interaction damping force acting on an element